The anti-tumor peptide Tat-Cx43$_{266-283}$ modulates the interplay between glioblastoma cells and tumor-associated astrocytes

Laura García Vicente

Tesis Doctoral

The anti-tumor peptide Tat-Cx43$_{266\text{-}283}$ Modulates the interplay between glioblastoma cells and tumor-associated astrocytes

PhD Thesis

Laura García Vicente

Universidad de Salamanca

2022

Directora: Aránzazu Tabernero Urbieta

VNiVERSiDAD Ð SALAMANCA

INSTITUTO DE NEUROCIENCIAS CASTILLA Y LEÓN

Dª ARÁNZAZU TABERNERO URBIETA, Catedrática de Universidad, adscrita al Instituto de Neurociencias de Castilla y León y al departamento de Bioquímica y Biología Molecular, de la Universidad de Salamanca.

AUTORIZA:

La presentación de la Tesis Doctoral titulada "The anti-tumor peptide Tat-Cx43$_{266-283}$ modulates the interplay between glioblastoma cells and tumor-associated astrocytes", realizada bajo su dirección por la graduada en Biología Dª LAURA GARCÍA VICENTE en el Instituto de Neurociencias de Castilla y León y en el Departamento de Bioquímica y Biología Molecular, de la Universidad de Salamanca. Además, considera que esta Tesis reúne los requisitos, calidad y rigor científico necesarios para que Dª LAURA GARCÍA VICENTE opte al grado de Doctora en Neurociencias con Mención Internacional por la Universidad de Salamanca.

Y para que así conste firma el siguiente documento en Salamanca a 4 de octubre de 2022.

Fdo. Aránzazu Tabernero Urbieta

Cuando emprendas tu viaje a Ítaca
pide que el camino sea largo,
lleno de aventuras, lleno de experiencias.
No temas a los lestrigones ni a los cíclopes
ni al colérico Poseidón,
seres tales jamás hallarás en tu camino,
si tu pensar es elevado, si selecta
es la emoción que toca tu espíritu y tu cuerpo.
Ni a los lestrigones ni a los cíclopes
ni al salvaje Poseidón encontrarás,
si no los llevas dentro de tu alma,
si no los yergue tu alma ante ti.
Pide que el camino sea largo,
que muchas sean las mañanas de verano
en que llegues -¡con qué placer y alegría!-
a puertos nunca vistos antes.
Detente en los emporios de Fenicia
y hazte con hermosas mercancías,
nácar y coral, ámbar y ébano
y toda suerte de perfumes sensuales,
cuantos más abundantes perfumes sensuales puedas.
Ve a muchas ciudades egipcias
a aprender, a aprender de sus sabios.
Ten siempre a Ítaca en tu mente.
Llegar allí es tu destino.
Mas no apresures nunca el viaje.
Mejor que dure muchos años
y atracar, viejo ya, en la isla,
enriquecido de cuanto ganaste en el camino
sin aguardar a que Ítaca te enriquezca.
Ítaca te brindó tan hermoso viaje.
Sin ella no habrías emprendido el camino.
Pero no tiene ya nada que darte.
Aunque la halles pobre, Ítaca no te ha engañado.
Así, sabio como te has vuelto, con tanta experiencia,
entenderás ya qué significan las Ítacas.

Konstantinos Kavafis

A todos los seres que hacen

el mundo un hogar.

To all.

Agradecimientos

A menudo nos olvidamos de que somos lo que somos gracias a lo que hemos sido, que la vida es continuo aprendizaje, que estamos siempre en evolución. Por eso, y porque no me voy a ver en otra igual, quiero aprovechar esta ocasión para agradecer a todas las personas importantes en mi vida, que no son pocas.

Gracias, mamá y papá, porque sin vosotros sencillamente no estaría aquí. Gracias por enseñarme que el esfuerzo da sus frutos y que las cosas bien hechas, bien hechas están. Creo que he heredado muchas cosas buenas de vosotres, a nivel genético y epigenético. Gracias por acompañarme; por tener siempre vuestra mano tendida hacia mí, pero dejarme alzar el vuelo cuando lo he necesitado. Gracias por vuestra infinita paciencia y vuestro apoyo incondicional. Esta Tesis, como todo lo que soy, es vuestra.

Gracias a las Miguel: mujeres luchadoras y empoderadas. Gracias por enseñarme a ser buena (pero no tonta), lo bonito de cuidar a los que nos rodean y que nunca estaré sola. Yaya, gracias por hacer que esta familia sea familia y por cuidar de tu reinita. Siempre serás mi persona favorita en el mundo. Tía Carmen, gracias por tener siempre la puerta abierta. Y los brazos. Tía Montse, por ser ejemplo de fortaleza. Gracias a las dos por entenderme cuando no me entiendo ni yo. Gracias, Yolanda, Ángel, Jesús y Esther, por crecer a mi lado. Carlos, por enseñarnos a ser esencialmente felices. Alba, por ser tan como yo y a la vez tan diferente y por dejarme descubrirte cada día. Gracias yayo, abuelo y Loli. Gracias, Duna, compañera, por enseñarme el amor incondicional y descubrirme otra manera de vivir.

Gracias, Demetrio, por enseñarme nudos que nunca se deshacen y hacia dónde tengo que mirar si me siento sola, por abrirme camino y por no dejarme caer. Gracias por estar a mi lado cuando estás cerca y cuando estás lejos, por hacerme reír y dejarme llorar, por quererme sin límites, por demostrarme que todo es posible, por hacerme fuerte. *Grazie mille*.

Gracias, Estefanía, por toda una vida y por la certeza de que siempre estarás. Gracias, Ali, mi Nita, por las idas y venidas que nos han hecho crecer y por querer siempre que te cuente lo que hago y dejarme ver el orgullo en tus ojos. Gracias, Andrea, por el camino compartido. Gracias, Carmen, por llenar mi vida de pequeños y grandes detalles. Gracias, Javi, por quererme feliz, libre y salvaje y cuidar siempre de mi lobita y de mí.

Gracias a todas mis maestras por ayudarme a forjar la persona que soy ahora. Gracias Marisa, Mercedes, Marisa, Pini y Sagrario, porque vuestras enseñanzas me han guiado a lo largo de los años. Gracias, Manuela, porque tus clases de Física eran clases de la vida y porque me hiciste querer ser como tú. Gracias a les que

Gracias a todo el Departamento de Bioquímica y Biología Molecular y, en especial, a José Manuel y Fernando por vuestra ayuda y disposición. Gracias Rodri, Marta, Carla y Violeta por las prácticas compartidas y por todo lo demás.

Gracias a Innova por recordarme el poder de personas luchando juntas. Gracias a la sección "in the wild" por las aventuras. Gracias a Precarios, el mejor equipo de Trivial, porque no ganaremos, pero las risas siempre fueron el mejor premio. Gracias a todos, pero sobre todo a Moisés, Nacho, Carlos, Dani, Anas, Julián, Álex, Paula, Zaki y Lorena. Gracias a la FJI por todo lo luchado y conseguido.

Thanks to the CZ Biohub for being a home away from home and to the Genomics Platform for taking so good care of me. Thank you, Spyros and Ashley, for your trust and help initiating the project. Thank you, Norma, for all your support and for being one of the strongest women I know. Vanessa, for embracing the project as yours. Mike, for listening to my never-ending questions and always being there for me. Alejandro, for your endless help and for making me be organized. Angela P, for being an inspiration. Thank you, Angela D, Honey, Sheryl, Aaron, Yang-Joon, Snighda and Maurizio for all your help.

Thank you, Tahreem, for every stolen laugh and every "you're smart", so necessary. Thank you, Ellie, for being a sister to me. Thank you, Samira and Fiona. Thank you to all the wanderers who hiked through California with me. I had some of the best conversations of my life under sequoias. Thank you, Beta Breakers, for every climb and every night around the fire, and for taking me to stunning Yosemite once and again. Thank you, Myriam, for introverting with me. Saurabh, for seeing the little kid inside of me and taking care of her. Vibhu, for teaching me how to open my hands to keep the birds free, and for not flying away.

Gracias al Lab 15 por ser casa y a todes les que lo componen por ser familia. Gracias, Marta y Myriam, por enseñarme cómo se vive aquí y guiarme en mis primeros pasos. Cuántas veces os he echado de menos. Gracias, Ana, por tu inigualable disposición y tu infinita bondad. Tomy, por tener siempre una palabra amable, por tus ganas de ayudar y por darle un toque especial a los lunes por la tarde. Gracias, Josefi, por llorar de la risa conmigo. Gracias por preocuparte siempre por mis huesos rotos y por los yogures de los primeros años, que me han durado para una tesis entera. Gracias, José María, por las mil enseñanzas, sobre bioquímica y sobre la vida a partes iguales, y por crear tan buena escuela. Gracias, Sara, por dejarme seguir tus pasos y salvarme el culo tantas veces, y por todas las aventuras compartidas. Rocío, por tu fuerza y tu optimismo y por siempre, siempre cuidar a tu gente. Gracias a mis Supernenas por ser precisamente eso (y un poco el Comité de Bioética), por recordarme que puedo con lo que me proponga y por las risas que nos han alargado la vida. Andrea, mamá de ratones, compañera de cultivos a las 10 de la noche (porque todos sabemos que a esa hora las células se portan mejor), proveedora de dulces desconocidos, gracias por reír y llorar conmigo. Raquel, mi descubrimiento más veloz, gracias por tu franqueza y por la conexión que nos une. Gracias, Pilar, por traer frescura y por estar siempre dispuesta a ayudar. Y por los postres, claro.

Camilo, por tu sentido del humor y tu bondad. Claudia, por tanto, en tan poco tiempo. Gracias, María P, por llegar pisando fuerte. Gracias a todes les pollites y, en especial, a Pablo, por vuestra paciencia y por enseñarme a enseñar. Gracias, María TFM, por llegar para quedarte.

Gracias, Arantxa. Gracias y mil veces gracias. Daría igual cuántas veces lo dijera, que no serían suficientes. Gracias por darme la oportunidad de descubrir la ciencia a tu lado, pero también por permitirme conocer lugares diferentes. Gracias por rescatarme cuando estaba perdida y ayudarme a retomar el vuelo. Gracias por tu disponibilidad, tu amabilidad y tu entusiasmo, que contagias a quienes tenemos la suerte de estar a tu alrededor. Gracias por confiar ciegamente en mí y darme ese empujoncito que muchas veces me hace falta para luchar por mis sueños, pero gracias también por saber frenarme cuando no sé hacerlo yo sola. Gracias por darme la libertad para marcar mi propio camino sin dejarme sola ni un momento. Gracias por todo.

Note

Part of the results presented in this PhD Thesis have been published in a peer-reviewed journal. The publication is included at the end of the document.

Parte de los resultados presentados en esta Tesis Doctoral han sido publicados en una revista revisada por pares. La publicación está incluida al final de este documento.

Publication details

Connexin43 peptide, TAT-Cx43$_{266\text{-}283}$, selectively targets glioma cells, impairs malignant growth, and enhances survival in mouse models in vivo

Myriam Jaraíz-Rodríguez, Rocío Talaverón, Laura García-Vicente, Sara G Pelaz, Marta Domínguez-Prieto, Andrea Álvarez-Vázquez, Raquel Flores-Hernández, Wun Chey Sin, John Bechberger, José M Medina, Christian C Naus, Arantxa Tabernero

Neuro-Oncology (2020), 22(4), 493–504

doi: 10.1093/neuonc/noz243

PMID: 31883012

PMCID: PMC7158688

Abbreviations

ANOVA	Analysis of variance
b-FGF	Basic fibroblast growth factor
BDNF	Brain-derived neurotrophic factor
BER	Base excision repair
BSA	Bovine serum albumin
CNS	Central nervous system
CPP	Cell-penetrating peptide
Cx43	Connexin43
DAPI	4 ',6-diamidino-2-fenilindol
DGE	Differential gene expression
DIV	Days in vitro
DMEM	Dulbecco's modified Eagle's Medium
DMSO	Dimethyl sulfoxide
DNA	Desoxyribonucleic acid
dpi	Days post-injection
DSB	Double strand break
EGF	Epidermal growth factor
Erk	Extracellular signal-regulated kinase
FACS	Fluorescence activated cell sorting
FCS	Fetal calf serum
GAPDH	Glyceraldehyde 3-phosphate dehydrogenase
GFAP	Glial fibrillar acidic protein
GL261-AC	GL261 growing as adherent cells in differentiation medium
GL261-NS	GL261 growing as neurospheres in stem cell medium
GSC	Glioma stem cell
HR	Homologous recombination
Id-1	Inhibitor of differentiation 1
IP	Intraperitoneal
IR	Ionizing radiation

JAK	Janus kinase
MAP-2	Microtubule associated protein 2
MBP	Myelin basic protein
MMP-2	Metalloproteinase 2
MMR	Mismatch repair
MTT	3-(4,5-dimethylthiazol-2-yl)-2,5-diphenyltetrazolium bromide
NG2	Neural/glial antigen 2
ns	Not significant
NSC	Neural stem cell
NT	Non-target
OPC	Oligodendrocyte precursor cell
PBS	Phosphate buffered saline
PCA	Principal component analysis
PCNA	Proliferating cell nuclear antigen
PCR	Polymerase chain reaction
RNA	Ribonucleic acid
ROI	Region of interest
RPL19	Ribosomal protein L19
RT	Reverse transcription
RTK	Receptor tyrosine kinase
SEM	Standard error of the mean
SA-β-Gal	Senescence-associated β-Galactosidase
SBS	STAT3 binding site
scRNA-Seq	Single-cell RNA sequencing
SFK	Src family kinase
siRNA	Small interference RNA
snRNA-Seq	Single-nucleus RNA sequencing
STAT3	Signal transducer and activator of transcription
TAA	Tumor-associated astrocyte
TAM	Tumor associated microglia/macrophage
TMZ	Temozolomide
TrkB	Tropomyosin kinase receptor B
UMAP	Uniform manifold approximation and projection

UMI	Unique molecular identifier
Tat-Cx43$_{266\text{-}283}$	Cell-penetrating peptide containing amino acids 266-283 of connexin43

Index

ABSTRACT

Abstract

Glioblastoma is the most aggressive and frequent form of primary brain tumor and, despite continuous effort to find an effective treatment, is considered as one of the deadliest types of cancer, with a median survival of only 16 months. Glioblastomas are characterized by fast and aggressive growth, high infiltrative capacity, and resistance to current treatments. These tumors are composed of a heterogeneous population of cells, including some with stem cell properties (glioblastoma stem cells, GSCs), which are highly tumorigenic and have high oncogenic Src activity. The presence of tumor cells in the brain triggers the activation of the astrocytes in the tumor microenvironment, which ultimately cooperate with glioblastoma cells to promote tumor progression. Previous results from our laboratory show that a cell-penetrating peptide that mimics the inhibitory effect of connexin43 on Src (Tat-Cx43$_{266-283}$) exerts potent anti-tumoral effects in glioblastoma cells in vitro and in vivo, without deleterious effects in healthy brain cells.

In this PhD thesis, we explore the mechanisms of astrocyte activation in the context of glioblastoma and analyze the effect of Tat-Cx43$_{266-283}$ in the crosstalk between tumor cells and astrocytes.

First, we use ex vivo and in vitro co-culture models to study astrocyte activation. We show that the presence of glioblastoma cells promotes a change in the phenotype of astrocytes that is characterized by an increase in the phosphorylation and nuclear translocation of the transcription factor STAT3. We find that laminin activates astrocytes, increasing the activity of STAT3 and the expression of its target genes N-cadherin and β-catenin. Importantly, we find that the treatment with Tat-Cx43$_{266-283}$ reverts these effects.

Second, we set up an in vivo model consisting in the intracranial injection of GL261 GSCs in immunocompetent syngeneic mice. We show that the treatment of GSCs derived from GL261 with Tat-Cx43$_{266-283}$ reduces Src levels and activity, diminishes proliferation, and promotes differentiation towards an oligodendrocyte-like state that favors temozolomide (TMZ) anti-tumor effect. We generate drug-resistant GL261 GSCs and characterize their response to Tat-Cx43$_{266-283}$ and TMZ treatments.

Third, we use the in vivo model to confirm the effect of Tat-Cx43$_{266-283}$ on astrocyte activation. We find that tumor progression induces a vast response of astrocytes, including STAT3 activation, and that Tat-Cx43$_{266-283}$ reverts this effect.

Finally, we take advantage of high-throughput single-cell technologies to confirm the main findings of this PhD Thesis and obtain a global picture that helps understanding glioblastoma biology and, ultimately, provide a cure for this deadly malignancy.

In summary, the results presented in this PhD Thesis confirm the anti-tumor effect of Tat-Cx43$_{266-283}$ in glioblastoma cells and uncover a new role for this peptide in the modulation of astrocyte activation. The combination of these effects disrupts the cross-communication between glioblastoma cells and astrocytes, contributing to the reduction of tumor growth and invasion.

Resumen

Los glioblastomas constituyen la forma más frecuente y agresiva de tumor cerebral. A pesar de continuos esfuerzos por encontrar una cura, el glioblastoma es considerado uno de los cánceres más mortales, con una supervivencia media de apenas 16 meses. Estos tumores se caracterizan por seguir un patrón de crecimiento rápido y agresivo, tener gran capacidad infiltrativa y ser resistentes a los tratamientos actuales. Una de las principales características de los glioblastomas es su gran heterogeneidad, conteniendo una población de células con características de célula madre (células madre de glioma o GSCs, por sus siglas en inglés), las cuales son altamente tumorigénicas y presentan alta actividad de la oncoproteína Src. La presencia de células tumorales en el cerebro desencadena la activación de los astrocitos presentes en su microambiente, condicionándolos para que contribuyan a la progresión tumoral. Previos estudios realizados en nuestro laboratorio demostraron que un péptido penetrante basado en la conexina 43 (Tat-Cx43$_{266-283}$) es capaz de recrear la inhibición de Src promovida por esta proteína, ejerciendo de esta manera un potente efecto antitumoral sobre las células de glioblastoma in vitro e in vivo. Notablemente, este péptido no tiene efectos deletéreos sobre las células sanas del cerebro.

En esta Tesis Doctoral, exploramos los mecanismos por los que se produce la activación de los astrocitos en el contexto del glioblastoma y analizamos el efecto de Tat-Cx43$_{266-283}$ en la comunicación entre las células tumorales y los astrocitos.

Primero, empleamos modelos de co-cultivo para estudiar la activación de los astrocitos in vitro y ex vivo. De esta manera, observamos que la presencia de células de glioblastoma promueve un cambio en el fenotipo de los astrocitos, caracterizado por un aumento en la fosforilación del factor de transcripción STAT3 y su traslocación al núcleo. Además, observamos que la laminina activa los astrocitos, aumentando la actividad de STAT3 y la expresión de sus genes diana N-cadherina y β-catenina. Cabe destacar que el tratamiento con Tat-Cx43$_{266-283}$ revierte esta activación.

Segundo, ponemos a punto un modelo de glioblastoma in vivo, en el cual inyectamos de manera singénica células madre obtenidas a partir de la línea de glioma de ratón GL261 en ratones inmunocompetentes. El tratamiento de estas células con Tat-Cx43$_{266-283}$ reduce la fosforilación de Src y sus niveles totales, disminuye la proliferación y promueve la diferenciación hacia un linaje de tipo oligodendrocítico, favoreciendo el efecto anti-tumoral del quimioterapéutico empleado actualmente, la temozolomida (TMZ). Además, generamos células resistentes a Tat-Cx43$_{266-283}$ y TMZ y caracterizamos su respuesta ante estos tratamientos.

Tercero, nos servimos de este modelo de ratón para confirmar el efecto de Tat-Cx43$_{266-283}$ sobre la activación de los astrocitos. Observamos que la progresión tumoral induce una fuerte respuesta en los astrocitos, con activación de STAT3, y que el tratamiento con Tat-Cx43$_{266-283}$ revierte este efecto.

Por último, realizamos estudios de célula única de alto rendimiento con el objetivo de confirmar los principales resultados de esta Tesis y obtener una visión global que nos permita una mejor comprensión de la biología del glioblastoma y dirija los pasos hacia la obtención de un tratamiento efectivo frente a estos tumores.

En resumen, los resultados presentados en esta Tesis Doctoral confirman el efecto antitumoral de Tat-Cx43$_{266-283}$ sobre las células de glioblastoma y descubren una nueva función de este péptido en la modulación de la activación de los astrocitos. Estos efectos tienen un notable efecto combinatorio, dando lugar a la pérdida de comunicación entre las células de glioblastoma y los astrocitos en su microambiente y comprometiendo así la progresión tumoral.

INTRODVCTION

Introduction

Gliomas and glioma stem cells

The most frequent primary tumors of the central nervous system (CNS) are those of glial origin, called gliomas, and are considered to originate from glial progenitor cells (Zong, Verhaak, and Canoll 2014). Gliomas have been traditionally classified according to histologic features and malignancy grade (Perry and Wesseling 2016). Grade 1 gliomas are circumscribed, whereas grades 2, 3 and 4 show extensive infiltration in the CNS parenchyma and are thus called diffuse gliomas. The latest World Health Organization (WHO) classification, WHO CNS5, takes into consideration molecular diagnostics and assigns common adult-type diffuse gliomas to three groups: astrocytoma, IDH-mutant (grades 2-4); oligodendroglioma, IDH-mutant and 1p/19q-codeleted (grades 2-3); and glioblastoma, IDH-wildtype (grade 4) (Louis, et al. 2021). Traditionally, grade 4 was given attending to histological features such as necrosis and/or microvascular proliferation. However, since the last classification, molecular alterations are enough to classify a tumor as grade 4. Glioblastoma, formerly termed glioblastoma multiforme because of its complex phenotype, is the most common and the most aggressive form of glioma. Histologically, glioblastoma is characterized by high cellularity, pleomorphic cells with nuclear atypia and high mitotic activity, and microvascular proliferation and/or necrosis. In the absence of such histological characteristics, TERT promoter mutation, EGFR amplification, or concomitant gain of chromosome 7 and loss of chromosome 10 are enough to classify a glioma as glioblastoma (Louis, et al. 2021). Main altered pathways are summarized in **Scheme 1**.
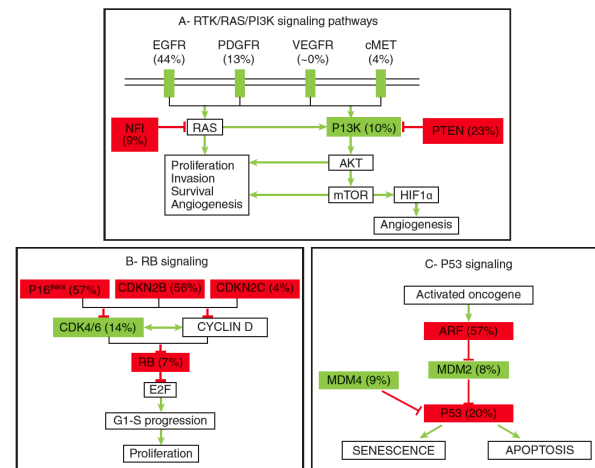
Scheme 1. Major key altered pathways in glioblastoma. Taken from (De Vleeschouwer 2017).

Glioblastomas are infiltrative but non-metastatic, and present poor immunogenicity. Prognosis has slightly improved over the years, and current median survival for glioblastoma patients is only 16 months (Miller, et al. 2021). The standard of care for these tumors follows the Stupp protocol: maximal safe surgical resection followed by ionizing radiation and adjuvant chemotherapy (Stupp, et al. 2005). To date, the most effective drug to treat glioblastoma is the alkylating agent

temozolomide (TMZ). However, 50% of the patients treated with temozolomide do not respond to the treatment, and the increase in survival for those who do is just a few months (Aldape, et al. 2019). Glioblastoma diffuse migration pattern makes a complete surgical resection virtually impossible, and radiotherapy protocols only cover 2 cm beyond the visible tumor margin (Young, et al. 2015; Sherriff, et al. 2013). However, cells infiltrate further than this and the infiltrating edge is, in fact, enriched in the so-called glioma stem cells (GSCs), a population of cells with stem cell properties. These cells present self-renewal ability and the potential to recapitulate the heterogeneous phenotypes of glioblastoma cells, and are resistant to current chemotherapy, giving rise to tumor recurrence (Sherriff, et al. 2013; Eyler and Rich 2008). GSCs are thought to be generated by asymmetric division of neural stem cells (NSCs) or oligodendrocyte progenitor cells (OPCs), with whom they share markers (Lee, et al. 2018; Wang, et al. 2021). Chemotherapeutic drugs that induce DNA damage can kill fast proliferating cells, but not GSCs, thus, targeting GSCs may help chemotherapy and radiotherapy.

Tumor progression in the brain microenvironment

The dynamic cross-communication between tumor cells and the cells in the surrounding tumor microenvironment (TME) plays a crucial role in promoting tumor progression and is thus being explored as a therapeutic target (Quail and Joyce

2017). Cellular components of the glioblastoma TME include brain-resident cell types (microglia, astrocytes, oligodendrocytes, endothelial cells, pericytes, and neurons) and peripherally derived immune cells (macrophages, lymphocytes, dendritic cells, and neutrophils) (Scheme 2).

Although the microenvironment of the normal brain is usually immunosuppressive, glioblastoma cells interact with the TME, especially with tumor-associated microglia/macrophages (TAMs), the main immune population in the TME, to suppress an anti-tumor immune response (Wei, et al. 2019; Poon, et al. 2017; Hambardzumyan, Gutmann, and Kettenmann 2016). Other cell populations, including astrocytes, neurons, and endothelial cells secrete factors that stimulate stemness, survival, proliferation, and migration of tumor cells (Infanger, et al. 2013; Brandao, et al. 2019; Venkatesh, et al. 2015; Venkatesh, et al. 2017).

The brain TME presents unique features that challenge glioblastoma treatment, including the presence of a blood brain barrier (BBB) and a distinct composition of the extracellular matrix (ECM), which is particularly soft compared to other solid tissues (Bellail, et al. 2004; van Tellingen, et al. 2015; Budday, et al. 2015). Anatomical tracts such as myelinated axons and the vasculature provide haptotactic cues for the migration of glioblastoma cells (Gritsenko, Ilina, and Friedl 2012; Gritsenko, Leenders, and Friedl 2017; Giese and Westphal 1996), which invade the perivascular space, disrupting astrocytic endfeet contacts with the endothelial cells and damaging the BBB (Watkins, et al. 2014). In the actively invading

regions of the tumor, however, the BBB is usually intact and impenetrable for most chemotherapeutics (de Vries, et al. 2006; van Tellingen, et al. 2015).

The high cellular density reached at the tumor core leads to the appearance of hypoxic regions and necrosis. Tumor cells migrate away from the necrotic core forming a characteristic pattern known as pseudopalisades, with very high cellularity (Brat, et al. 2004). The hypoxic niche contributes to the maintenance of GSCs through the activation of alternative transcriptional programs that promote survival and angiogenesis (Colwell, et al. 2017; Soeda, et al. 2009). Although glioblastoma is characterized by its high vascularity, tumor vessels differ from healthy vessels in that they are disorganized and highly permeable, leading to infiltration of immune cells from the peripheral circulation (Weiss, et al. 2009).

Reactive astrocytes

Astrocytes constitute approximately the 30% of the cells in the CNS and perform many functions critical for its physiology (Sofroniew and Vinters 2010). In the healthy brain, astrocytes contribute to neuronal development and function, playing an active role in synaptic activity and plasticity (Chung, Allen, and Eroglu 2015). The endfeet of astrocytes closely associate with endothelial cells and pericytes to form the BBB (Zhao, et al. 2015).
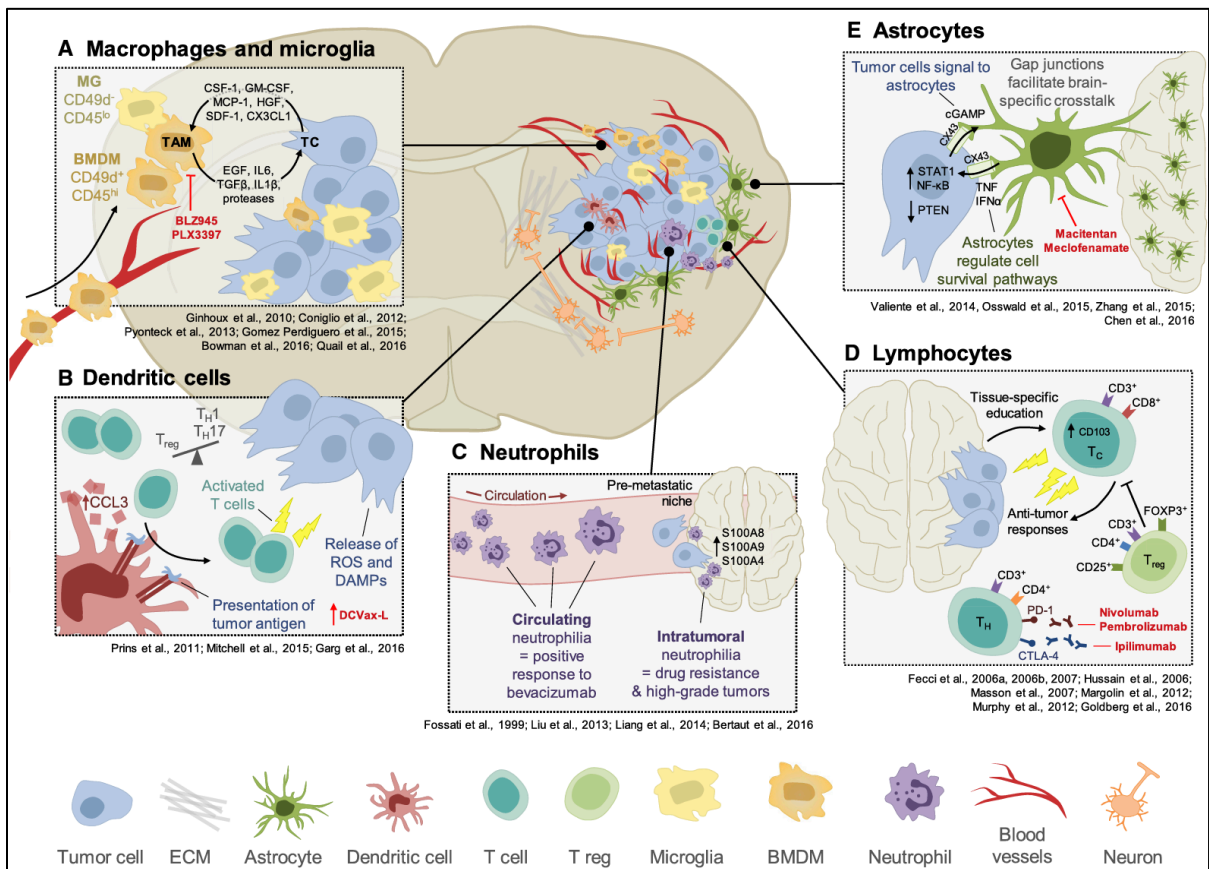
Scheme 2. Cellular components of the brain tumor microenvironment. Taken from (Quail and Joyce 2017).

Under pathological situations, astrocytes lose homeostatic functions and may gain protective and/or detrimental roles. These astrocytes that undergo morphological, molecular, and functional remodeling in response to CNS injury are collectively known as reactive astrocytes (Escartin, et al. 2021). The main component of astrocyte intermediate filaments, glial fibrillary acidic protein (GFAP), is usually upregulated in reactive astrocytes and often GFAP labeling shows reactive astrocytes forming a border around CNS lesions (Voskuhl, et al. 2009). Reactive astrocytes may upregulate other cytoskeleton proteins (i.e., Nestin, Vimentin), growth factors and cytokines (i.e., brain derived neurotrophic factor, BDNF; interleukin 6, IL-6; C-C motif chemokine ligand 2, CCL2), cell adhesion proteins (i.e., CD44) and extracellular matrix components (i.e., collagen, versican) (Escartin, et al. 2021)

Reactive astrocytes have been observed and characterized over the years in the context of different pathological conditions, including traumatic brain or spinal cord injury (Bush, et al. 1999; Ren, et al. 2013; Bundesen, et al. 2003; Bloom 2014; Anderson, et al. 2016), stroke (Cekanaviciute, et al. 2014; Zamanian, et al. 2012; Gao, Li, and Chopp 2005), inflammation (Zamanian, et al. 2012; Hasel, et al. 2021), and neurodegenerative diseases (Liedtke, et al. 1998; Lepore, et al. 2008; Kraft, et al. 2013; Ben Haim, et al. 2015; Liddelow, et al. 2017; Heppner, Ransohoff, and Becher 2015; Galea, et al. 2022). In the context of brain tumors, invasion of the brain parenchyma promotes reactive astrogliosis, in an initial attempt to repair the damaged tissue. However, signaling from glioma cells turns the activation of astrocytes into tumor-associated astrocytes (TAAs), which ultimately tumor growth (O'Brien, Howarth, and Sibson 2013; Lee, et al. 2011; J. K. Kim, et al. 2014; Placone, Quiñones-Hinojosa, and Searson 2016; Brandao, et al. 2019). Activation of astrocytes upon tumor growth has been associated to NF-κB triggering by RANKL (J. K. Kim, et al. 2014) and, more recently, to STAT3 signaling (Priego, et al. 2018; Henrik Heiland, et al. 2019). Activated TAAs release factors that enhance proliferation and invasion of tumor cells, including tumor growth factor-β (TGF-β) (J. K. Kim, et al. 2014), tumor necrosis factor-α (TNF-α), IL-1β (Seike, et al. 2011), insulin growth factor-1 (IGF-1), glial-cell derived neurotrophic factor (GDNF) (Shabtay-Orbach, et al. 2015), osteopontin, IL-6, and IL-8 (Nagashima, et al. 2002; Rath, et al. 2013). Astrocytes in the TME promote migration of tumor cells by mediating the activation of matrix metalloproteinases (MMPs), such as MMP-2 (Le, et al. 2003), and help to the adaptation of glioblastoma cells to hypoxia (Jin, et al. 2018). In addition, several studies pinpoint to a role for TAAs in chemoprotection (Chen, et al. 2015; Chen, et al. 2016) and immunoprotection (Huang, et al. 2010; J. E. Kim, et al. 2014).

STAT3 and related pathways

Signal transduction and activator of transcription (STAT) proteins are important mediators of the extracellular signals that promote

survival, proliferation, or differentiation (Darnell, Kerr, and Stark 1994; Darnell 1997). STAT3 is activated by cytokines and growth factors and is involved in the regulation of immune responses and other cellular events such as proliferation, survival, or differentiation in healthy and tumor cells (Hirano, Ishihara, and Hibi 2000; Yu, Pardoll, and Jove 2009).

Upon stimulation, STAT3 is phosphorylated by Janus kinases (JAKs) or other intracellular or receptor tyrosine kinases. STAT3 is primarily phosphorylated at tyrosine 705 (Y705), which stabilizes the dimerization through reciprocal phosphotyrosine-SH2 domain interactions and is critical for the activation of target genes (Yoshimura, Naka, and Kubo 2007; Hirano, Ishihara, and Hibi 2000) (**Scheme 3**). STAT3 is also phosphorylated at serine 727 (S727) by multiple Ser/Thr kinases. S727 phosphorylation increases STAT3 transcriptional activity (Wen, Zhong, and Darnell 1995; Abe, et al. 2001), but has also been shown to enhance Y705 dephosphorylation and inactivation (Wakahara, et al. 2012; Yang, et al. 2020).
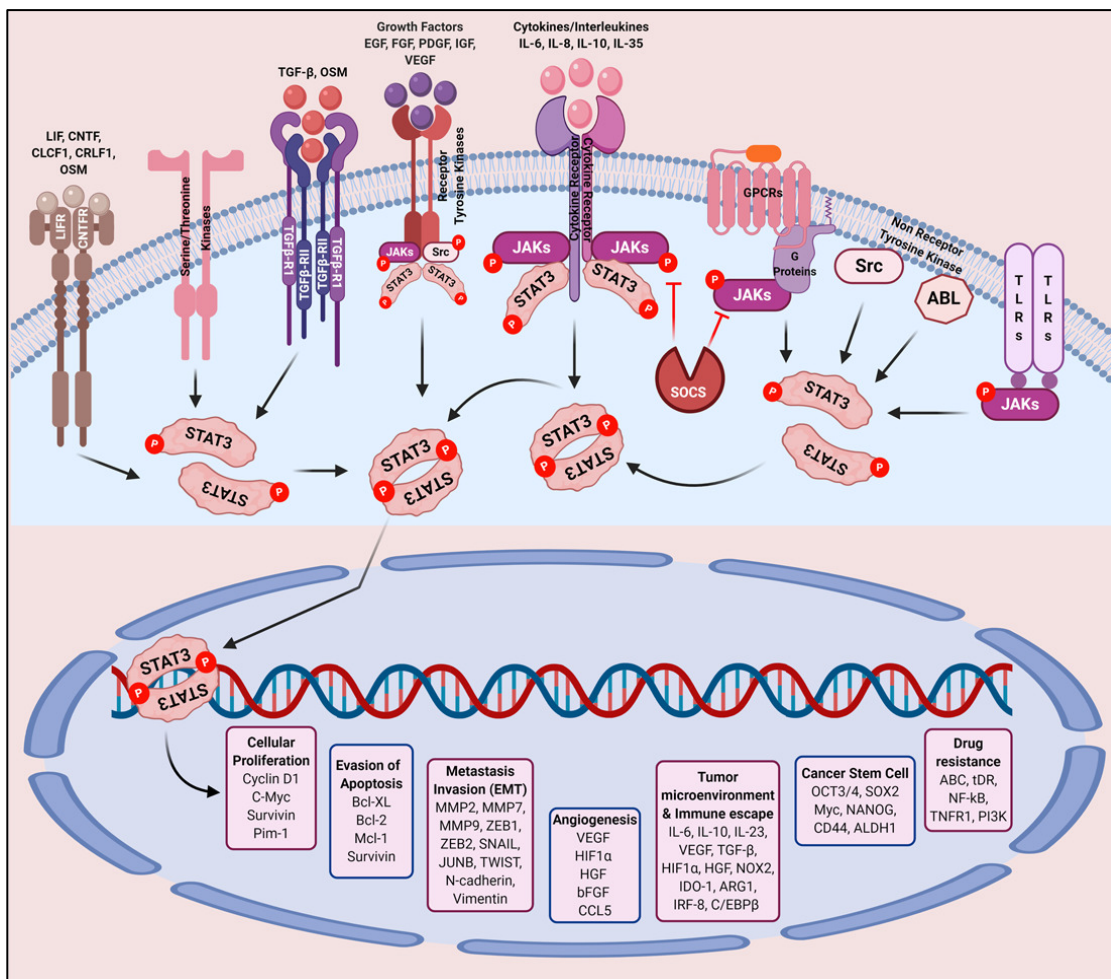
Scheme 3. Major key pathways involved in the activation of STAT3 and target genes in the context of cancer. Taken from (Garg, et al. 2020).

Among the various genes regulated by STAT3, one of the main groups includes proteins related to cell adhesion and invasion. Cadherins (named for "calcium-dependent adhesion") are Ca^{2+}-dependent transmembrane proteins. Cadherins mediate cell-cell adhesion through their extracellular domain, and associate through their intracytoplasmic tail with adaptors and signaling proteins, forming a complex that includes α-, β-, and p120-catenins. N-cadherin is involved in many activities in the CNS, such as differentiation, migration, and cell polarization (Takeichi 2007), and regulates cell-cell adhesion and cellular morphology in astrocytes (Kanemaru et al. 2013).

Mouse models of glioblastoma

Preclinical models are essential to advance our understanding of tumor biology and treatment. Although there is a variety of animal models of glioblastoma, the wide majority utilize mice. Mouse models can be grouped into three categories: genetically engineered mouse modes (GEMMs), syngeneic models and xenograft models, all of them featuring different advantages and disadvantages (Scheme 4). In syngeneic models, tumor cells of murine origin are implanted into mice of the same strain. These cells can be obtained from spontaneous tumors (Fraser 1971) or, more frequently, from tumors originated from exposure to mutagenic chemicals (Ausman, Shapiro, and Rall 1970). The main advantage of these models is an intact immune system, which makes them suitable for immunotherapy studies (Genoud, et al. 2018).

The GL261 model is the most widely used syngeneic model and is easily available. It has been used in studies of gene therapy, immune cell transfer, monoclonal antibodies, and cytokine therapies, checkpoint inhibitors, and dendritic vaccines (Maes and Van Gool 2011; Xu, et al. 2014; Wainwright, et al. 2014; Pellegatta, et al. 2006; Ciesielski, et al. 2006; A, et al. 2008). The GL261 model was generated by intracranial injection of 3-methylcholantrene into C57BL/6 mice and maintained by serial intracranial and subcutaneous transplantations of tumor pieces on the syngeneic strain (Ausman, Shapiro, and Rall 1970). Several in vitro cultures were stablished from the GL261 tumor in parallel during the 1990s.
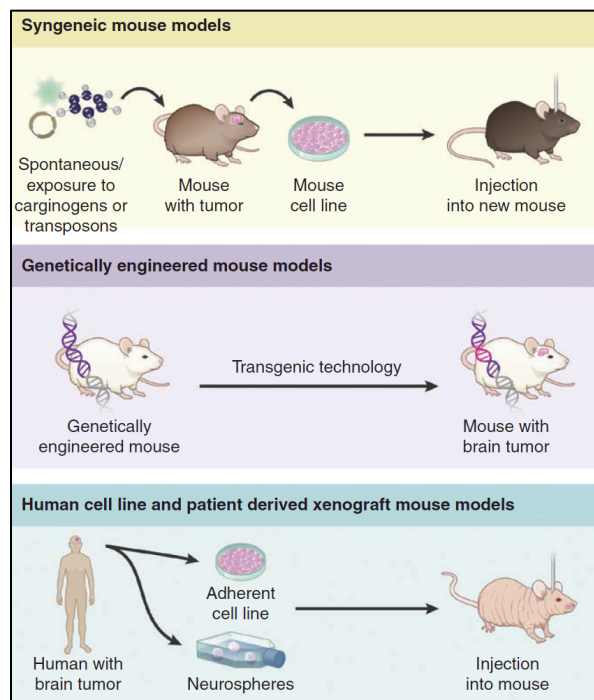
Scheme 4. Mouse models available to glioblastoma researchers. Taken from (Haddad, et al. 2021).

Although GL261 cells are widely used, they are poorly characterized. Szatmari and colleagues characterized the carcinogenic alterations of GL261 cells and found elevated expression of the myc oncogene and p53 tumor suppressor gene compared to normal brain, although p53 presented a homozygous point mutation at codon 153 of exon 5. This mutation is located at a non-conserved region, suggesting a low functional importance for it (Friend 1994). p53 gene mutations are a very commonly found in human brain tumors and indicate bad prognosis (Ishii, et al. 1999; Sidransky, et al. 1992). Interestingly, other studies also reported high p53 expression but did not find p53 mutations (Blaszczyk-Thurin, Ertl, and Ertl 2002). Although c-myc alterations are rare in humans, gene amplification and rearrangement and prolonged protein life have been described (Shindo, et al. 1993). GL261 cells present decreased H-ras expression and a mutation of K-ras in codon 12 of exon 1, one of its most frequently mutated sites. Ras mutations are a signature of chemical carcinogenesis but are not considered a driver mutation of glioblastoma, being probably a reflect of the chemical-carcinogen induced nature of the GL261 tumor (Verhaak, et al. 2010; Brennan, et al. 2013). Although they are more frequent in other tumor types, K-ras mutations have been reported in human brain tumors (Bos 1989).

Intracranially implanted GL261 cells grow rapidly and form tumors with 100% penetrance, with a median survival of 25 days (10^5 cells), 27 days (10^4 cells), 36 days (10^3 cells), and 55 days (10^2 cells) (Szatmári et al., 2006). Thus, these tumors can be considered aggressive and the GL261 model is, in fact, classified as glioblastoma. GL261 form both subcutaneous and intracranial tumors but are not metastatic. Intracranial tumors show rapid growth rate with slightly invasive growth pattern and low lymphocyte infiltration (Szatmári, et al. 2006). GL261 cells are moderately immunogenic, probably due to a slightly elevated MHCI expression, but MHCII levels are barely detectable. GL261 cells also express unique tumor antigens, which makes the GL261 model a preferent election for glioma immunotherapy studies (Maes and Van Gool 2011). Although GL261 growing in vitro are rather radio-sensitive, irradiation of tumor-bearing mouse did not show a curative effect (Szatmári, et al. 2006; Mathios, et al. 2016).

Temozolomide and mechanisms of drug resistance

TMZ (3-methyl-4-oxoimidazo[5,1-d][1,2,3,5] tetrazine-8-carboxamide) is a non-cell cycle specific alkylating prodrug. At physiological pH, TMZ is rapidly hydrolyzed to the active intermediate, 5-(3-methyltriazen-1-yl) imidazole-4-carboxamide (MTIC), a short-lived compound which is further hydrolyzed to 5-amino-imidazole-4-carboxamide (AIC) and methyl diazonium (Moody and Wheelhouse 2014; Reid, et al. 1997). The electrophilic methyl diazonium ion transfers its methyl group to negatively charged DNA, creating DNA adducts, preferentially at N^7 and O^6 sites on guanines (N^7-MeG, >70%; O^6-MeG, ~9%) and N^3

Temozolomide Metabolism

Adduct Formation

DNA Repair Mechanisms
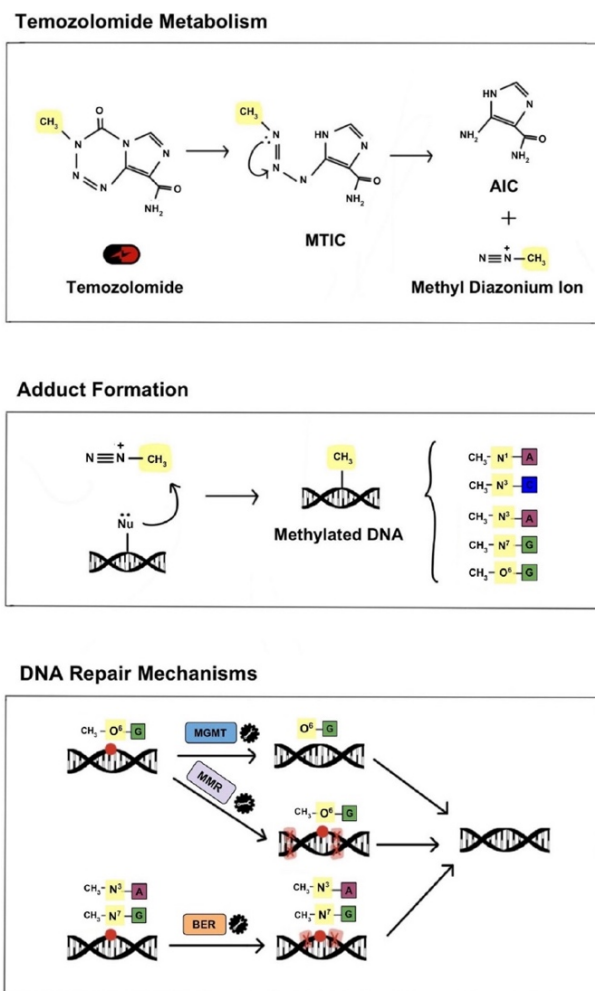
Scheme 5. TMZ mechanism of action. Taken from (Singh, et al. 2021).

site on adenines (N^3-MeA, ~10%) on genomic DNA. The cytotoxicity of TMZ is mainly derived from O^6-MeG lesions, which lead to the insertion of a thymine during subsequent DNA replication, causing either double-strand breaks (DSBs) in the DNA or GC to AT transition (Lee 2016). TMZ-induced DSBs can be repaired by homologous recombination (HR), whereas methylated DNA can be repaired by base excision repair (BER) or DNA mismatch repair (MMR) (Fujii, Sobol, and Fuchs 2022) (**Scheme 5**). The lack of such DNA repair pathways, which are necessary for the cytotoxicity

of TMZ, and/or overexpression of O^6-MeG methyltransferase (MGMT), the enzyme that reverses the methylation of guanine at O^6, are the main causes of TMZ resistance (Hickman and Samson 2004; Hunter, et al. 2006).

Connexin43, Src, and Tat-Cx43$_{266-283}$

Connexins are tetraspan membrane proteins with two extracellular loops and three intracellular regions, including the N- and C-terminal domains (Kumar and Gilula 1996). Connexins assemble in hexamers to form channels named connexons or hemichannels, that may form functional channels per se, connecting the cytoplasm and the extracellular milieu, or couple with a connexon in the adjacent cell to form gap junctions, which allow the intercellular exchange of small molecules.

Connexin43 (Cx43), encoded by the *GJA1/Gja1* gene (human/mouse), is the most abundant connexin in mammals and is widely expressed in many tissues, including the CNS, where it is highly expressed in astrocytes (Giaume, et al. 1991; Giaume, et al. 2021). Beyond its channel-related functions, Cx43 regulates a multitude of channel-independent processes. Cx43 possesses a large intracytoplasmic C-terminal domain (Cx43-CT, amino acids 232 to 382), which is mostly an intrinsically disordered region (IDR), and provides a large surface area and a high conformational flexibility, acting as a scaffolding hub for the interaction of different partners (Sorgen, et al. 2004; Grosely, et al. 2013) (**Scheme 6**).
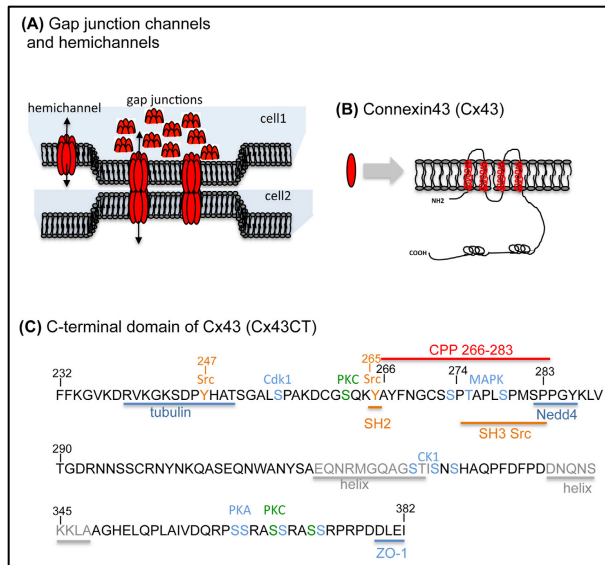
Scheme 6. Structure and interactions of connexin43 (Cx43). Taken from (Tabernero, et al. 2016).

In gliomas, Cx43 expression levels inversely correlate with the degree of malignancy, being almost inexistent in glioblastoma (Shinoura, et al. 1996; Huang, et al. 1999; Soroceanu, Manning, and Sontheimer 2001; Pu, et al. 2004). Ectopic expression of Cx43 in glioma cells reduces their stem cell potential and proliferation (Zhu, et al. 1991; Naus, et al. 1992; Yu, et al. 2012), making it to be considered as a tumor suppressor. However, Cx43 can also play pro-tumorigenic roles (Sin, Crespin, and Mesnil 2012), such as promoting invasion (Lin, et al. 2002; Oliveira, et al. 2005) and drug resistance (Murphy, et al. 2016; Grek, et al. 2018; Gielen, et al. 2013). Thus, it is important to carefully mimic the desired Cx43 effects when designing anti-tumoral tools based in this protein.

Among others, Cx43-CT contains the sequence required for Src binding (Src homology (SH)2- and SH3-binding domains). Src is a non-receptor tyrosine kinase that participates in different signaling pathways that control biological events such as proliferation, differentiation, survival, migration, and invasion (Courtneidge 2002; Caner, Asik, and Ozpolat 2021) (**Scheme 7**). Src activity is upregulated in several types of tumors, where it contributes to tumor progression by regulating the abovementioned processes and is, therefore, considered a proto-oncoprotein (Frame 2004; Frame 2002; Irby and Yeatman 2000; Kim, Song, and Haura 2009; Summy and Gallick 2003). In glioblastoma, c-Src itself and other Src family kinases (SFKs) are highly expressed and overactivated, representing a target for the inhibition of proliferation and migration in GSCs (Han, et al. 2014; Weissenberger, et al. 1997; Du, et al. 2009).
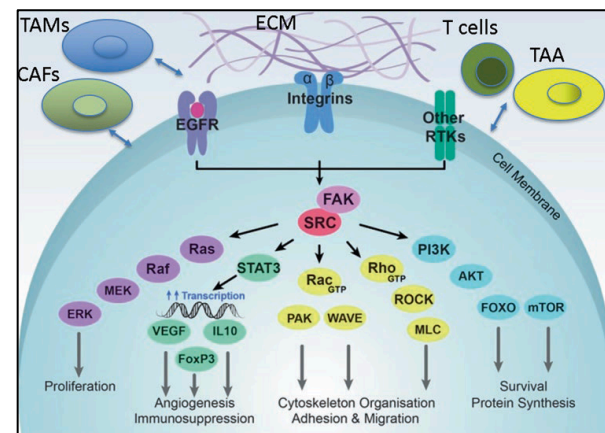
Scheme 7. Src signaling network. Taken from (Caner, Asik, and Ozpolat 2021). TAMs: tumor-associated microglia/macrophages, CAFs: cancer associated fibroblasts, ECM: extracellular matrix, TAA: tumor-associated astrocyte.

Importantly, Cx43 inhibits the oncogenic activity of Src in glioma cells and reverses the stem

cell phenotype (Herrero-González, et al. 2010; Gangoso, et al. 2014). As a tentative to benefit from the anti-tumor Src-inhibiting capacity of Cx43 without its pro-tumor functions, Tabernero and colleagues designed a cell-penetrating peptide (CPP) containing the sequence of Cx43 that interacts with Src (amino acids 266-283), including the SH3-binding motif, fused to the Tat sequence for its autonomous internalization into the cells (Vivès, Brodin, and Lebleu 1997). This peptide, termed Tat-Cx43$_{266-283}$, recruits Src together with its inhibitors Csk and PTEN and, in fact, inhibits Src in GSCs (Gangoso, et al. 2014; González-Sánchez, et al. 2016) (**Scheme 8**). Tat-Cx43$_{266-283}$ mimics the Src inhibitory function of Cx43 and reverses the stem cell phenotype through downregulation of two important transcriptional regulators, Sox-2 and Id1, and promotes N- to E-cadherin switch, reversing the epithelial-mesenchymal transition (Gangoso, et al. 2014). In addition, Tat-Cx43$_{266-283}$ impairs metabolic plasticity and autophagy in GSCs in a nutrient-context-independent way (Pelaz, et al. 2020; Pelaz, et al. 2021) and reduces migration and invasion through inhibition of the Src-FAK axis (Jaraíz-Rodríguez, et al. 2017b). Importantly, these anti-tumor effects have been confirmed in vivo and have been shown to be specific of GSCs, with no effects in healthy brain cells (Jaraíz-Rodríguez, et al. 2020; Pelaz, et al. 2020). Taking together all these considerations, Tat-Cx43$_{266-283}$ appears as a promising therapeutic strategy against glioblastoma.
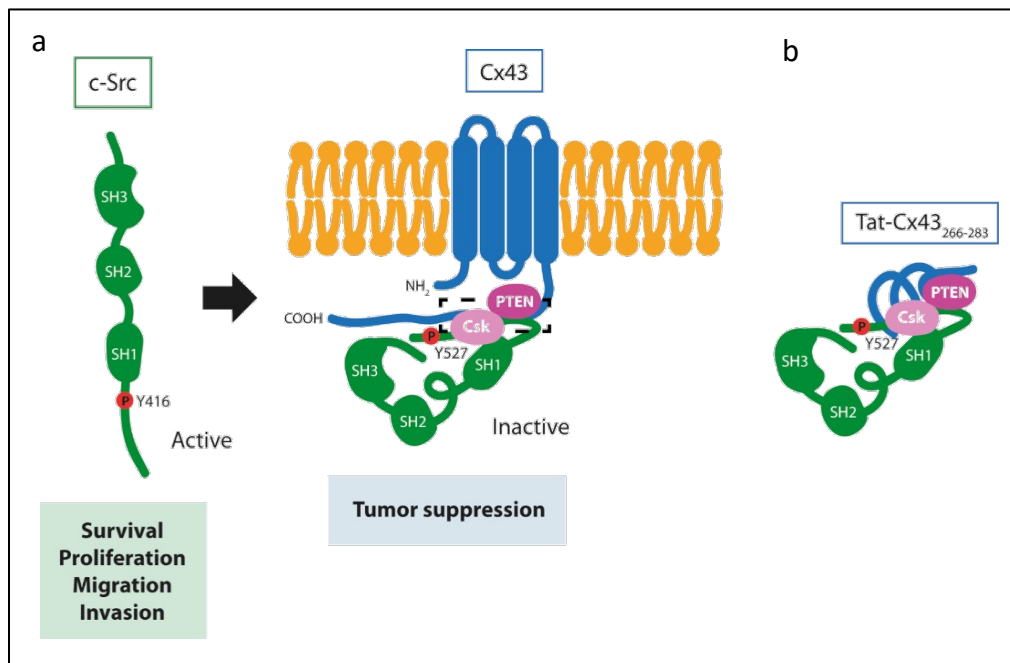
Scheme 8. Mechanism of action of Tat-Cx43$_{266-283}$. Mechanism of Src inhibition by **(a)** Cx43 and **(b)** Tat-Cx43$_{266-283}$.

OBJECTIVES

Objectives
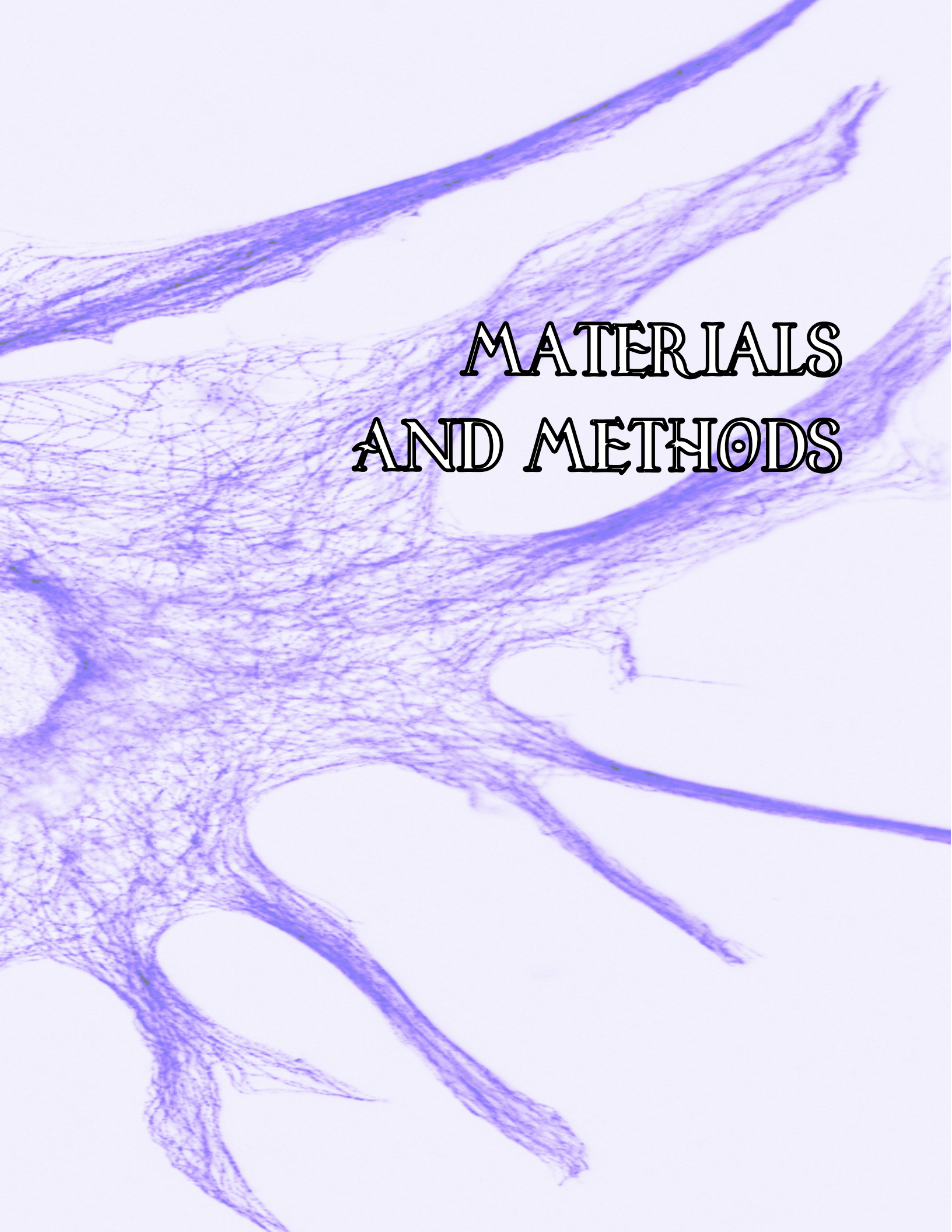
One of the hallmarks of glioblastoma is the presence in the tumor microenvironment of reactive astrocytes that promote tumor growth. Glioblastoma cells secrete factors that activate astrocytes, turning them into tumor-supportive and ultimately facilitating glioblastoma cell proliferation, migration, and invasion. Our group has previously shown that, through Src inhibition, Tat-Cx43$_{266-283}$ exerts an anti-tumorigenic effect and reduces proliferation, migration, and invasion of glioblastoma cells.

Given that Src is involved in the regulation of astrogliosis, and that Tat-Cx43$_{266-283}$ alters the phenotype of glioblastoma cells, we aimed to understand the impact of Tat-Cx43$_{266-283}$ on astrocyte activation and their crosstalk with glioblastoma cells.

The specific objectives of this Thesis were:

1. To explore the effect of Tat-Cx43$_{266-283}$ on reactive astrocytes.
2. To set up an in vivo model to study the glioblastoma tumor microenvironment.
3. To study the impact of Tat-Cx43$_{266-283}$ on the communication between glioblastoma cells and tumor-associated astrocytes in a physiological context.
4. To deepen our understanding of an immunocompetent syngeneic glioblastoma model through single-cell genomics.

MATERIALS AND METHODS

Materials and methods

Materials

Reagent or resource	Source	Identifier
ANTIBODIES		
Alpha actinin	Millipore	1682
Alpha tubulin	Sigma-Aldrich	#T9026
BDNF	Icosagen	327-100
Beta actin	Sigma-Aldrich	A5441
Beta catetin	BD	610153
Beta III tubulin	Covance	MMS-435P
Cx43	BD	610062
Cx43	Invitrogen	71-0700
ERK p42-p44	Cell signaling	#9102S
ERK phospho-T202-Y204	Cell signaling	#9106S
GAPDH	Applied Biosciences	AM4300
GFAP	Sigma-Aldrich	G3893
GFAP	Sigma-Aldrich	G9269
GFAP-AlexaFluor 488	ThermoFisher Scientific	53-9892-82
Goat anti-Mouse IgG (H+L) Cross-Adsorbed Secondary Antibody, Alexa Fluor™ 647	ThermoFisher Scientific	A-21235
Goat anti-Mouse IgG (H+L) Highly Cross-Adsorbed Secondary Antibody, Alexa Fluor™ 488	ThermoFisher Scientific	A-11029

Goat anti-Mouse IgG (H+L) Highly Cross-Adsorbed Secondary Antibody, Alexa Fluor™ 594	ThermoFisher Scientific	A-11032
Goat anti-Rabbit IgG (H+L) Cross-Adsorbed Secondary Antibody, Alexa Fluor™ 750	ThermoFisher Scientific	A-21039
Goat anti-Rabbit IgG (H+L) Cross-Adsorbed Secondary Antibody, Alexa Fluor™ 647	ThermoFisher Scientific	A21244
Goat anti-Rabbit IgG (H+L) Cross-Adsorbed Secondary Antibody, Alexa Fluor™ 594	ThermoFisher Scientific	A-11012
Goat anti-Rabbit IgG (H+L) Highly Cross-Adsorbed Secondary Antibody, Alexa Fluor™ 488	ThermoFisher Scientific	A-11034
Id1	Santa Cruz Biotechnology	sc-488
ITGA7	ThermoFisher Scientific	15947434
Laminin	Sigma-Aldrich	L939
Map2	Sigma-Aldrich	#M1406
MBP	Santa Cruz Biotechnology	271524
MMP2	Santa Cruz Biotechnology	13595
N-cadherin	Santa Cruz Biotechnology	sc-7939
Nestin	Santa Cruz Biotechnology	sc-377-380
NeuN	Millipore	MAB377
NG2	Millipore	AB5320
P21	BD	556431
PCNA	GeneTex	GTX20029
PD-L1/CD274	Proteintech	66248-1-Ig
Peroxidase-conjugated Goat Anti-Mouse IgG (H+L)	Jackson ImmunoResearch	115-035-003

Peroxidase-conjugated Goat Anti-Rabbit IgG (H+L)	Jackson ImmunoResearch	111-035-003
RPL19	Santa Cruz Biotechnology	sc-100830
Sox2	Abcam	Ab97597
Src	Cell Signaling	#2110
Src phospho-Y 416	Cell Signaling	#2101
STAT3 alpha	Cell Signaling	#8768
STAT3 phospho-S 727	Santa Cruz Biotechnology	136193
STAT3 phospho-Y 705	Cell Signaling	#9145
TrkB	BD	610102

CHEMICALS

100 bp DNA Ladder	ThermoFisher Scientific	15628019
2-Mercaptoethanol	Gibco	31350-010
2-propanol, minimum 99%	Sigma-Aldrich	I9516
50 bp DNA Ladder	ThermoFisher Scientific	11518626
Accutase	ThermoFisher Scientific	00-4555-56
Amphotericin B	Sigma-Aldrich	A9528
Animal Free Recombinant Human EGF	PeproTech	AF-100-15
B-27 supplement	Invitrogen	17504-044
Bovine Albumin Fraction V	Gibco	15260-037
Bradford Reagent	Bio-Rad	500-006
Brain-derived neurotrophic factor	Sigma-Aldrich	B3795
Cell culture inserts	Millipore	PICM03050
Chloroform, minimum 99%	Sigma-Aldrich	C2432
Clodronate liposomes	Liposoma	SKU: C-005
Cy2-conjugated streptavidin	Jackson Immunoresearch	016-220-084

Cytosine-β-arabinofuranoside	Sigma-Aldrich	C6645
Dasatinib	Selleck Chemicals	S1021
dATP	Invitrogen	55082
dCTP	Invitrogen	55083
dGTP	Invitrogen	55084
Dimethyl sulfoxide for UV-spectroscopy, ≥99.8%	Sigma-Aldrich	41641
DMEM	Sigma-Aldrich	D5523
DMEM/Nutrient Mixture F-12 Ham	Sigma-Aldrich	D6421
DNase I grade II	Roche	10104159001
dTTP	Invitrogen	55085
Fetal calf serum	Gibco	N/A
High Sensitivity D5000 Reagents	Agilent	5067-5593
High Sensitivity D5000 ScreenTape	Agilent	5067-5592
Horse serum	Thermofisher Scientific	26050088
iBlot 2 NC Regular Stacks	ThermoFisher Scientific	IB23001
IGEPAL® CA-630	Sigma-Aldrich	I8896
Kapa Library Quantification Kit	Roche	07960140001
Laminin I	R&D Systems	446-005-01
Lipofectamine 2000	Invitrogen	11668-019
MEM Non-Essential Amino Acids	ThermoFisher Scientific	11140050
N-2 supplement	Invitrogen	17502-048
NuPAGE™ Antioxidant	ThermoFisher Scientific	NP0005
NuPAGE™ MOPS SDS Running Buffer	ThermoFisher Scientific	NP0001

NuPAGE™ Novex Bis-Tris (4-12%) midigels	ThermoFisher Scientific	WG1402BOX
NuPAGE™ Transfer Buffer	ThermoFisher Scientific	NP00061
Opti-MEM™ I Reduced Serum Medium, no phenol red	ThermoFisher Scientific	11058021
PCR master mix	Promega	M750B
Penicillin G	Sigma-Aldrich	P3032
Pierce™ BCA Protein Assay Kit	ThermoFisher Scientific	23227
PKH26 Red Fluorescent Cell Linker	Sigma-Aldrich	MINI26-1KT
Poly-L-lysine hydrobromide	Sigma-Aldrich	P1524-25MG
Ponceau solution	Sigma-Aldrich	P7170
Precision Plus Protein Dual Color Standards	Bio-Rad	161-0374
Protease Inhibitor Cocktail Set III	Calbiochem	539134
Random hexamer primers	Invitrogen	48190011
Recombinant Human FGF-basic	PeproTech	100-18B
RNAsin® Ribonuclease Inhibitor	Promega	N2511
Ruxolitinib	MedChemExpress	HY-50856
Silencer™ Negative Control No. 1 siRNA	ThermoFisher Scientific	AM4635
SlowFade® Gold antifade reagent	Invitrogen	S36936
Sodium orthovanadate	Merck Milipore	567540
Stat3 siRNA	Santa Cruz Biotechnology	sc-270027
Streptomycin	Sigma-Aldrich	S9137

SuperScriptII Reverse Transcriptase	Invitrogen	18064014
Syber Safe DNA gel stain	Invitrogen	S33102
Tat peptide	GenScript	N/A
Tat-Cx43$_{266-283}$ peptide	GenScript	Patent ID: WO2014191608A1
Trizol reagent	Invitrogen	15596-026
Trypsin/EDTA	Invitrogen	25300-062
Turbo DNA-Free Kit	Invitrogen	AM1907
Tween 20	Fisher	BP337-500
Western blotting luminol reagent	Santa Cruz Biotechnology	sc-2048
X-Gal	Eppendorf	0032006.400
COMMERCIAL ASSAYS		
Chromium Single Cell Multiome ATAC + Gene Expression	10x Genomics	https://www.10xgenomics.com/products/single-cell-multiome-atac-plus-gene-expression
GemCode Single-Cell 5' Bead and Library kit	10x Genomics	https://www.10xgenomics.com/support/single-cell-immune-profiling
ANIMALS		
C57BL/6	Charles River	N/A
NOD-SCID	Charles River	N/A
WISTAR	SEA-USAL	N/A
CELL LINES		
G166	BioRep	RRID: CVCL_DG66
GL261	DSMZ	RRID: CVCL_Y003
RECOMBINANT DNA		
pcDNA mCherry	C. Naus	Addgene_128744

OLIGONUCLEOTIDES		
Primers for RT-PCR	Sigma-Aldrich	See **Table 5**

EQUIPMENT		
4150 TapeStation System	Agilent	https://www.agilent.com/en/product/automated-electrophoresis/tapestation-systems
AATI Fragment Analyzer	Agilent	https://www.agilent.com/en/product/automated-electrophoresis/fragment-analyzer-systems
C1000 Touch Thermal	Biorad	https://www.bio-rad.com/es-es/product/c1000-touch-thermal-cycler?ID=LGTW9415
Chromium controller	10x Genomics	https://www.10xgenomics.com/instruments/chromium-controller
Countess Automatic Cell Counter	ThermoFisher Scientific	https://www.thermofisher.com/es/es/home/life-science/cell-analysis/cell-analysis-instruments/automated-cell-counters.html
MicroChemi imaging system	Bioimaging Stystems	https://dnr-is.com/products/microchemi/
Nanodrop 2000 Spectrophotometer	ThermoFisher Scientific	https://www.thermofisher.com/order/catalog/product/ND-2000
NextSeq 2000 Sequencing System	Illumina	https://www.illumina.com/systems/sequencing-platforms/nextseq-1000-2000.html
NovaSeq 6000 Sequencing system	Illumina	https://www.illumina.com/systems/sequencing-platforms/novaseq.html
SH800S cell sorter	Sony	https://www.sonybiotechnology.com/us/instruments/sh800s-cell-sorter/
Stellaris 8 Confocal Microscope	Leica Microsystems	https://www.leica-microsystems.com/c/em/lsr-c/confocal-microscopy-reimagined/

Zeiss Axio Observer Z1 microscope for Live-Cell Imaging	Carl Zeiss Microscopy	https://www.zeiss.com/microscopy/en/products/light-microscopes/widefield-microscopes/axio-observer-for-life-science-research.html
SOFTWARE AND ALGORITHMS		
Leica Application Suite X	Leica Microsystems CMS GmbH	https://www.leica-microsystems.com/de/produkte/mikroskop-software/p/leica-las-x-ls/
Enrichr	(Chen, et al. 2013)	https://maayanlab.cloud/Enrichr/
GSEApy	Z. Fang	https://gseapy.readthedocs.io/en/latest/
ImageJ2 v2.3.0	ImageJ2 Team, 2017	https://imagej.net/
bcl2fastq v2.19.0.316	Illumina	https://emea.support.illumina.com/sequencing/sequencing_software/bcl2fastq-conversion-software/downloads.html
Scanpy Python package v.1.4.2	(Wolf, Angerer, and Theis 2018)	https://scanpy.readthedocs.io/en/stable/
STAR v2.5.2b	(Dobin, et al. 2013)	https://github.com/alexdobin/STAR
HTSEQ v0,6,1p1	(Putri, et al. 2022)	https://htseq.readthedocs.io/en/master/
CellRanger v2.0.1	10x Genomics	https://support.10xgenomics.com/single-cell-gene-expression/software/overview/welcome
Zen Blue 3.5	Zeiss	https://www.zeiss.com/microscopy/int/products/microscope-software/zen.html
GraphPad Prism v9.0.1	GraphPad Software	https://graphpad.com/
Wound-healing tool for Fiji	MRI	https://github.com/MontpellierRessourcesImagerie/imagej_macros_and_scripts/wiki/Wound-Healing-Tool

Experimental methods

Animals

Albino Wistar rats were obtained from the animal facility of the University of Salamanca (Servicio de Experimentación Animal, SEA). NOD/SCID mice and C57BL/6 mice were shipped from Charles River to the animal facility of the University of Salamanca at INCYL (SEA-INCYL). At all locations, animals were housed on a 12h/12h light/dark cycle and provided with food and water ad libitum. Mice were maintained singly from the start of the experiments, and were monitored for signs of humane endpoints daily, including changes in behavior and weight. All animal procedures were approved by the ethics committee of the University of Salamanca and the Junta de Castilla y León and were carried out in accordance with European Community Council directives (2010/63/UE), and Spanish law (RD 53/2013 BOE 34/11370–420, 2013) for the use and care of laboratory animals.

Cells

G166 human GSCs were obtained from BioRep (Okawa, et al. 2017). GL261 mouse glioma cells were obtained from DSMZ.

Human GSCs were cultured in adherent conditions (Pollard, et al. 2009; Jaraíz-Rodríguez, et al. 2017b), in stem cell medium containing Dulbecco's modified Eagle's medium (DMEM)/Nutrient Mixture F-12 Ham supplemented with 1% Minimum Essential Medium-Non-Essential Amino Acids (MEM-NEAA), 3.9 mM glucose, 1 mM L-glutamine, 0.07% β-mercaptoethanol, 121.8 μg/mL bovine serum albumin (BSA), 1% B-27 supplement, 0.5% N-2 supplement, 10 ng/ml epidermal growth factor (EGF) , and 10 ng/ml basic fibroblast growth factor (b-FGF). 4 μg/ml laminin was added to the culture medium to promote cell adherence to the culture surface. Cells were grown to confluence, dissociated using Accutase, and then split to convenience. Cells were counted using a Countess Automatic Cell Counter, using specific protocols for cell shape and size. Cells were observed using an inverted microscope and we routinely used cultures expanded for no more than 15 passages.

GL261 cells were grown adherently (GL261-AC) in differentiation medium containing DMEM supplemented with 10% fetal calf serum (FCS), dissociated using trypsin/EDTA, and split to convenience. Neurospheres (GL261-NS) were obtained from GL261 adherent cultures as previously described (Yi, et al. 2013) and cultured in stem cell medium. Neurospheres were dissociated using Accutase and subcultured at a density of 10^4 cells/ml every 8-10 days. For differentiation studies, neurospheres were cultured in differentiation medium for the indicated times.

All culture media were supplemented with 50 U/ml penicillin G, 37.5 U/ml Streptomycin and 0.23 μg/ml Amphotericin B to avoid bacterial and fungal contamination. Cells were maintained at

37°C in an atmosphere of 95% air/5% CO_2 and with 90-95% humidity.

GL261 cells and G166 GSCs were stably transfected with pcDNA3.1-mCherry plasmid (a kind gift from C. Naus) using Lipofectamine 2000 Transfection Reagent according to manufacturer's instructions. Cells were plated at low density and mCherry+ colonies were selected and amplified.

For the indicated experiments, G166 cells were labeled with 2 µL/ml PKH26 (Red Fluorescent Cell kit) following manufacturer instructions.

Astrocyte cultures

Primary astrocyte cultures were prepared from the forebrains of 1-2-day-old Wistar rats or C57BL/6 mice as previously described (Tabernero, Orfao, and Medina 1996). Briefly, animals were decapitated, and their brains immediately excised. After removing the meninges and blood vessels, the forebrains were placed in Earle's balanced solution (EBS) containing 20 µg/ml DNase I, and 0.3% (w/v) BSA. The tissue was minced, washed, centrifuged, and incubated in 0.025% trypsin and 60 µg/ml DNase I for 15 minutes at 37 ℃. Trypsinization was terminated by the addition of DMEM containing 10% FCS. The tissue was then dissociated by passing it through a cell strainer and the resulting cell suspension was centrifuged. The cells were then resuspended in DMEM containing 10% FCS and plated on Petri dishes coated with 10 mg/ml poly-L-lysine hydrobromide at a density of 10^5 cells/cm².

Except otherwise stated, cytosine-β-arabinofuranoside was added to the culture medium of confluent astrocytes of at least 10 DIV for 72 hours to avoid microglia proliferation. Where indicated, 5 mg/ml clodronate liposomes were added to the culture medium of astrocytes for 72 hours.

For astrocyte-GSC co-cultures, GSCs were plated on confluent astrocytes of at least 21 DIV. Co-cultures were maintained for the indicated times in differentiation medium, stem cell medium or a combination. Human G166-GSCs were plated on top of rat astrocytes and GL261-GSCs were plated on top of mouse astrocytes.

Organotypic Brain Slice Cultures

Organotypic brain slice cultures were prepared as described (Polo-Hernández, et al. 2010). 350-µm-thick brain slices were obtained from 1-2-day-old Wistar rats and cultured onto cell culture inserts for 19–20 days in organotypic medium containing DMEM supplemented with 10% horse serum and glucose (33 mM final concentration).

For GSC-organotypic brain slice co-cultures, 2,500 PKH26-labeled G166-GSCs were placed onto each brain slice and allowed to engraft for 2 days prior to the experiment. GSC-organotypic brain slice co-cultures were maintained in organotypic or stem cell medium, as indicated.

Intracranial implantation of glioma cells

mCherry-GL261-GSCs were injected into 8-week-old C57BL/6 mice. An equal number of males and females was used.

Mice were anesthetized by isoflurane inhalation, placed on a stereotaxic frame, and window-trephined in the parietal bone. A unilateral intracerebral injection to the right cortex was performed with a Hamilton microsyringe. 1 µl of physiological saline containing 5,000 cells was injected at the following coordinates: 1 mm rostral to lambda, 1 mm lateral, and 2 mm deep. To minimize the inflammatory response from damaged brain tissue due to the needle injection, tumoral cells were slowly injected into the brain and the needle was held in place for an additional 2 minutes before removal. Cellular suspensions were kept on ice while the surgery was being performed and allowed to temperate for five minutes once loaded into the microsyringe.

At the indicated times, mice were anesthetized with pentobarbital (120 mg/kg, 0.2 ml) and transcardially perfused with 15 ml of physiological saline followed by 25 ml of 4% paraformaldehyde in 0.1 M phosphate buffer (pH 7.4). Brains were removed and cryoprotected by immersion in a solution of 30% sucrose in phosphate buffered saline (PBS) until they sank. Then, 20-40 µm-thick coronal sections were obtained with a cryostat to be processed for immunostaining. For STAT3 immunofluorescence and single cell studies, mice were perfused with physiological saline only and brains were snap-frozen in liquid nitrogen for 10 min and kept at -80 ºC. Sections were obtained and fixed with 4% paraformaldehyde for 25 minutes at room temperature.

Tissue dissociation and sample preparation for single-cell experiments

A tissue piece was collected from each brain (see Results **Fig. 20**). Mice samples were kept blinded during experimental handling and QC.

Each sample included tumor core and peritumoral space. Nuclei suspensions from frozen tissue were obtained using a density gradient medium as described (https://www.protocols.io/view/nuclei-isolation-prep-and-protocol-5qpvoneedl4o/v1). Tissue pieces were mechanically digested in ice-cold buffer containing protease and RNAse inhibitors using a Dounce homogenizer and incubated in 0.35% IGEPAL® CA-630. Homogenized solutions were filtered using a 40 µm-pore cell strainer and carefully added to ultracentrifuge tubes with layered 40% and 30% Iodixanol solutions. Tubes were centrifuged at 10,000 *g* for 18 minutes and nuclei were collected from the interface between 40% and 30% Iodixanol solutions.

Nuclei suspensions from fresh cells were obtained following 10xGenomics protocol (https://www.10xgenomics.com/products/nuclei-isolation). Cells and neurospheres were

dissociated using Accutase and lysed in lysis buffer containing 0.3% IGEPAL® CA-630.

Nuclei were counted using a Countess Automated Cell Counter and nuclei quality was assessed in an inverted microscope. Cells and nuclei were loaded with a target output of 6,000 nuclei per sample.

Treatments

Synthetic peptides (>85% pure) were obtained from GenScript. YGRKKRRQRRR was used as the Tat sequence, which enables the cell penetration of peptides. The Tat-Cx43$_{266-283}$ sequence was Tat-AYFNGCSSPTAPLSPMSP (patent ID: WO2014191608A1). Tat-Cx43$_{266-283}$-B has a biotin molecule fused at its C-terminus.

For in vitro and ex vivo studies, the peptides were used at 50 or 100 μM as indicated, in culture medium at 37°C for the indicated times. For in vivo studies, 100 μM Tat or 100 μM Tat-Cx43$_{266-283}$ was intracranially injected in 1 μl of physiological saline together with the cells. For 28 day and survival experiments, 4 nmol/g Tat or Tat-Cx43$_{266-283}$ was intraperitonially injected twice per week, starting on day 8 and until the end of the experiment. An equivalent amount of saline was injected to control mice.

1 μM of Src inhibitor dasatinib 1 μM of Jak inhibitor ruxolitinib, or 0.1% (v/v) DMSO (vehicle) were added to the culture media at 37°C for the indicated times.

Laminin was added to the culture medium at 37°C for the indicated times at 4 μl/ml or the indicated concentration. Where indicated, 10 μg/ml anti-β1-integrin was added to the culture medium 30 minutes before.

Immunofluorescence

Cells and spheres were fixed in 4% (w/v) paraformaldehyde for 15 minutes at room temperature, rinsed in PBS and incubated for 1 hour in blocking/permeabilizing solution (PBS containing 10% FCS, 0.1 M lysine, 0.02% sodium azide, and 0.1% Triton X-100). Organotypic brain slices were fixed in 4% (w/v) paraformaldehyde for 25 minutes at room temperature, rinsed in PBS and incubated in blocking/permeabilizing solution for 24 hours at 4°C. For in vivo studies, sections were rinsed in PBS and incubated for 2 hours in BSA-blocking/permeabilizing solution (PBS containing 1% BSA, 0.02% sodium azide, and 0.2% Triton X-100). For STAT3 staining, cells and slices were incubated in 100% methanol for 20 minutes at -20°C to permeabilize cell membranes.

Samples were incubated overnight at 4°C with the indicated primary antibody (Table 1), washed, and incubated for 75 minutes (cells, spheres and organotypic brain slices) or 2 hours (brain sections) with the corresponding fluorophore-conjugated secondary antibody (Table 2) at room temperature. Antibodies were prepared in blocking/permeabilizing solution. For STAT3 immunofluorescence, samples were incubated for at least 48 hours at 4°C. Nuclear DNA was stained with 1 μg/ml DAPI for 4 minutes or TO-PRO™-3 Iodide for 10 minutes.

Protein	Host	Concentration
β-catetin	Mouse	1:400
GFAP	Mouse	1:500
GFAP	Mouse	1:500
Map2	Mouse	1:500
N-cadherin	Rabbit	1:200
Sox2	Rabbit	1:500
Src		
STAT3 alpha	Rabbit	1:400
STAT3 phospho-Y705	Rabbit	1:100
α-tubulin	Mouse	1:500

Table 1. Primary antibodies used for immunofluorescence.

Protein	Host	Fluorophore	Concentration (cells/slices)
Rabbit IgG	Goat	Alexa Fluor 750	1:1000/1:500
Rabbit IgG	Goat	Alexa Fluor 647	1:1000/1:500
Rabbit IgG	Goat	Alexa Fluor 594	1:1000/1:500
Rabbit IgG	Goat	Alexa Fluor 488	1:1000/1:500
Mouse IgG	Goat	Alexa Fluor 647	1:1000/1:500
Mouse IgG	Goat	Alexa Fluor 594	1:1000/1:500
Mouse IgG	Goat	Alexa Fluor 488	1:1000/1:500

Table 2. Secondary antibodies used for immunofluorescence.

For Tat-Cx43$_{266-283}$-B internalization experiments, samples were incubated with 3.6 µg/ml Cy2-Streptavidin for 75 minutes (Jaraíz-Rodríguez, et al. 2017a).

Samples were mounted using SlowFade™ Gold Antifade Mountant and imaged on an inverted Zeiss Axio Observer Z1 microscope for Live-Cell Imaging coupled to an Axio-Cam MRm camera and Zeiss Apotome (optical sectioning structured illumination microscopy; https://www.zeiss.com/microscopy/int/solutions/reference/all-tutorials/optical-sectioning/apotome-operation.html), or a Stellaris 8

48

Confocal Microscope with a pinhole aperture of 1 Airy Unit.

MTT Assay

Cells and neurospheres were incubated in culture medium containing 0.5 mg/ml MTT for 75 minutes. Medium was removed and DMSO was added and incubated for 10 minutes in the dark with mild shaking. Neurospheres were spined-down before removing the medium. The absorbance at 570 nm was measured using a microplate reader.

SA-β-Gal assay

Senescence-associated (SA)-β-Gal was assayed as previously described (Debacq-Chainiaux, et al. 2009). Briefly, cells were fixed in 4% (w/v) paraformaldehyde for 5 minutes at room temperature, rinsed in PBS and incubated in staining solution (40 mM citric acid/Na phosphate buffer, 5 mM $K_4[Fe(CN)_6]3H_2O$, 5 mM $K_3[Fe(CN)_6]$, 150 mM sodium chloride, 2 mM magnesium chloride and 1 mg/ml X-gal in distilled water), for 24 hours at 37ºC and no CO_2. After the staining, cells were washed with PBS and viewed by bright microscopy, and the number of blue (SA-β-Gal^{+}) cells was counted.

Wound-healing assay

A scratch was inflicted to confluent astrocyte monolayers using a 200 μl pipette tip. Then, the corresponding treatment was added. Phase-contrast photomicrographs were taken at 0, 2, 6, 20, 24, and 48 hours after the scratch was made on a Leica inverted fluorescence microscope connected to a digital video camera (Leica DC 100). Images were analyzed using the MRI wound-healing tool for Fiji to detect the cell-free gap area.

Protein extraction and quantification

Cells were washed with PBS and lysed in lysis buffer (5 nM Tris-HCl, pH 6.8; 2% SDS (w/v); 2 mM EDTA; 2 mM EGTA; 1 mM PMSF; 0.1% NaF; 0.1% sodium orthovanadate; 1 μl/ml (v/v) Protease Inhibitor Cocktail Set III). Lysates were heated for 5 minutes at 99ºC, sonicated for 5 minutes, and centrifuged at 14,000 x g for 15 minutes. The amount of protein present in each sample was quantified using Bradford Assay or Pierce™ BCA Protein Assay Kit, following manufacturer's instructions.

Lysates were mixed with Laemli buffer (0.18 M Tris-HCl, pH 6,8; 5 M glycerol; 3.7% (w/v) SDS; 0.6 M β-mercaptoethanol or 9 mM DTT; 0.04% (v/v) bromophenol blue) at a 3:1 ratio. Lysates were kept at -80ºC or at -20ºC once mixed with Laemli buffer.

Western blotting

Western blotting was performed as previously described (Herrero-González, et al. 2010). Briefly, equivalent amounts of proteins were separated on NuPAGE™ Novex Bis-Tris (4-12%) midigels using NuPAGE™ MOPS SDS Running Buffer.

Electrophoresis was performed at a constant voltage between 90 and 120 V. Nitrocellulose membranes were equilibrated in NuPAGE transfer buffer with 10% (v/v) methanol and proteins were transferred using an iBlot dry blotting system with a constant voltage of 23 V for 6 minutes.

Membranes were blocked for 1 hour in 20 mM Tris-buffered saline buffer (TBS, pH 7.5) with 1% Tween, and 5% (w/v) nonfat dry milk and incubated overnight at 4ºC with the primary antibodies (Table 3) prepared in TBS with 1% Tween. After extensive washing, the membranes were incubated with the corresponding peroxidase-conjugated secondary antibodies (Table 4) and developed with a chemiluminescent substrate in a MicroChemi imaging system. Densitometry analysis of the bands was performed using Fiji software. Whole membranes were incubated with 10% (v/v) Ponceau red was used to determine the total amount of protein loaded. Molecular weight was determined by comparison with the Precision Plus Protein Dual Color Standards.

Protein	Host	Concentration
β-actin	Mouse	1:5000
α-actinin	Mouse	1:1000
Akt	Rabbit	1:1000
Akt phospho-S473	Rabbit	1:2000
β-catetin	Mouse	1:1000
Cx43	Mouse	1:200
Erk	Rabbit	1:1000
Erk phospho-T202-Y204	Mouse	1:500
GAPDH	Mouse	1:5000
GFAP	Mouse	1:500
GFAP	Rabbit	1:1000
Id1	Rabbit	1:500
IL-6	Mouse	1:100
Laminin	Rabbit	1:1000
Map2	Mouse	1:1000
N-cadherin	Rabbit	1:500
NG2	Rabbit	1:250
PD-L1/CD274	Mouse	1:5000
PCNA	Mouse	1:200

PTEN	Mouse	1:500	
Sox2	Rabbit	1:500	
Src	Rabbit	1:500	
Src phospho-Y416	Rabbit	1:250	
STAT3 alpha	Rabbit	1:2000	
STAT3 phospho-Y705	Rabbit	1:2000	
STAT3 phospho-S727	Mouse	1:200	
α-tubulin	Mouse	1:5000	
βIII-tubulin	Mouse	1:1000	
MMP2	Mouse	1:500	
MBP	Mouse	1:100	
Nestin	Mouse	1:100	
NeuN	Mouse	1:1000	
MGMT	Mouse	1:1000	

Table 3. Primary antibodies used for western blotting.

Protein	Host	Concentration
Mouse IgG	Goat	1:2500
Rabbit IgG	Goat	1:5000

Table 4. Secondary antibodies used for western blotting.

RNA extraction

RNA was extracted from cells or brains using Trizol Reagent according to manufacturer's instructions. Briefly, 0.2 chloroform volume was added to each Trizol volume and tubes were vigorously agitated for 15 seconds and incubated for 3 minutes. Samples were then centrifuged at 12,000 x g for 15 minutes. The upper aqueous phase was collected and 0.5 volumes of isopropyl were added to precipitate RNA. Supernatant was removed and precipitated RNA was washed with 1 volume of 75% (v/v) ethanol. Samples were then centrifuged for 5 minutes at 7,500 x g at 4ºC. Precipitated RNA was dissolved in DEPC H_2O for 10 minutes at 55ºC. 0.05 volumes of Rnasin® Ribonuclease Inhibitor per final volume of resuspended RNA was added. Genomic DNA was removed using Turbo DNA-Free Kit, according to manufacturer's instructions. Samples were kept at -80ºC. RNA was quantified in a Nanodrop 2000.

RT-PCR

cDNA was obtained from mRNA using SuperScriptII Reverse Transcriptase, following

manufacturer's instructions. Briefly, 1 µg RNA was mixed with 200 ng random hexamer primers in a final volume of 11 µl DEPC-H_2O and incubated for 10 minutes at 70ºC, followed by 2 minutes on ice. Then, a mix of 10 mM deoxyribonucleotides (dNTPs), 1 µl RNAsin® Ribonuclease Inhibitor, 2 µl DTT, and 0.66 µl transcriptase was added. Volume was completed to 20 µl with DEPC H_2O. The cycling conditions for RT-PCR were: 20ºC for 10 minutes, 42ºC for 45 minutes, 99ºC for 5 minutes.

cDNA from mRNAs of interests was PCR-amplified using specific oligonucleotides (**Table 5**). 200 µg cDNA was mixed with the corresponding oligonucleotides (1 µM final concentration), 12.5 10 µl PCR master mix, and DEPC H_2O to a final volume of 25 µl. The cycling conditions for amplification were: 94°C for 5 min; 94°C for 30 s, 59°C for 45 s, 72ºC for 60 s for 40 cycles; 72 °C for 5 min. PCR products were separated on a 2.5 % (w/v) agarose gel containing Syber Safe DNA gel stain and visualized by UV-illumination. Gels were made and run in Tris-borate-EDTA (TBE) buffer. Molecular size was determined by comparison with the 50 bp or the 100 bp DNA Ladder.

Transcript	Sequences
TrkB.FL (mouse)	Common forward: AGCAATCGGGAGCATCTCT Reverse: CTGGCAGAGTCATCGTCGT
TrkB.T1 (mouse)	Common forward: AGCAATCGGGAGCATCTCT Reverse: TACCCATCCAGTGGGATCTT
TrkB.T2 (mouse)	Common forward: AGCAATCGGGAGCATCTCT Reverse: TCATGAGCCAAAAATGAGTCC
Bdnf (mouse)	Forward: CGACATCACTGGCTGACACT Reverse: CAAAGGCACTTGACTGCTGA
Ntf5 (mouse)	Forward: TGGCTCATCAAAACGGACGA Reverse: CAGATGAGTACCACCGTGCA
Gapdh	Forward: ATCCTGCACCACCAACTGCT Reverse: GGGCCATCCACAGTCTTCTG

Table 5. Oligonucleotides used for PCR-amplification. FL: full-length, T1: truncated isoform 1, T2: truncated isoform 2.

siRNA transfection

18-21 DIV astrocytes were transfected with 50 nM validated non-targeting siRNA or with a pool of 3 STAT3-specific siRNA. siRNAs were diluted in Opti-MEM™, incubated for 5 minutes, and mixed with 2.5 µl/ml Lipofectamine 2000 Transfection Reagent diluted in OptiMEM™

medium, according to the manufacturer's instructions. Mix was performed drop by drop with gentle vortex agitation and incubated for an additional 20 minutes. Culture medium was replaced with antibiotic-free medium and 200 µl/ml mix was gently added drop by drop to minimize breakage of the complexes. Medium containing siRNAs was replaced with antibiotic-containing fresh medium 8 hours after transfection. The reduction in protein expression was assessed by western blot.

FACS sorting

All protocols used in this study are described in detail elsewhere (Consortium 2018), including preparation of lysis plates, FACS sorting, cDNA synthesis using the Smart-Seq2 protocol (Darmanis, et al. 2015; Picelli, et al. 2013), library preparation using an in-house version of Tn5 (Hennig, et al. 2018; Picelli, et al. 2014), library pooling and quality control, and sequencing. For further details please refer to https://doi.org/10.17504/protocols.io.2uwgexe.

Single-cell suspensions were sorted by a SONY SH800 Cell Sorter. All events were gated with forward scatter-area (FCS-A)/side scatter-area (SSC-A) and FCS-height (FCS-H)/FCS-width (FCS-W). Single cells were sorted in 96-well plates containing 4 µL lysis buffer (4U Recombinant RNase Inhibitor, 0.05% Triton X-100, 2.5 mM dNTP mix, 2.5 µM Oligo-dT30VN (5′-AAGCAGTGGTATCAACGCAGAGTACT30V

N-3′), spun down for 2 min at $1,000 \times g$, and snap frozen. Plates containing sorted cells were stored at −80°C until processing.

Reverse transcription and PCR amplification were performed according to the Smart-seq2 protocol described previously (Picelli, et al. 2013). In brief, 96-well plates containing single-cell lysates were thawed on ice followed by incubation at 72°C for 3 min and placed immediately on ice. Reverse transcription was carried out after adding 6 µL of reverse transcription-mix (100 U SMARTScribe Reverse Transcriptase (Takara Bio), 10 U Recombinant RNase Inhibitor (Takara Bio), 1× First-Strand Buffer (Takara Bio), 8.5 mM DTT (Invitrogen), 0.4 mM betaine (Sigma), 10 mM $MgCl_2$ (Sigma), and 1.6 µM TSO (5′-AAGCAGTGGTATCAACGCAGAGTACATrG rG+G-3′) for 90 min at 42°C, followed by 5 min at 70°C. Reverse transcription was followed by PCR amplification. PCR was performed with 15 µL PCR mix (1× KAPA HiFi HotStart ReadyMix), 0.16 µM ISPCR oligo (5′-AAGCAGTGGTATCAACGCAGAGT-3′), and 0.56 U Lambda exonuclease according to the following thermal-cycling protocol: (1) 37°C for 30 min; (2) 95°C for 3 min; (3) 21 cycles of 98°C for 20 s, 67°C for 15 s, and 72°C for 4 min; and (4) 72°C for 5 min. PCR was followed by bead purification using 0.7× AMPure beads, capillary electrophoresis, and smear analysis using a Fragment Analyzer. Calculated smear concentrations within the size range of 500 and 5,000 bp for each single cell were used to dilute

samples for Nextera library preparation as described previously (Darmanis, et al. 2015).

Microfluidic droplet single-cell analysis

Single cells or nuclei were captured in droplet emulsions using the Chromium instrument (10x Genomics) and scRNA-seq libraries were constructed as per the 10x Genomics protocol using GemCode Single-Cell 5' Bead and Library kit. Single nuclei were processed using the 10x Multiome ATAC + Gene Expression kit.

All reactions were performed in the Biorad C1000 Touch Thermal cycler with 96-Deep Well Reaction Module. The number of cycles used for cDNA amplification and sample index PCR was determined following 10x guidelines. Amplified cDNA and final libraries were evaluated on a TapeStation System using a High Sensitivity D5000 ScreenTape. The average fragment length of the libraries was quantitated on a TapeStation System, and by qPCR with the Kapa Library Quantification kit for Illumina. Each library was diluted to 2 nM and equal volumes of up to 8 libraries were pooled for each sequencing run. Pools were sequenced with X cycle run kits with B bases for Read 1, X bases for Index 1, and 90 bases for Read 2. A PhiX control library was spiked in at 1%. Libraries were sequenced on a NovaSeq 6000 or a NextSeq 2000 Sequencing System (Illumina).

Computational methods

Image analysis

Images were analyzed using Fiji Software. For in vitro and ex vivo experiments, details of the image analysis are specified in the corresponding figure legend. Were indicated, maximum z projections were obtained from confocal stack images.

Sequencing data extraction and pre-processing

Sequences were de-multiplexed using bcl2fastq v2.19.0.316. Reads were aligned to the mm10plus genome using STAR v2.5.2b with parameters TK. Gene counts were produced using HTSEQ v0,6,1p1 with default parameters, except 'stranded' was set to 'false', and 'mode' was set to 'intersection-nonempty'.

Sequences from the microfluidic droplet platform were de-multiplexed and aligned using CellRanger v2.0.1, with default parameters.

Gene count tables were combined with the metadata variables using the Scanpy Python package v.1.4.2. We removed genes that were not expressed in at least 3 cells and then cells that did not have at least 250 detected genes. For FACS we removed cells with fewer than 5,000 counts, and for the droplet method we removed cells with fewer than 2,500 unique molecular identifiers (UMIs). The data was then normalized using size factor normalization such that every cell has 10,000 counts and log transformed. We computed highly variable genes using default parameters and then scaled the data to a maximum value of 10. We

then computed principal component analysis, neighborhood graph and clustered the data using the Leiden algorithm (Traag, Waltman, and van Eck 2019). The data was visualized using UMAP projection (Becht, et al. 2018). When performing batch correction to remove the technical artifacts introduced by the technologies, we replaced the neighborhood graph computation with bbknn (Polański, et al. 2020).

Statistical Analyses

The number of technical replicates and independent experiments is indicated for each experiment in its corresponding figure or figure legend and was determined according to the previous experience of the research group.

For comparison between two groups, data were analyzed by two-tailed Student's t-test. When more than two groups were compared, data were analyzed by one-way ANOVA, and confidence intervals and significance were corrected for multiple comparisons with the Tukey test.

General Discussion

General discussion

Glioblastoma is an aggressive tumor with very poor prognosis. The standard of care for patients with this harmful malignancy has remained almost invariable for the last 20 years, and the urgent need to find new effective therapies is challenged by the unique characteristics of glioblastoma, including high intra and intertumoral heterogeneity and an extraordinarily infiltrative potential, accompanied by an immunosuppressive TME (Perrin, et al. 2019). Several strategies have been proposed to advance knowledge towards curing glioblastoma: the use of neuroscience research, understanding the TME, development of accurate preclinical models, and studies of potential drug targets for precision medicine (Aldape, et al. 2019). In this PhD Thesis, we aim to address some of the actual challenges by focusing on the study of the relationship of tumor cells with the astrocytes in their TME, developing and characterizing a syngeneic preclinical model of glioblastoma, and gaining deeper understanding of the mechanism of action of Tat-Cx43$_{266-283}$ as a Src-targeted therapy. To achieve these goals and with the purpose of obtaining comprehensive information, we combine classical cell and molecular biology techniques with high-throughput state-of-the art single-cell technologies.

Over the last years, immunotherapy has gained importance in the treatment of different types of cancer, including brain tumors (Waldman, Fritz, and Lenardo 2020; D'Errico, Machado, and Sainz 2017; Sanders and Debinski 2020). However, the efficacy of immunotherapeutic strategies in glioblastoma is low and a better knowledge of the neuroimmune system is needed to improve its prospects (Bausart, Préat, and Malfanti 2022). Glioblastomas hijack different cell types in the brain TME to support tumor progression, via secreted molecules and vesicles, but also direct communication through gap junctions and tunnelling nanotubes and microtubes (Broekman, et al. 2018). Tumor cells thwart the immune response, causing a state of reduced T cell effector function commonly known as T cell exhaustion (Woroniecka and Fecci 2018). Understanding how immune cells enter the brain and what mechanisms the tumor utilizes to suppress the immune response lays the groundwork for the application of new strategies that mobilize an effective anti-tumoral immune response. Unfortunately, human glioblastoma cells cannot be used to achieve this goal, given that fully immunocompetent animal models must be used. To overcome this limitation of PDX implantation, humanized mouse models, consistent in immunodeficient mice with a human immune system, are gaining importance. These models can be generated with peripheral blood

mononuclear cells (PBMCs) derived from the same patient, recreating their immune system (Buqué and Galluzzi 2018), however, the interaction between cells from different genetic backgrounds is still present. In this respect, immunocompetent models such as the widely used GL261 model present the advantage of permitting implantation into completely immunocompetent mice with an intact immune system that can be interrogated. As every other, the GL261 model is not perfect and poses some drawbacks worth noting, primarily a high mutational load and elevated immunogenicity compared to human glioblastomas (Johanns, et al. 2016). This may explain the failure in clinical trials of immunotherapy studies that were successful in the GL261 model (Genoud, et al. 2018; Maes and Van Gool 2011; Filley, Henriquez, and Dey 2017). A wise model selection is crucial when analyzing tumor biology and testing therapeutic strategies. The application of state-of-the-art scRNA-Seq has provided tremendous insights into glioblastoma heterogeneity (Patel, et al. 2014; Caruso, et al. 2022; Neftel, et al. 2019; Darmanis, et al. 2017). The in-depth characterization of the GL261-NS—C57BL/6 model using scRNA-Seq and snRNA-Seq carried out in this study contributes to clarifying its biology and will provide researchers with tools for the proper application of this model in preclinical studies and the interpretation of the results obtained from it. Notably, our results show how this model recapitulates most of the hallmarks of human glioblastoma.

The use of targeted therapies is at the forefront of cancer treatment. However, most clinical trials of targeted therapies against glioblastoma have failed due to the appearance of resistance after long-term use, which leads to rapid disease progression and tumor recurrence (Jain 2018). This is likely to be a result of the number of pathways altered and implied in the development of glioblastoma. Thus, the field is moving towards the application of combined therapies to simultaneously attack multiple targets. In this respect, Tat-Cx43$_{266-283}$ treatment favors the response to TMZ, arguing in favor of a beneficial combination of both drugs. Oncogenic driver mutations often create a dependency on the signaling of the affected pathway (Weinstein 2002). With this basis, nearly all targeted cancer therapies today relay on this phenomenon of "oncogene addiction", as it is the case for BRAF inhibitors in *BRAF^{V600E}* mutant melanoma, ABL inhibitors in *BCR-ABL* translocated chronic myeloid leukemia, trastuzumab in *HER2* amplified breast cancer, or EGFR inhibitors in *EGFR* mutant lung cancer (Sun and Bernards 2014). Therapies directed against an oncogene, however, bring the problematic of the appearance of acquired resistance, and do not translate into a meaningful overall survival. Noteworthy, it has been observed in patients the so-known "drug holiday effect", by which patients that have developed resistance to a treatment show a stabilization of the tumor, or even a decline, when the therapy is discontinued (Szakács, et al. 2014; Imamovic and Sommer 2013). This suggests that

resistant cells have developed a new vulnerability, which can be exploited as a new target, making a point for the characterization of the mechanisms of acquired resistance. Tat-Cx43$_{266-283}$- and TMZ-resistant GSCs generated in this Thesis can serve as a useful tool to design rational therapies strategies of drug combination.

The data presented in this work, together with previous observations (Jaraíz-Rodríguez, et al. 2020; Pelaz, et al. 2020), confirm that Tat-Cx43$_{266-283}$ does not have deleterious effects on healthy cells, constituting an advantage over other Src inhibitors. Because healthy astrocytes might play an important role during brain tumor treatment, it could be speculated that that deleterious effect of dasatinib in healthy astrocytes might be involved in the lack of positive results in clinical trials for glioblastoma (Galanis, et al. 2019). Tat-Cx43$_{266-283}$ does, however, affect malignant cells while it modulates astrocyte activation, compromising the communication between tumor cells and the TME. STAT3 is a point of convergence for multiple signaling pathways with oncogenic potential, and is constitutively activated in tumor cells and immune cells in the TME, constituting a key node in the crosstalk between tumor cells and their microenvironment (Yu, Pardoll, and Jove 2009; Yu, Kortylewski, and Pardoll 2007). In fact, STAT3 has emerged as a promising target and multitude of studies have focused on its inhibition as a therapeutic strategy against cancer, including brain metastases (Priego, et al. 2018). In this study, we show that astrocytes respond to glioblastoma cells by activating STAT3. Interestingly, we found that laminin, through integrin receptors, promotes a reciprocal signaling activation of STAT3 and Src in TAAs, triggering the subsequent signaling cascade. Tat-Cx43$_{266-283}$, by inhibiting Src, efficiently inhibits STAT3 in TAAs, decreasing expression of hallmark proteins of the reactive astrocyte phenotype. This new role adds on value to Tat-Cx43$_{266-283,}$ complementing that in malignant cells, disrupting the communication between tumor cells and TAAs and ultimately leading to decreased tumor proliferation, migration, and invasion (Jaraíz-Rodríguez, et al. 2020).

In summary, the research conducted in this Thesis provides meaningful insights into the biology of the C57BL/6—GL261 model, the mechanisms of glioblastoma-TME communication, and the value of Tat-Cx43$_{266}$ for glioblastoma therapy.
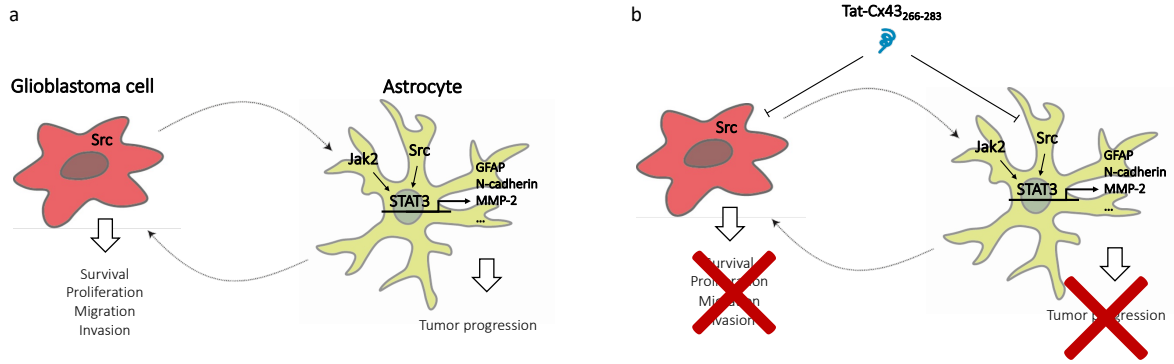
Scheme 9. Proposed mechanism for Tat-Cx43$_{266-283}$ the inhibition of glioblastoma-astrocyte communication.

CONCLVSIONS

Conclusions

I. Different in vitro, ex vivo and in vivo models show that Tat-Cx43$_{266-283}$ is taken up by reactive astrocytes affecting their phenotype and response to tumor cells or injury.

II. GSCs obtained from mouse GL261 cells present high Src activity, analogously to human GSCs. Treatment with Tat-Cx43$_{266-283}$ inhibits Src activity, neurosphere-forming ability, MTT reduction potential, and tumor-forming capacity of GL261 GSCs.

III. Differentiated GL261 cells exhibit high levels of the neurotrophin receptor TrkB, while GSCs obtained from GL261 cells upregulate BDNF, which is compatible with the reported neurotrophin feedback loop between the stem and differentiated tumor cell populations that favors tumor growth.

IV. Tat-Cx43$_{266-283}$ shifts the phenotype of GL261 GSCs towards an oligodendrocyte-like phenotype with increased TMZ sensitivity, arguing in favor of a beneficial combination of both drugs for glioblastoma therapy. Indeed, when GL261 GSCs acquire Tat-Cx43$_{266-283}$ or TMZ resistance after the exposure to prolonged and increasing concentrations of these drugs, some of the resistant clones become sensitive to the other drug.

V. The implantation of GL261 GSCs in the brain of syngeneic mice originates tumors that recapitulate the hallmarks of human glioblastoma, including high cellularity, heterogenicity, development of a necrotic core, presence of pseudopalisades in the infiltrating rims, and an extensive astrocytic response.

VI. In vitro and in vivo glioblastoma preclinical models show that astrocytes respond to glioblastoma cells by activating the transcription factor STAT3, as judged by increased expression, phosphorylation at tyrosine 705 and nuclear translocation.

VII. Our study unveils a new role for laminin in the activation of STAT3 in tumor-associated astrocytes. Indeed, laminin, through integrin receptor, promotes a reciprocal signaling activation of STAT3 and Src that results in increased levels of the hallmark astrocyte proteins GFAP, N-cadherin, β-catenin, α-actinin, MMP-2, and Cx43.

VIII. Tat-Cx43$_{266-283}$, through Src inhibition, impairs STAT3 activation triggered by glioblastoma cells and laminin in astrocytes, which contributes to its antitumor effect. Importantly, most of these

results were confirmed by immunohistochemistry, Western blot and sc-RNAseq in vitro, ex vivo and in the in vivo syngeneic model of glioblastoma developed and characterized in this PhD thesis.

Final conclusion

The results presented in this PhD Thesis confirm the anti-tumoral effect of Tat-Cx43$_{266\text{-}283}$ on the inhibition of GSCs and uncover a new role for this peptide on targeting the reactive astrocytes in the tumor microenvironment, disrupting the communication between glioblastoma cells and astrocytes, and favoring a better outcome. These discoveries reinforce the idea that glioblastomas develop in a complex brain environment where the different components should be considered when aiming to design an effective therapy and supports the use of Tat-Cx43$_{266\text{-}283}$ for the treatment of glioblastoma.

Conclusión final

Los resultados presentados en esta Tesis Doctoral confirman el efecto antitumoral de Tat-Cx43$_{266\text{-}283}$ en la inhibición de las células madre de glioblastoma y revelan un nuevo papel de este péptido sobre los astrocitos del microambiente tumoral. El tratamiento con Tat-Cx43$_{266\text{-}283}$ compromete la comunicación entre las células tumorales y los astrocitos, favoreciendo un mejor desenlace. Estos descubrimientos refuerzan la idea de que los glioblastomas se desarrollan en un ambiente complejo, cuyos diferentes components deben ser tenidos en cuenta con el fin de desarrollar un tratamiento efectivo, y apoya el uso de Tat-Cx43$_{266\text{-}283}$ en el tratamiento de estos fatales tumores.

REFERENCES

References

A, Wu, et al. 2008. "Persistence of Cd133+ Cells in Human and Mouse Glioma Cell Lines: Detailed Characterization of Gl261 Glioma Cells with Cancer Stem Cell-Like Properties." *Stem cells and development* 17, no. 1 (2008 Feb). http://dx.doi.org/10.1089/scd.2007.0133 .

Aasland, D., et al. 2019. "Temozolomide Induces Senescence and Repression of Dna Repair Pathways in Glioblastoma Cells Via Activation of Atr-Chk1, P21, and Nf-Kb." *Cancer Res* 79, no. 1 (01 01): 99-113. http://dx.doi.org/10.1158/0008-5472.CAN-18-1733.

Abe, K., et al. 2001. "The Yxxq Motif in Gp 130 Is Crucial for Stat3 Phosphorylation at Ser727 through an H7-Sensitive Kinase Pathway." *Oncogene* 20, no. 27 (Jun 14): 3464-74. http://dx.doi.org/10.1038/sj.onc.1204461 .

Acarin, L., B. González, and B. Castellano. 2000. "Neuronal, Astroglial and Microglial Cytokine Expression after an Excitotoxic Lesion in the Immature Rat Brain." *Eur J Neurosci* 12, no. 10 (Oct): 3505-20. http://dx.doi.org/10.1046/j.1460-9568.2000.00226.x.

Al-Mayhani, M. T., et al. 2011. "Ng2 Expression in Glioblastoma Identifies an Actively Proliferating Population with an Aggressive Molecular Signature." *Neuro Oncol* 13, no. 8 (Aug): 830-45.
http://dx.doi.org/10.1093/neuonc/nor088 .

Alcantara Llaguno, S., et al. 2009. "Malignant Astrocytomas Originate from Neural Stem/Progenitor Cells in a Somatic Tumor Suppressor Mouse Model." *Cancer Cell* 15, no. 1 (Jan 06): 45-56. http://dx.doi.org/10.1016/j.ccr.2008.12.006.

Alcantara Llaguno, Sheila, et al. 2019. "Cell-of-Origin Susceptibility to Glioblastoma Formation Declines with Neural Lineage Restriction." *Nature Neuroscience* 22, no. 4 (2019-02-18): 545-555. http://dx.doi.org/doi:10.1038/s41593-018-0333-8.

Aldape, K., et al. 2019. "Challenges to Curing Primary Brain Tumours." *Nat Rev Clin Oncol* 16, no. 8 (08): 509-520. http://dx.doi.org/10.1038/s41571-019-0177-5.

Ampofo, E., et al. 2017. "The Regulatory Mechanisms of Ng2/Cspg4 Expression." *Cell Mol Biol Lett* 22: 4. http://dx.doi.org/10.1186/s11658-017-0035-3.

Ancot, F., et al. 2009. "Proteolytic Cleavages Give Receptor Tyrosine Kinases the Gift of Ubiquity." *Oncogene* 28, no. 22 (Jun 04): 2185-95. http://dx.doi.org/10.1038/onc.2009.88.

Anderson, M. A., et al. 2016. "Astrocyte Scar Formation Aids Central Nervous System Axon Regeneration." *Nature* 532, no. 7598 (Apr 14): 195-200. http://dx.doi.org/10.1038/nature17623.

Arimori, T., et al. 2021. "Structural Mechanism of Laminin Recognition by Integrin." *Nat Commun* 12, no. 1 (06 29): 4012. http://dx.doi.org/10.1038/s41467-021-24184-8.

Arévalo, J. C., and S. H. Wu. 2006. "Neurotrophin Signaling: Many Exciting Surprises!" *Cell Mol Life Sci* 63, no. 13 (Jul): 1523-37. http://dx.doi.org/10.1007/s00018-006-6010-1.

Aumailley, M. 2013. "The Laminin Family." *Cell Adh Migr* 7, no. 1 (2013 Jan-Feb): 48-55. http://dx.doi.org/10.4161/cam.22826.

Ausman, J. I., W. R. Shapiro, and D. P. Rall. 1970. "Studies on the Chemotherapy of Experimental Brain Tumors: Development of an Experimental Model." *Cancer Res* 30, no. 9 (Sep): 2394-400.

Bausart, M., V. Préat, and A. Malfanti. 2022. "Immunotherapy for Glioblastoma: The Promise of Combination Strategies." *J Exp Clin Cancer Res* 41, no. 1 (Jan 25): 35. http://dx.doi.org/10.1186/s13046-022-02251-2.

Baxter, G. T., et al. 1997. "Signal Transduction Mediated by the Truncated Trkb Receptor Isoforms, Trkb.T1 and Trkb.T2." *J Neurosci* 17, no. 8 (Apr 15): 2683-90.

Becht, E., et al. 2018. "Dimensionality Reduction for Visualizing Single-Cell Data Using Umap." *Nat Biotechnol* (Dec 03). http://dx.doi.org/10.1038/nbt.4314.

Bellail, A. C., et al. 2004. "Microregional Extracellular Matrix Heterogeneity in Brain Modulates Glioma Cell Invasion." *Int J Biochem Cell Biol* 36, no. 6 (Jun): 1046-69. http://dx.doi.org/10.1016/j.biocel.2004.01.013.

Beloribi-Djefaflia, S., S. Vasseur, and F. Guillaumond. 2016. "Lipid Metabolic Reprogramming in Cancer Cells." *Oncogenesis* 5 (Jan 25): e189. http://dx.doi.org/10.1038/oncsis.2015.49.

Beltzig, L., et al. 2022. "Senescence Is the Main Trait Induced by Temozolomide in Glioblastoma Cells." *Cancers (Basel)* 14, no. 9 (Apr 29). http://dx.doi.org/10.3390/cancers14092233.

Ben Haim, L., et al. 2015. "The Jak/Stat3 Pathway Is a Common Inducer of Astrocyte Reactivity in Alzheimer's and Huntington's Diseases." *J Neurosci* 35, no. 6 (Feb 11): 2817-29. http://dx.doi.org/10.1523/jneurosci.3516-14.2015.

Bhaduri, A., et al. 2020. "Outer Radial Glia-Like Cancer Stem Cells Contribute to Heterogeneity of Glioblastoma." *Cell Stem Cell* 26, no. 1 (01 02): 48-63.e6. http://dx.doi.org/10.1016/j.stem.2019.11.015.

Blaszczyk-Thurin, M., I. O. Ertl, and H. C. Ertl. 2002. "An Experimental Vaccine

Expressing Wild-Type P53 Induces Protective Immunity against Glioblastoma Cells with High Levels of Endogenous P53." *Scand J Immunol* 56, no. 4 (Oct): 361-75. http://dx.doi.org/10.1046/j.1365-3083.2002.01119.x.

Bloom, O. 2014. "Non-Mammalian Model Systems for Studying Neuro-Immune Interactions after Spinal Cord Injury." *Exp Neurol* 258 (Aug): 130-40. http://dx.doi.org/10.1016/j.expneurol.2013.12.023.

Bos, J. L. 1989. "Ras Oncogenes in Human Cancer: A Review." *Cancer Res* 49, no. 17 (Sep 01): 4682-9.

Bovenga, F., C. Sabbà, and A. Moschetta. 2015. "Uncoupling Nuclear Receptor Lxr and Cholesterol Metabolism in Cancer." *Cell Metab* 21, no. 4 (Apr 07): 517-26. http://dx.doi.org/10.1016/j.cmet.2015.03.002.

Brandao, M., et al. 2019. "Astrocytes, the Rising Stars of the Glioblastoma Microenvironment." *Glia* 67, no. 5 (May): 779-790. http://dx.doi.org/10.1002/glia.23520.

Brat, D. J., et al. 2004. "Pseudopalisades in Glioblastoma Are Hypoxic, Express Extracellular Matrix Proteases, and Are Formed by an Actively Migrating Cell Population." *Cancer Res* 64, no. 3 (Feb 01): 920-7. http://dx.doi.org/10.1158/0008-5472.can-03-2073.

Brennan, C. W., et al. 2013. "The Somatic Genomic Landscape of Glioblastoma." *Cell* 155, no. 2 (Oct 10): 462-77.

http://dx.doi.org/10.1016/j.cell.2013.09.034.

Broadfield, L. A., et al. 2021. "Lipid Metabolism in Cancer: New Perspectives and Emerging Mechanisms." *Dev Cell* 56, no. 10 (05 17): 1363-1393. http://dx.doi.org/10.1016/j.devcel.2021.04.013.

Broekman, M. L., et al. 2018. "Multidimensional Communication in the Microenvirons of Glioblastoma." *Nat Rev Neurol* 14, no. 8 (08): 482-495. http://dx.doi.org/10.1038/s41582-018-0025-8.

Budday, S., et al. 2015. "Mechanical Properties of Gray and White Matter Brain Tissue by Indentation." *J Mech Behav Biomed Mater* 46 (Jun): 318-30. http://dx.doi.org/10.1016/j.jmbbm.2015.02.024.

Bundesen, L. Q., et al. 2003. "Ephrin-B2 and Ephb2 Regulation of Astrocyte-Meningeal Fibroblast Interactions in Response to Spinal Cord Lesions in Adult Rats." *J Neurosci* 23, no. 21 (Aug 27): 7789-800.

Buqué, A., and L. Galluzzi. 2018. "Modeling Tumor Immunology and Immunotherapy in Mice." *Trends Cancer* 4, no. 9 (09): 599-601. http://dx.doi.org/10.1016/j.trecan.2018.07.003.

Burg, M. A., A. Nishiyama, and W. B. Stallcup. 1997. "A Central Segment of the Ng2 Proteoglycan Is Critical for the Ability of Glioma Cells to Bind and Migrate toward Type Vi Collagen." *Exp Cell Res* 235, no. 1 (Aug 25): 254-64.

http://dx.doi.org/10.1006/excr.1997.3674.

Bush, T. G., et al. 1999. "Leukocyte Infiltration, Neuronal Degeneration, and Neurite Outgrowth after Ablation of Scar-Forming, Reactive Astrocytes in Adult Transgenic Mice." *Neuron* 23, no. 2 (Jun): 297-308. http://dx.doi.org/10.1016/s0896-6273(00)80781-3.

Campisi, J., and F. d'Adda di Fagagna. 2007. "Cellular Senescence: When Bad Things Happen to Good Cells." *Nat Rev Mol Cell Biol* 8, no. 9 (Sep): 729-40. http://dx.doi.org/10.1038/nrm2233.

Caner, A., E. Asik, and B. Ozpolat. 2021. "Src Signaling in Cancer and Tumor Microenvironment." *Adv Exp Med Biol* 1270: 57-71. http://dx.doi.org/10.1007/978-3-030-47189-7_4.

Caruso, Francesca Pia, et al. 2022. "A Map of Tumor–Host Interactions in Glioma at Single-Cell Resolution." *GigaScience* 9, no. 10. http://dx.doi.org/10.1093/gigascience/giaa109.

Cekanaviciute, E., et al. 2014. "Astrocytic Transforming Growth Factor-Beta Signaling Reduces Subacute Neuroinflammation after Stroke in Mice." *Glia* 62, no. 8 (Aug): 1227-40. http://dx.doi.org/10.1002/glia.22675.

Chang, M. L., et al. 2007. "Reactive Changes of Retinal Astrocytes and Müller Glial Cells in Kainate-Induced Neuroexcitotoxicity." *J Anat* 210, no. 1 (Jan): 54-65.

http://dx.doi.org/10.1111/j.1469-7580.2006.00671.x.

Chen, E. Y., et al. 2013. "Enrichr: Interactive and Collaborative Html5 Gene List Enrichment Analysis Tool." *BMC Bioinformatics* 14 (Apr 15): 128. http://dx.doi.org/10.1186/1471-2105-14-128.

Chen, Q., et al. 2016. "Carcinoma-Astrocyte Gap Junctions Promote Brain Metastasis by Cgamp Transfer." *Nature* 533, no. 7604 (05 26): 493-498. http://dx.doi.org/10.1038/nature18268.

Chen, W., et al. 2015. "Glioma Cells Escaped from Cytotoxicity of Temozolomide and Vincristine by Communicating with Human Astrocytes." *Med Oncol* 32, no. 3 (Mar): 43. http://dx.doi.org/10.1007/s12032-015-0487-0.

Cheng, C., et al. 2018. "Lipid Metabolism Reprogramming and Its Potential Targets in Cancer." *Cancer Commun (Lond)* 38, no. 1 (05 21): 27. http://dx.doi.org/10.1186/s40880-018-0301-4.

Cho, S., A. Wood, and M. R. Bowlby. 2007. "Brain Slices as Models for Neurodegenerative Disease and Screening Platforms to Identify Novel Therapeutics." *Curr Neuropharmacol* 5, no. 1 (Mar): 19-33. http://dx.doi.org/10.2174/157015907780077105.

Chrétien, A., et al. 2008. "Role of Tgf-Beta1-Independent Changes in Protein Neosynthesis, P38alphamapk, and Cdc42 in Hydrogen Peroxide-Induced

Senescence-Like Morphogenesis." *Free Radic Biol Med* 44, no. 9 (May 01): 1732-51. http://dx.doi.org/10.1016/j.freeradbiomed.2008.01.026.

Chung, W. S., N. J. Allen, and C. Eroglu. 2015. "Astrocytes Control Synapse Formation, Function, and Elimination." *Cold Spring Harb Perspect Biol* 7, no. 9 (Feb 06): a020370. http://dx.doi.org/10.1101/cshperspect.a020370.

Ciesielski, M. J., et al. 2006. "Antitumor Effects of a Xenogeneic Survivin Bone Marrow Derived Dendritic Cell Vaccine against Murine Gl261 Gliomas." *Cancer Immunol Immunother* 55, no. 12 (Dec): 1491-503. http://dx.doi.org/10.1007/s00262-006-0138-6.

Collado, M., M. A. Blasco, and M. Serrano. 2007. "Cellular Senescence in Cancer and Aging." *Cell* 130, no. 2 (Jul 27): 223-33. http://dx.doi.org/10.1016/j.cell.2007.07.003.

Colwell, N., et al. 2017. "Hypoxia in the Glioblastoma Microenvironment: Shaping the Phenotype of Cancer Stem-Like Cells." *Neuro Oncol* 19, no. 7 (Jul 01): 887-896. http://dx.doi.org/10.1093/neuonc/now258.

Consortium, The Tabula Muris. 2018. "Single-Cell Transcriptomics of 20 Mouse Organs Creates a Tabula Muris." *Nature* 562, no. 7727 (2018 Oct). http://dx.doi.org/10.1038/s41586-018-0590-4.

Courtneidge, S. A. 2002. "Role of Src in Signal Transduction Pathways. The Jubilee Lecture." *Biochem Soc Trans* 30, no. 2 (Apr): 11-7. http://dx.doi.org/10.1042/.

D'Errico, G., H. L. Machado, and B. Sainz. 2017. "A Current Perspective on Cancer Immune Therapy: Step-by-Step Approach to Constructing the Magic Bullet." *Clin Transl Med* 6, no. 1 (Dec): 3. http://dx.doi.org/10.1186/s40169-016-0130-5.

Darmanis, S., et al. 2017. "Single-Cell Rna-Seq Analysis of Infiltrating Neoplastic Cells at the Migrating Front of Human Glioblastoma." *Cell Rep* 21, no. 5 (10 31): 1399-1410. http://dx.doi.org/10.1016/j.celrep.2017.10.030.

---. 2015. "A Survey of Human Brain Transcriptome Diversity at the Single Cell Level." *Proc Natl Acad Sci U S A* 112, no. 23 (Jun 09): 7285-90. http://dx.doi.org/10.1073/pnas.1507125112.

Darnell, J. E. 1997. "Stats and Gene Regulation." *Science* 277, no. 5332 (Sep 12): 1630-5. http://dx.doi.org/10.1126/science.277.5332.1630.

Darnell, J. E., I. M. Kerr, and G. R. Stark. 1994. "Jak-Stat Pathways and Transcriptional Activation in Response to Ifns and Other Extracellular Signaling Proteins." *Science* 264, no. 5164 (Jun 03): 1415-21. http://dx.doi.org/10.1126/science.8197455.

De Vleeschouwer, S. 2017. "Glioblastoma."

de Vries, N. A., et al. 2006. "Blood-Brain Barrier and Chemotherapeutic Treatment of Brain Tumors." *Expert Rev Neurother* 6, no. 8 (Aug): 1199-209. http://dx.doi.org/10.1586/14737175.6.8.1199.

Debacq-Chainiaux, F., et al. 2009. "Protocols to Detect Senescence-Associated Beta-Galactosidase (Sa-Betagal) Activity, a Biomarker of Senescent Cells in Culture and in Vivo." *Nat Protoc* 4, no. 12: 1798-806. http://dx.doi.org/10.1038/nprot.2009.191.

Dobin, A., et al. 2013. "Star: Ultrafast Universal Rna-Seq Aligner." *Bioinformatics* 29, no. 1 (Jan 01): 15-21. http://dx.doi.org/10.1093/bioinformatics/bts635.

Donato, R. 2003. "Intracellular and Extracellular Roles of S100 Proteins." *Microsc Res Tech* 60, no. 6 (Apr 15): 540-51. http://dx.doi.org/10.1002/jemt.10296.

Du, J., et al. 2009. "Bead-Based Profiling of Tyrosine Kinase Phosphorylation Identifies Src as a Potential Target for Glioblastoma Therapy." *Nat Biotechnol* 27, no. 1 (Jan): 77-83. http://dx.doi.org/10.1038/nbt.1513.

Escartin, C., et al. 2021. "Reactive Astrocyte Nomenclature, Definitions, and Future Directions." *Nat Neurosci* 24, no. 3 (03): 312-325. http://dx.doi.org/10.1038/s41593-020-00783-4.

Eyler, C. E., and J. N. Rich. 2008. "Survival of the Fittest: Cancer Stem Cells in Therapeutic Resistance and Angiogenesis." *J Clin Oncol* 26, no. 17 (Jun 10): 2839-45. http://dx.doi.org/10.1200/JCO.2007.15.1829.

Fenner, B. M. 2012. "Truncated Trkb: Beyond a Dominant Negative Receptor." *Cytokine Growth Factor Rev* 23, no. 1-2 (2012 Feb-Apr): 15-24. http://dx.doi.org/10.1016/j.cytogfr.2012.01.002.

Filley, A. C., M. Henriquez, and M. Dey. 2017. "Recurrent Glioma Clinical Trial, Checkmate-143: The Game Is Not over Yet." *Oncotarget* 8, no. 53 (Oct 31): 91779-91794. http://dx.doi.org/10.18632/oncotarget.21586.

Fischer, J., and T. Ayers. 2021. "Single Nucleus Rna-Sequencing: How It's Done, Applications and Limitations." *Emerg Top Life Sci* 5, no. 5 (11 12): 687-690. http://dx.doi.org/10.1042/ETLS20210074.

Fortin, D., et al. 2001. "Pcv for Oligodendroglial Tumors: In Search of Prognostic Factors for Response and Survival." *Can J Neurol Sci* 28, no. 3 (Aug): 215-23. http://dx.doi.org/10.1017/s0317167100001359.

Fossey, S. L., et al. 2009. "Characterization of Stat3 Activation and Expression in Canine and Human Osteosarcoma." *BMC Cancer* 9 (Mar 10): 81. http://dx.doi.org/10.1186/1471-2407-9-81.

Frame, M. C. 2002. "Src in Cancer: Deregulation and Consequences for Cell Behaviour." *Biochim Biophys Acta* 1602, no. 2 (Jun

21): 114-30. http://dx.doi.org/10.1016/s0304-419x(02)00040-9.

---. 2004. "Newest Findings on the Oldest Oncogene; How Activated Src Does It." *J Cell Sci* 117, no. Pt 7 (Mar 01): 989-98. http://dx.doi.org/10.1242/jcs.01111.

Fraser, H. 1971. "Astrocytomas in an Inbred Mouse Strain." *J Pathol* 103, no. 4 (Apr): 266-70. http://dx.doi.org/10.1002/path.1711030410.

Frattini, V., et al. 2013. "The Integrated Landscape of Driver Genomic Alterations in Glioblastoma." *Nat Genet* 45, no. 10 (Oct): 1141-9. http://dx.doi.org/10.1038/ng.2734.

Friend, S. 1994. "P53: A Glimpse at the Puppet Behind the Shadow Play." *Science* 265, no. 5170 (Jul 15): 334-5. http://dx.doi.org/10.1126/science.8023155.

Fuchs, S. M., and R. T. Raines. 2006. "Internalization of Cationic Peptides: The Road Less (or More?) Traveled." *Cell Mol Life Sci* 63, no. 16 (Aug): 1819-22. http://dx.doi.org/10.1007/s00018-006-6170-z.

Fujii, S., R. W. Sobol, and R. P. Fuchs. 2022. "Double-Strand Breaks: When Dna Repair Events Accidentally Meet." *DNA Repair (Amst)* 112 (04): 103303. http://dx.doi.org/10.1016/j.dnarep.2022.103303.

Fulgenzi, G., et al. 2020. "Novel Metabolic Role for Bdnf in Pancreatic B-Cell Insulin Secretion." *Nat Commun* 11, no. 1 (04

23): 1950. http://dx.doi.org/10.1038/s41467-020-15833-5.

Galanis, E., et al. 2019. "A Phase 1 and Randomized, Placebo-Controlled Phase 2 Trial of Bevacizumab Plus Dasatinib in Patients with Recurrent Glioblastoma: Alliance/North Central Cancer Treatment Group N0872." *Cancer* 125, no. 21 (11 01): 3790-3800. http://dx.doi.org/10.1002/cncr.32340.

Galea, E., et al. 2022. "Multi-Transcriptomic Analysis Points to Early Organelle Dysfunction in Human Astrocytes in Alzheimer's Disease." *Neurobiol Dis* 166 (05): 105655. http://dx.doi.org/10.1016/j.nbd.2022.105655.

Gangemi, R. M., et al. 2009. "Sox2 Silencing in Glioblastoma Tumor-Initiating Cells Causes Stop of Proliferation and Loss of Tumorigenicity." *Stem Cells* 27, no. 1 (Jan): 40-8. http://dx.doi.org/10.1634/stemcells.2008-0493.

Gangoso, E., et al. 2012. "Reduced Connexin43 Expression Correlates with C-Src Activation, Proliferation, and Glucose Uptake in Reactive Astrocytes after an Excitotoxic Insult." *Glia* 60, no. 12 (Dec): 2040-9. http://dx.doi.org/10.1002/glia.22418.

---. 2017. "A C-Src Inhibitor Peptide Based on Connexin43 Exerts Neuroprotective Effects through the Inhibition of Glial Hemichannel Activity." *Front Mol Neurosci* 10: 418. http://dx.doi.org/10.3389/fnmol.2017.00418.

---. 2014. "A Cell-Penetrating Peptide Based on the Interaction between C-Src and Connexin43 Reverses Glioma Stem Cell Phenotype." *Cell Death Dis* 5 (Jan): e1023. http://dx.doi.org/10.1038/cddis.2013.560.

Gao, Q., Y. Li, and M. Chopp. 2005. "Bone Marrow Stromal Cells Increase Astrocyte Survival Via Upregulation of Phosphoinositide 3-Kinase/Threonine Protein Kinase and Mitogen-Activated Protein Kinase Kinase/Extracellular Signal-Regulated Kinase Pathways and Stimulate Astrocyte Trophic Factor Gene Expression after Anaerobic Insult." *Neuroscience* 136, no. 1: 123-34. http://dx.doi.org/10.1016/j.neuroscience.2005.06.091.

Garg, M., et al. 2020. "The Pleiotropic Role of Transcription Factor Stat3 in Oncogenesis and Its Targeting through Natural Products for Cancer Prevention and Therapy." *Med Res Rev* (Dec 01). http://dx.doi.org/10.1002/med.21761.

Genoud, V., et al. 2018. "Responsiveness to Anti-Pd-1 and Anti-Ctla-4 Immune Checkpoint Blockade in Sb28 and Gl261 Mouse Glioma Models." *Oncoimmunology* 7, no. 12 (2018): e1501137. http://dx.doi.org/10.1080/2162402X.2018.1501137.

Giaume, C., et al. 1991. "Gap Junctions in Cultured Astrocytes: Single-Channel Currents and Characterization of Channel-Forming Protein." *Neuron* 6, no. 1 (Jan): 133-43. http://dx.doi.org/10.1016/0896-6273(91)90128-m.

---. 2021. "Glial Connexins and Pannexins in the Healthy and Diseased Brain." *Physiol Rev* 101, no. 1 (01 01): 93-145. http://dx.doi.org/10.1152/physrev.00043.2018.

Gielen, P. R., et al. 2013. "Connexin43 Confers Temozolomide Resistance in Human Glioma Cells by Modulating the Mitochondrial Apoptosis Pathway." *Neuropharmacology* 75 (Dec): 539-48. http://dx.doi.org/10.1016/j.neuropharm.2013.05.002.

Giese, A., and M. Westphal. 1996. "Glioma Invasion in the Central Nervous System." *Neurosurgery* 39, no. 2 (Aug): 235-50; discussion 250-2. http://dx.doi.org/10.1097/00006123-199608000-00001.

Gogolla, N., et al. 2006. "Preparation of Organotypic Hippocampal Slice Cultures for Long-Term Live Imaging." *Nat Protoc* 1, no. 3: 1165-71. http://dx.doi.org/10.1038/nprot.2006.168.

González-Sánchez, A., et al. 2016. "Connexin43 Recruits Pten and Csk to Inhibit C-Src Activity in Glioma Cells and Astrocytes." *Oncotarget* 7, no. 31 (Aug): 49819-49833. http://dx.doi.org/10.18632/oncotarget.10454.

Graham, V., et al. 2003. "Sox2 Functions to Maintain Neural Progenitor Identity." *Neuron* 39, no. 5 (Aug 28): 749-65. http://dx.doi.org/10.1016/s0896-6273(03)00497-5.

Grek, C. L., et al. 2018. "Novel Approach to Temozolomide Resistance in Malignant Glioma: Connexin43-Directed Therapeutics." *Curr Opin Pharmacol* 41 (Aug): 79-88. http://dx.doi.org/10.1016/j.coph.2018.05.002.

Gritsenko, P. G., O. Ilina, and P. Friedl. 2012. "Interstitial Guidance of Cancer Invasion." *J Pathol* 226, no. 2 (Jan): 185-99. http://dx.doi.org/10.1002/path.3031.

Gritsenko, P., W. Leenders, and P. Friedl. 2017. "Recapitulating in Vivo-Like Plasticity of Glioma Cell Invasion Along Blood Vessels and in Astrocyte-Rich Stroma." *Histochem Cell Biol* 148, no. 4 (Oct): 395-406. http://dx.doi.org/10.1007/s00418-017-1604-2.

Grosely, R., et al. 2013. "Effects of Phosphorylation on the Structure and Backbone Dynamics of the Intrinsically Disordered Connexin43 C-Terminal Domain." *J Biol Chem* 288, no. 34 (Aug 23): 24857-70. http://dx.doi.org/10.1074/jbc.M113.454389.

Guo, D., E. H. Bell, and A. Chakravarti. 2013. "Lipid Metabolism Emerges as a Promising Target for Malignant Glioma Therapy." *CNS Oncol* 2, no. 3 (May): 289-99. http://dx.doi.org/10.2217/cns.13.20.

Günther, W., et al. 2003. "Temozolomide Induces Apoptosis and Senescence in Glioma Cells Cultured as Multicellular Spheroids." *Br J Cancer* 88, no. 3 (Feb 10): 463-9. http://dx.doi.org/10.1038/sj.bjc.6600711.

Habib, N., et al. 2016. "Div-Seq: Single-Nucleus Rna-Seq Reveals Dynamics of Rare Adult Newborn Neurons." *Science* 353, no. 6302 (08 26): 925-8. http://dx.doi.org/10.1126/science.aad7038.

Haddad, A. F., et al. 2021. "Mouse Models of Glioblastoma for the Evaluation of Novel Therapeutic Strategies." *Neurooncol Adv* 3, no. 1 (2021 Jan-Dec): vdab100. http://dx.doi.org/10.1093/noajnl/vdab100.

Hambardzumyan, D., D. H. Gutmann, and H. Kettenmann. 2016. "The Role of Microglia and Macrophages in Glioma Maintenance and Progression." *Nat Neurosci* 19, no. 1 (Jan): 20-7. http://dx.doi.org/10.1038/nn.4185.

Han, X., et al. 2014. "The Role of Src Family Kinases in Growth and Migration of Glioma Stem Cells." *Int J Oncol* 45, no. 1 (Jul): 302-10. http://dx.doi.org/10.3892/ijo.2014.2432.

Hangauer, M. J., et al. 2017. "Drug-Tolerant Persister Cancer Cells Are Vulnerable to Gpx4 Inhibition." *Nature* 551, no. 7679 (11 09): 247-250. http://dx.doi.org/10.1038/nature24297.

Hasel, P., et al. 2021. "Neuroinflammatory Astrocyte Subtypes in the Mouse Brain." *Nat Neurosci* 24, no. 10 (10): 1475-1487. http://dx.doi.org/10.1038/s41593-021-00905-6.

Hennig, B. P., et al. 2018. "Large-Scale Low-Cost Ngs Library Preparation Using a

Robust Tn5 Purification and Tagmentation Protocol." *G3 (Bethesda)* 8, no. 1 (01 04): 79-89. http://dx.doi.org/10.1534/g3.117.300257.

Henrik Heiland, D., et al. 2019. "Tumor-Associated Reactive Astrocytes Aid the Evolution of Immunosuppressive Environment in Glioblastoma." *Nat Commun* 10, no. 1 (Jun 11): 2541. http://dx.doi.org/10.1038/s41467-019-10493-6.

Heppner, F. L., R. M. Ransohoff, and B. Becher. 2015. "Immune Attack: The Role of Inflammation in Alzheimer Disease." *Nat Rev Neurosci* 16, no. 6 (Jun): 358-72. http://dx.doi.org/10.1038/nrn3880.

Herrero-González, S., et al. 2010. "Connexin43 Inhibits the Oncogenic Activity of C-Src in C6 Glioma Cells." *Oncogene* 29, no. 42 (Oct): 5712-23. http://dx.doi.org/10.1038/onc.2010.299.

Herrmann, J. E., et al. 2008. "Stat3 Is a Critical Regulator of Astrogliosis and Scar Formation after Spinal Cord Injury." *J Neurosci* 28, no. 28 (Jul 9): 7231-43. http://dx.doi.org/10.1523/jneurosci.1709-08.2008.

Hickman, M. J., and L. D. Samson. 2004. "Apoptotic Signaling in Response to a Single Type of Dna Lesion, O(6)-Methylguanine." *Mol Cell* 14, no. 1 (Apr 09): 105-16. http://dx.doi.org/10.1016/s1097-2765(04)00162-5.

Hirano, T., K. Ishihara, and M. Hibi. 2000. "Roles of Stat3 in Mediating the Cell Growth, Differentiation and Survival Signals Relayed through the Il-6 Family of Cytokine Receptors." *Oncogene* 19, no. 21 (May 15): 2548-56. http://dx.doi.org/10.1038/sj.onc.1203551.

Huang, J. Y., et al. 2010. "Extracellular Matrix of Glioblastoma Inhibits Polarization and Transmigration of T Cells: The Role of Tenascin-C in Immune Suppression." *J Immunol* 185, no. 3 (Aug 01): 1450-9. http://dx.doi.org/10.4049/jimmunol.0901352.

Huang, R. P., et al. 1999. "Reduced Connexin43 Expression in High-Grade Human Brain Glioma Cells." *J Surg Oncol* 70, no. 1 (Jan): 21-4. http://dx.doi.org/10.1002/(sici)1096-9098(199901)70:1<21::aid-jso4>3.0.co;2-0.

Huang, S. H., et al. 2009. "Essential Role of Hrs in Endocytic Recycling of Full-Length Trkb Receptor but Not Its Isoform Trkb.T1." *J Biol Chem* 284, no. 22 (May 29): 15126-36. http://dx.doi.org/10.1074/jbc.M809763200.

Huang, Y. Z., and J. O. McNamara. 2010. "Mutual Regulation of Src Family Kinases and the Neurotrophin Receptor Trkb." *J Biol Chem* 285, no. 11 (Mar 12): 8207-17. http://dx.doi.org/10.1074/jbc.M109.091041.

Hunter, C., et al. 2006. "A Hypermutation Phenotype and Somatic Msh6 Mutations in Recurrent Human Malignant Gliomas after Alkylator Chemotherapy." *Cancer Res* 66, no. 8 (Apr 15): 3987-91.

http://dx.doi.org/10.1158/0008-5472.CAN-06-0127.

HUTCHISON, D. J. 1963. "Cross Resistance and Collateral Sensitivity Studies in Cancer Chemotherapy." *Adv Cancer Res* 7: 235-50. http://dx.doi.org/10.1016/s0065-230x(08)60984-7.

Imamovic, L., and M. O. Sommer. 2013. "Use of Collateral Sensitivity Networks to Design Drug Cycling Protocols That Avoid Resistance Development." *Sci Transl Med* 5, no. 204 (Sep 25): 204ra132. http://dx.doi.org/10.1126/scitranslmed.3006609.

Infanger, D. W., et al. 2013. "Glioblastoma Stem Cells Are Regulated by Interleukin-8 Signaling in a Tumoral Perivascular Niche." *Cancer Res* 73, no. 23 (Dec 01): 7079-89. http://dx.doi.org/10.1158/0008-5472.CAN-13-1355.

Irby, R. B., and T. J. Yeatman. 2000. "Role of Src Expression and Activation in Human Cancer." *Oncogene* 19, no. 49 (Nov 20): 5636-42. http://dx.doi.org/10.1038/sj.onc.1203912.

Ishii, N., et al. 1999. "Cells with Tp53 Mutations in Low Grade Astrocytic Tumors Evolve Clonally to Malignancy and Are an Unfavorable Prognostic Factor." *Oncogene* 18, no. 43 (Oct 21): 5870-8. http://dx.doi.org/10.1038/sj.onc.1203241.

Itahana, K., J. Campisi, and G. P. Dimri. 2007. "Methods to Detect Biomarkers of Cellular Senescence: The Senescence-Associated Beta-Galactosidase Assay." *Methods Mol Biol* 371: 21-31. http://dx.doi.org/10.1007/978-1-59745-361-5_3.

Jain, K. K. 2018. "A Critical Overview of Targeted Therapies for Glioblastoma." *Front Oncol* 8: 419. http://dx.doi.org/10.3389/fonc.2018.00419.

Janiszewska, M., et al. 2012. "Imp2 Controls Oxidative Phosphorylation and Is Crucial for Preserving Glioblastoma Cancer Stem Cells." *Genes Dev* 26, no. 17 (Sep 01): 1926-44. http://dx.doi.org/10.1101/gad.188292.112.

Jaraíz-Rodríguez, M., et al. 2017a. "Biotinylated Cell-Penetrating Peptides to Study Intracellular Protein-Protein Interactions." *J Vis Exp*, no. 130 (12 20). http://dx.doi.org/10.3791/56457.

---. 2017b. "A Short Region of Connexin43 Reduces Human Glioma Stem Cell Migration, Invasion, and Survival through Src, Pten, and Fak." *Stem Cell Reports* 9, no. 2 (Aug): 451-463. http://dx.doi.org/10.1016/j.stemcr.2017.06.007.

---. 2020. "Connexin43 Peptide, Tat-Cx43266-283, Selectively Targets Glioma Cells, Impairs Malignant Growth, and Enhances Survival in Mouse Models in Vivo." *Neuro Oncol* 22, no. 4 (04 15): 493-504. http://dx.doi.org/10.1093/neuonc/noz243.

Jin, P., et al. 2018. "Astrocyte-Derived Ccl20 Reinforces Hif-1-Mediated Hypoxic

Responses in Glioblastoma by Stimulating the Ccr6-Nf-Kappab Signaling Pathway." *Oncogene* 37, no. 23 (Jun): 3070-3087. http://dx.doi.org/10.1038/s41388-018-0182-7.

Johanns, T. M., et al. 2016. "Endogenous Neoantigen-Specific Cd8 T Cells Identified in Two Glioblastoma Models Using a Cancer Immunogenomics Approach." *Cancer Immunol Res* 4, no. 12 (12): 1007-1015. http://dx.doi.org/10.1158/2326-6066.CIR-16-0156.

Johnson, J. I., et al. 2001. "Relationships between Drug Activity in Nci Preclinical in Vitro and in Vivo Models and Early Clinical Trials." *Br J Cancer* 84, no. 10 (May 18): 1424-31. http://dx.doi.org/10.1054/bjoc.2001.1796.

Jones, D. T., et al. 2013. "Recurrent Somatic Alterations of Fgfr1 and Ntrk2 in Pilocytic Astrocytoma." *Nat Genet* 45, no. 8 (Aug): 927-32. http://dx.doi.org/10.1038/ng.2682.

Jucker, M., M. Tian, and D. K. Ingram. 1996. "Laminins in the Adult and Aged Brain." *Mol Chem Neuropathol* 28, no. 1-3 (1996 May-Aug): 209-18. http://dx.doi.org/10.1007/BF02815224.

Justicia, C., C. Gabriel, and A. M. Planas. 2000. "Activation of the Jak/Stat Pathway Following Transient Focal Cerebral Ischemia: Signaling through Jak1 and Stat3 in Astrocytes." *Glia* 30, no. 3 (May): 253-70. http://dx.doi.org/10.1002/(sici)1098-1136(200005)30:3<253::aid-glia5>3.0.co;2-o.

Kim, J. E., et al. 2014. "Stat3 Activation in Glioblastoma: Biochemical and Therapeutic Implications." *Cancers (Basel)* 6, no. 1 (Feb 10): 376-95. http://dx.doi.org/10.3390/cancers6010376.

Kim, J. K., et al. 2014. "Tumoral Rankl Activates Astrocytes That Promote Glioma Cell Invasion through Cytokine Signaling." *Cancer Lett* 353, no. 2 (Oct 28): 194-200. http://dx.doi.org/10.1016/j.canlet.2014.07.034.

Kim, L. C., L. Song, and E. B. Haura. 2009. "Src Kinases as Therapeutic Targets for Cancer." *Nat Rev Clin Oncol* 6, no. 10 (Oct): 587-95. http://dx.doi.org/10.1038/nrclinonc.2009.129.

Kitange, G. J., et al. 2009. "Induction of Mgmt Expression Is Associated with Temozolomide Resistance in Glioblastoma Xenografts." *Neuro Oncol* 11, no. 3 (Jun): 281-91. http://dx.doi.org/10.1215/15228517-2008-090.

Knizhnik, A. V., et al. 2013. "Survival and Death Strategies in Glioma Cells: Autophagy, Senescence and Apoptosis Triggered by a Single Type of Temozolomide-Induced Dna Damage." *PLoS One* 8, no. 1: e55665. http://dx.doi.org/10.1371/journal.pone.0055665.

Kong, X., et al. 2017. "Cancer Drug Addiction Is Relayed by an Erk2-Dependent Phenotype Switch." *Nature* 550, no.

7675 (10 12): 270-274. http://dx.doi.org/10.1038/nature24037.

Kraft, A. W., et al. 2013. "Attenuating Astrocyte Activation Accelerates Plaque Pathogenesis in App/Ps1 Mice." *FASEB J* 27, no. 1 (Jan): 187-98. http://dx.doi.org/10.1096/fj.12-208660.

Kumar, N. M., and N. B. Gilula. 1996. "The Gap Junction Communication Channel." *Cell* 84, no. 3 (Feb 09): 381-8. http://dx.doi.org/10.1016/s0092-8674(00)81282-9.

Kuzu, O. F., M. A. Noory, and G. P. Robertson. 2016. "The Role of Cholesterol in Cancer." *Cancer Res* 76, no. 8 (04 15): 2063-70. http://dx.doi.org/10.1158/0008-5472.CAN-15-2613.

Lang, B., et al. 2004. "Astrocytes in Injured Adult Rat Spinal Cord May Acquire the Potential of Neural Stem Cells." *Neuroscience* 128, no. 4: 775-83. http://dx.doi.org/10.1016/j.neuroscience.2004.06.033.

Le, D. M., et al. 2003. "Exploitation of Astrocytes by Glioma Cells to Facilitate Invasiveness: A Mechanism Involving Matrix Metalloproteinase-2 and the Urokinase-Type Plasminogen Activator-Plasmin Cascade." *J Neurosci* 23, no. 10 (May): 4034-43.

Lee, J., et al. 2011. "Non-Invasive Quantification of Brain Tumor-Induced Astrogliosis." *BMC Neurosci* 12 (Jan): 9. http://dx.doi.org/10.1186/1471-2202-12-9.

Lee, J. H., et al. 2018. "Human Glioblastoma Arises from Subventricular Zone Cells with Low-Level Driver Mutations." *Nature* 560, no. 7717 (08): 243-247. http://dx.doi.org/10.1038/s41586-018-0389-3.

Lee, S. Y. 2016. "Temozolomide Resistance in Glioblastoma Multiforme." *Genes Dis* 3, no. 3 (Sep): 198-210. http://dx.doi.org/10.1016/j.gendis.2016.04.007.

Lepore, A. C., et al. 2008. "Selective Ablation of Proliferating Astrocytes Does Not Affect Disease Outcome in Either Acute or Chronic Models of Motor Neuron Degeneration." *Exp Neurol* 211, no. 2 (Jun): 423-32. http://dx.doi.org/10.1016/j.expneurol.2008.02.020.

Li, J., et al. 2022. "Overcoming Temozolomide Resistance in Glioblastoma Via Enhanced Nad." *Cancers (Basel)* 14, no. 15 (Jul 22). http://dx.doi.org/10.3390/cancers14153572.

Liddelow, S. A., et al. 2017. "Neurotoxic Reactive Astrocytes Are Induced by Activated Microglia." *Nature* 541, no. 7638 (Jan 26): 481-487. http://dx.doi.org/10.1038/nature21029.

Liedtke, W., et al. 1998. "Experimental Autoimmune Encephalomyelitis in Mice Lacking Glial Fibrillary Acidic Protein Is Characterized by a More Severe Clinical Course and an Infiltrative Central Nervous System Lesion." *Am J Pathol* 152, no. 1 (Jan): 251-9.

Lin, H., et al. 2017. "Fatty Acid Oxidation Is Required for the Respiration and Proliferation of Malignant Glioma Cells." *Neuro Oncol* 19, no. 1 (01): 43-54. http://dx.doi.org/10.1093/neuonc/now128.

Lin, J. H., et al. 2002. "Connexin 43 Enhances the Adhesivity and Mediates the Invasion of Malignant Glioma Cells." *J Neurosci* 22, no. 11 (Jun 01): 4302-11. http://dx.doi.org/20026450.

Lombardo, L. J., et al. 2004. "Discovery of N-(2-Chloro-6-Methyl- Phenyl)-2-(6-(4-(2-Hydroxyethyl)- Piperazin-1-Yl)-2-Methylpyrimidin-4- Ylamino)Thiazole-5-Carboxamide (Bms-354825), a Dual Src/Abl Kinase Inhibitor with Potent Antitumor Activity in Preclinical Assays." *J Med Chem* 47, no. 27 (Dec 30): 6658-61. http://dx.doi.org/10.1021/jm049486a.

Louis, David N, et al. 2021. "The 2021 Who Classification of Tumors of the Central Nervous System: A Summary." *Neuro-Oncology* 23, no. 8: 1231-1251. http://dx.doi.org/10.1093/neuonc/noab106.

Luberg, K., et al. 2010. "Human Trkb Gene: Novel Alternative Transcripts, Protein Isoforms and Expression Pattern in the Prefrontal Cerebral Cortex During Postnatal Development." *J Neurochem* 113, no. 4 (May): 952-64. http://dx.doi.org/10.1111/j.1471-4159.2010.06662.x.

Macias, M., et al. 2005. "Confocal Visualization of the Effect of Short-Term Locomotor Exercise on Bdnf and Trkb Distribution in the Lumbar Spinal Cord of the Rat: The Enhancement of Bdnf in Dendrites?" *Acta Neurobiol Exp (Wars)* 65, no. 2: 177-82.

Maes, W., and S. W. Van Gool. 2011. "Experimental Immunotherapy for Malignant Glioma: Lessons from Two Decades of Research in the Gl261 Model." *Cancer Immunol Immunother* 60, no. 2 (Feb): 153-60. http://dx.doi.org/10.1007/s00262-010-0946-6.

Marin-Valencia, I., et al. 2012. "Analysis of Tumor Metabolism Reveals Mitochondrial Glucose Oxidation in Genetically Diverse Human Glioblastomas in the Mouse Brain in Vivo." *Cell Metab* 15, no. 6 (Jun 06): 827-37. http://dx.doi.org/10.1016/j.cmet.2012.05.001.

Marques-Torrejon, M. A., E. Gangoso, and S. M. Pollard. 2017. "Modelling Glioblastoma Tumour-Host Cell Interactions Using Adult Brain Organotypic Slice Co-Culture." *Dis Model Mech* (Dec). http://dx.doi.org/10.1242/dmm.031435.

Mathios, D., et al. 2016. "Anti-Pd-1 Antitumor Immunity Is Enhanced by Local and Abrogated by Systemic Chemotherapy in Gbm." *Sci Transl Med* 8, no. 370 (Dec 21): 370ra180. http://dx.doi.org/10.1126/scitranslmed.aag2942.

Meijer, D. H., et al. 2012. "Separated at Birth? The Functional and Molecular Divergence of Olig1 and Olig2." *Nat Rev Neurosci* 13, no. 12 (Dec): 819-31. http://dx.doi.org/10.1038/nrn3386.

Meyer, M., et al. 2015. "Single Cell-Derived Clonal Analysis of Human Glioblastoma Links Functional and Genomic Heterogeneity." *Proc Natl Acad Sci U S A* 112, no. 3 (Jan 20): 851-6. http://dx.doi.org/10.1073/pnas.1320611111.

Middeldorp, J., and E. M. Hol. 2011. "Gfap in Health and Disease." *Prog Neurobiol* 93, no. 3 (Mar): 421-43. http://dx.doi.org/10.1016/j.pneurobio.2011.01.005.

Miller, K. D., et al. 2021. "Brain and Other Central Nervous System Tumor Statistics, 2021." *CA Cancer J Clin* 71, no. 5 (09): 381-406. http://dx.doi.org/10.3322/caac.21693.

Moody, C. L., and R. T. Wheelhouse. 2014. "The Medicinal Chemistry of Imidazotetrazine Prodrugs." *Pharmaceuticals (Basel)* 7, no. 7 (Jul 10): 797-838. http://dx.doi.org/10.3390/ph7070797.

Moss, S. E., and R. O. Morgan. 2004. "The Annexins." *Genome Biol* 5, no. 4: 219. http://dx.doi.org/10.1186/gb-2004-5-4-219.

Murphy, S. F., et al. 2016. "Connexin 43 Inhibition Sensitizes Chemoresistant Glioblastoma Cells to Temozolomide." *Cancer Res* 76, no. 1 (Jan 1): 139-49. http://dx.doi.org/10.1158/0008-5472.can-15-1286.

Nagashima, G., et al. 2002. "Immunohistochemical Analysis of Reactive Astrocytes around Glioblastoma: An Immunohistochemical Study of Postmortem Glioblastoma Cases." *Clin Neurol Neurosurg* 104, no. 2 (May): 125-31. http://dx.doi.org/10.1016/s0303-8467(01)00197-4.

Naus, C. C., et al. 1992. "In Vivo Growth of C6 Glioma Cells Transfected with Connexin43 Cdna." *Cancer Res* 52, no. 15 (Aug 01): 4208-13.

Neftel, C., et al. 2019. "An Integrative Model of Cellular States, Plasticity, and Genetics for Glioblastoma." *Cell* 178, no. 4 (08 08): 835-849.e21. http://dx.doi.org/10.1016/j.cell.2019.06.024.

O'Brien, E. R., C. Howarth, and N. R. Sibson. 2013. "The Role of Astrocytes in Cns Tumors: Pre-Clinical Models and Novel Imaging Approaches." *Front Cell Neurosci* 7: 40. http://dx.doi.org/10.3389/fncel.2013.00040.

Ogura, M., et al. 2012. "Mitochondrial C-Src Regulates Cell Survival through Phosphorylation of Respiratory Chain Components." *Biochem J* 447, no. 2 (Oct 15): 281-9. http://dx.doi.org/10.1042/BJ20120509.

Ohba, S., K. Yamashiro, and Y. Hirose. 2021. "Inhibition of Dna Repair in Combination with Temozolomide or Dianhydrogalactiol Overcomes Temozolomide-Resistant Glioma Cells." *Cancers (Basel)* 13, no. 11 (May 24). http://dx.doi.org/10.3390/cancers13112570.

Ohira, K., et al. 2006. "Trkb-T1 Regulates the Rhoa Signaling and Actin Cytoskeleton in Glioma Cells." *Biochem Biophys Res*

Commun 342, no. 3 (Apr 14): 867-74. http://dx.doi.org/10.1016/j.bbrc.2006.02.033.

---. 2005. "A Truncated Tropomyosin-Related Kinase B Receptor, T1, Regulates Glial Cell Morphology Via Rho Gdp Dissociation Inhibitor 1." *J Neurosci* 25, no. 6 (Feb 09): 1343-53. http://dx.doi.org/10.1523/JNEUROSCI.4436-04.2005.

Okawa, S., et al. 2017. "Proteome and Secretome Characterization of Glioblastoma-Derived Neural Stem Cells." *Stem Cells* 35, no. 4 (04): 967-980. http://dx.doi.org/10.1002/stem.2542.

Oliveira, R., et al. 2005. "Contribution of Gap Junctional Communication between Tumor Cells and Astroglia to the Invasion of the Brain Parenchyma by Human Glioblastomas." *BMC Cell Biol* 6, no. 1 (Feb 16): 7. http://dx.doi.org/10.1186/1471-2121-6-7.

Park, H. K., et al. 2019. "Interplay between Trap1 and Sirtuin-3 Modulates Mitochondrial Respiration and Oxidative Stress to Maintain Stemness of Glioma Stem Cells." *Cancer Res* 79, no. 7 (04 01): 1369-1382. http://dx.doi.org/10.1158/0008-5472.CAN-18-2558.

Patel, A. P., et al. 2014. "Single-Cell Rna-Seq Highlights Intratumoral Heterogeneity in Primary Glioblastoma." *Science* 344, no. 6190 (Jun 20): 1396-401. http://dx.doi.org/10.1126/science.1254257.

Pattwell, S. S., et al. 2020. "A Kinase-Deficient Ntrk2 Splice Variant Predominates in Glioma and Amplifies Several Oncogenic Signaling Pathways." *Nat Commun* 11, no. 1 (06 12): 2977. http://dx.doi.org/10.1038/s41467-020-16786-5.

Pelaz, S. G., et al. 2020. "Targeting Metabolic Plasticity in Glioma Stem Cells in Vitro and in Vivo through Specific Inhibition of C-Src by Tat-Cx43." *EBioMedicine* 62 (Dec): 103134. http://dx.doi.org/10.1016/j.ebiom.2020.103134.

---. 2021. "Impairment of Autophagic Flux Participates in the Antitumor Effects of Tat-Cx43." *Cancers (Basel)* 13, no. 17 (Aug 24). http://dx.doi.org/10.3390/cancers13174262.

Pellegatta, S., et al. 2006. "Dendritic Cells Pulsed with Glioma Lysates Induce Immunity against Syngeneic Intracranial Gliomas and Increase Survival of Tumor-Bearing Mice." *Neurol Res* 28, no. 5 (Jul): 527-31. http://dx.doi.org/10.1179/016164106X116809.

Perrin, S. L., et al. 2019. "Glioblastoma Heterogeneity and the Tumour Microenvironment: Implications for Preclinical Research and Development of New Treatments." *Biochem Soc Trans* 47, no. 2 (04 30): 625-638. http://dx.doi.org/10.1042/BST20180444.

Perry, A., and P. Wesseling. 2016. "Histologic Classification of Gliomas." *Handb Clin Neurol* 134: 71-95.

http://dx.doi.org/10.1016/B978-0-12-802997-8.00005-0.

Persson, A. I., et al. 2010. "Non-Stem Cell Origin for Oligodendroglioma." *Cancer Cell* 18, no. 6 (Dec 14): 669-82. http://dx.doi.org/10.1016/j.ccr.2010.10.033.

Picelli, S. 2019. "Full-Length Single-Cell Rna Sequencing with Smart-Seq2." *Methods Mol Biol* 1979: 25-44. http://dx.doi.org/10.1007/978-1-4939-9240-9_3.

Picelli, S., et al. 2014. "Tn5 Transposase and Tagmentation Procedures for Massively Scaled Sequencing Projects." *Genome Res* 24, no. 12 (Dec): 2033-40. http://dx.doi.org/10.1101/gr.177881.114.

---. 2013. "Smart-Seq2 for Sensitive Full-Length Transcriptome Profiling in Single Cells." *Nat Methods* 10, no. 11 (Nov): 1096-8. http://dx.doi.org/10.1038/nmeth.2639.

Placone, A. L., A. Quiñones-Hinojosa, and P. C. Searson. 2016. "The Role of Astrocytes in the Progression of Brain Cancer: Complicating the Picture of the Tumor Microenvironment." *Tumour Biol* 37, no. 1 (Jan): 61-9. http://dx.doi.org/10.1007/s13277-015-4242-0.

Polański, K., et al. 2020. "Bbknn: Fast Batch Alignment of Single Cell Transcriptomes." *Bioinformatics* 36, no. 3 (02 01): 964-965. http://dx.doi.org/10.1093/bioinformatics/btz625.

Pollard, S. M., et al. 2009. "Glioma Stem Cell Lines Expanded in Adherent Culture Have Tumor-Specific Phenotypes and Are Suitable for Chemical and Genetic Screens." *Cell Stem Cell* 4, no. 6 (Jun): 568-80. http://dx.doi.org/10.1016/j.stem.2009.03.014.

Polo-Hernández, E., et al. 2010. "Oleic Acid Synthesized in the Periventricular Zone Promotes Axonogenesis in the Striatum During Brain Development." *J Neurochem* 114, no. 6 (Sep): 1756-66. http://dx.doi.org/10.1111/j.1471-4159.2010.06891.x.

Poon, C. C., et al. 2017. "Glioblastoma-Associated Microglia and Macrophages: Targets for Therapies to Improve Prognosis." *Brain* 140, no. 6 (Jun 01): 1548-1560. http://dx.doi.org/10.1093/brain/aww355.

Priego, N., et al. 2018. "Stat3 Labels a Subpopulation of Reactive Astrocytes Required for Brain Metastasis." *Nat Med* 24, no. 7 (07): 1024-1035. http://dx.doi.org/10.1038/s41591-018-0044-4.

Pu, P., et al. 2004. "Altered Expression of Cx43 in Astrocytic Tumors." *Clin Neurol Neurosurg* 107, no. 1 (Dec): 49-54. http://dx.doi.org/10.1016/j.clineuro.2004.03.006.

Putri, G. H., et al. 2022. "Analysing High-Throughput Sequencing Data in Python with Htseq 2.0." *Bioinformatics* 38, no. 10 (05 13): 2943-2945. http://dx.doi.org/10.1093/bioinformatics/btac166.

Quail, D. F., and J. A. Joyce. 2017. "The Microenvironmental Landscape of Brain Tumors." *Cancer Cell* 31, no. 3 (Mar 13): 326-341. http://dx.doi.org/10.1016/j.ccell.2017.02.009.

Rath, B. H., et al. 2013. "Astrocytes Enhance the Invasion Potential of Glioblastoma Stem-Like Cells." *PLoS One* 8, no. 1: e54752. http://dx.doi.org/10.1371/journal.pone.0054752.

Ravi, V. M., et al. 2022. "Spatially Resolved Multi-Omics Deciphers Bidirectional Tumor-Host Interdependence in Glioblastoma." *Cancer Cell* 40, no. 6 (06 13): 639-655.e13. http://dx.doi.org/10.1016/j.ccell.2022.05.009.

Reid, J. M., et al. 1997. "Pharmacokinetics of 3-Methyl-(Triazen-1-Yl)Imidazole-4-Carboximide Following Administration of Temozolomide to Patients with Advanced Cancer." *Clin Cancer Res* 3, no. 12 Pt 1 (Dec): 2393-8.

Ren, Z., et al. 2013. "'Hit & Run' Model of Closed-Skull Traumatic Brain Injury (Tbi) Reveals Complex Patterns of Post-Traumatic Aqp4 Dysregulation." *J Cereb Blood Flow Metab* 33, no. 6 (Jun): 834-45. http://dx.doi.org/10.1038/jcbfm.2013.30.

Richards, L. M., et al. 2021. "Gradient of Developmental and Injury Response Transcriptional States Defines Functional Vulnerabilities Underpinning Glioblastoma Heterogeneity." *Nat Cancer* 2, no. 2 (02): 157-173.

http://dx.doi.org/10.1038/s43018-020-00154-9.

Rivers, L. E., et al. 2008. "Pdgfra/Ng2 Glia Generate Myelinating Oligodendrocytes and Piriform Projection Neurons in Adult Mice." *Nat Neurosci* 11, no. 12 (Dec): 1392-401. http://dx.doi.org/10.1038/nn.2220.

Rose, J., et al. 2020. "Mitochondrial Metabolism in Astrocytes Regulates Brain Bioenergetics, Neurotransmission and Redox Balance." *Front Neurosci* 14: 536682. http://dx.doi.org/10.3389/fnins.2020.536682.

Sanai, N., et al. 2004. "Unique Astrocyte Ribbon in Adult Human Brain Contains Neural Stem Cells but Lacks Chain Migration." *Nature* 427, no. 6976 (Feb 19): 740-4. http://dx.doi.org/10.1038/nature02301.

Sanders, S., and W. Debinski. 2020. "Challenges to Successful Implementation of the Immune Checkpoint Inhibitors for Treatment of Glioblastoma." *Int J Mol Sci* 21, no. 8 (Apr 16). http://dx.doi.org/10.3390/ijms21082759.

Sarmiento Soto, M., et al. 2020. "Stat3-Mediated Astrocyte Reactivity Associated with Brain Metastasis Contributes to Neurovascular Dysfunction." *Cancer Res* 80, no. 24 (12 15): 5642-5655. http://dx.doi.org/10.1158/0008-5472.CAN-20-2251.

Satija, Rahul, et al. 2015. "Spatial Reconstruction of Single-Cell Gene Expression Data." *Nature Biotechnology* 33, no. 5 (2015-04-13): 495-502. http://dx.doi.org/doi:10.1038/nbt.3192.

Sato, A., et al. 2011. "Mek-Erk Signaling Dictates Dna-Repair Gene Mgmt Expression and Temozolomide Resistance of Stem-Like Glioblastoma Cells Via the Mdm2-P53 Axis." *Stem Cells* 29, no. 12 (Dec): 1942-51. http://dx.doi.org/10.1002/stem.753.

Schiffer, D., et al. 2018. "The Significance of Chondroitin Sulfate Proteoglycan 4 (Cspg4) in Human Gliomas." *Int J Mol Sci* 19, no. 9 (Sep 12). http://dx.doi.org/10.3390/ijms19092724.

Segerman, A., et al. 2016. "Clonal Variation in Drug and Radiation Response among Glioma-Initiating Cells Is Linked to Proneural-Mesenchymal Transition." *Cell Rep* 17, no. 11 (12 13): 2994-3009. http://dx.doi.org/10.1016/j.celrep.2016.11.056.

Seike, T., et al. 2011. "Interaction between Lung Cancer Cells and Astrocytes Via Specific Inflammatory Cytokines in the Microenvironment of Brain Metastasis." *Clin Exp Metastasis* 28, no. 1 (Jan): 13-25. http://dx.doi.org/10.1007/s10585-010-9354-8.

Shabtay-Orbach, A., et al. 2015. "Paracrine Regulation of Glioma Cells Invasion by Astrocytes Is Mediated by Glial-Derived Neurotrophic Factor." *Int J Cancer* 137, no. 5 (Sep 1): 1012-20. http://dx.doi.org/10.1002/ijc.29380.

Shao, Z., et al. 2011. "Induced Differentiation of Neural Stem Cells of Astrocytic Origin to Motor Neurons in the Rat." *Stem Cells Dev* 20, no. 7 (Jul): 1163-70. http://dx.doi.org/10.1089/scd.2010.0262.

Sherriff, J., et al. 2013. "Patterns of Relapse in Glioblastoma Multiforme Following Concomitant Chemoradiotherapy with Temozolomide." *Br J Radiol* 86, no. 1022 (Feb): 20120414. http://dx.doi.org/10.1259/bjr.20120414.

Shin, Y. J., et al. 2013. "Characterization of Nestin Expression and Vessel Association in the Ischemic Core Following Focal Cerebral Ischemia in Rats." *Cell Tissue Res* 351, no. 3 (Mar): 383-95. http://dx.doi.org/10.1007/s00441-012-1538-x.

Shindo, H., et al. 1993. "Stabilization of C-Myc Protein in Human Glioma Cells." *Acta Neuropathol* 86, no. 4: 345-52. http://dx.doi.org/10.1007/BF00369446.

Shinoura, N., et al. 1996. "Protein and Messenger Rna Expression of Connexin43 in Astrocytomas: Implications in Brain Tumor Gene Therapy." *J Neurosurg* 84, no. 5 (May): 839-45; discussion 846. http://dx.doi.org/10.3171/jns.1996.84.5.0839.

Sidransky, D., et al. 1992. "Clonal Expansion of P53 Mutant Cells Is Associated with Brain Tumour Progression." *Nature* 355, no. 6363 (Feb 27): 846-7. http://dx.doi.org/10.1038/355846a0.

Silva, C. M. 2004. "Role of Stats as Downstream Signal Transducers in Src Family Kinase-Mediated Tumorigenesis." *Oncogene* 23, no. 48 (Oct 18): 8017-23. http://dx.doi.org/10.1038/sj.onc.1208159.

Sin, W. C., S. Crespin, and M. Mesnil. 2012. "Opposing Roles of Connexin43 in

Glioma Progression." *Biochim Biophys Acta* 1818, no. 8 (Aug): 2058-67. http://dx.doi.org/10.1016/j.bbamem.2011.10.022.

Singh, N., et al. 2021. "Mechanisms of Temozolomide Resistance in Glioblastoma - a Comprehensive Review." *Cancer Drug Resist* 4: 17-43. http://dx.doi.org/10.20517/cdr.2020.79.

Slyper, M., et al. 2020. "A Single-Cell and Single-Nucleus Rna-Seq Toolbox for Fresh and Frozen Human Tumors." *Nat Med* 26, no. 5 (05): 792-802. http://dx.doi.org/10.1038/s41591-020-0844-1.

Soeda, A., et al. 2009. "Hypoxia Promotes Expansion of the Cd133-Positive Glioma Stem Cells through Activation of Hif-1alpha." *Oncogene* 28, no. 45 (Nov 12): 3949-59. http://dx.doi.org/10.1038/onc.2009.252.

Sofroniew, M. V., and H. V. Vinters. 2010. "Astrocytes: Biology and Pathology." *Acta Neuropathol* 119, no. 1 (Jan): 7-35. http://dx.doi.org/10.1007/s00401-009-0619-8.

Sorgen, P. L., et al. 2004. "Structural Changes in the Carboxyl Terminus of the Gap Junction Protein Connexin43 Indicates Signaling between Binding Domains for C-Src and Zonula Occludens-1." *J Biol Chem* 279, no. 52 (Dec 24): 54695-701. http://dx.doi.org/10.1074/jbc.M409552200.

Soroceanu, L., T. J. Manning, and H. Sontheimer. 2001. "Reduced Expression of Connexin-43 and Functional Gap Junction Coupling in Human Gliomas."

Glia 33, no. 2 (Feb): 107-17. http://dx.doi.org/10.1002/1098-1136(200102)33:2<107::aid-glia1010>3.0.co;2-4.

Sriram, K., et al. 2004. "Induction of Gp130-Related Cytokines and Activation of Jak2/Stat3 Pathway in Astrocytes Precedes up-Regulation of Glial Fibrillary Acidic Protein in the 1-Methyl-4-Phenyl-1,2,3,6-Tetrahydropyridine Model of Neurodegeneration: Key Signaling Pathway for Astrogliosis in Vivo?" *J Biol Chem* 279, no. 19 (May 7): 19936-47. http://dx.doi.org/10.1074/jbc.M309304200.

Stallcup, W. B., and F. J. Huang. 2008. "A Role for the Ng2 Proteoglycan in Glioma Progression." *Cell Adh Migr* 2, no. 3 (2008 Jul-Sep): 192-201. http://dx.doi.org/10.4161/cam.2.3.6279.

Steindler, D. A., and E. D. Laywell. 2003. "Astrocytes as Stem Cells: Nomenclature, Phenotype, and Translation." *Glia* 43, no. 1 (Jul): 62-9. http://dx.doi.org/10.1002/glia.10242.

Stupp, R., et al. 2005. "Radiotherapy Plus Concomitant and Adjuvant Temozolomide for Glioblastoma." *N Engl J Med* 352, no. 10 (Mar 10): 987-96. http://dx.doi.org/10.1056/NEJMoa043330.

Summy, J. M., and G. E. Gallick. 2003. "Src Family Kinases in Tumor Progression and Metastasis." *Cancer Metastasis Rev* 22, no. 4 (Dec): 337-58. http://dx.doi.org/10.1023/a:1023772912750.

Sun, C., and R. Bernards. 2014. "Feedback and Redundancy in Receptor Tyrosine Kinase Signaling: Relevance to Cancer Therapies." *Trends Biochem Sci* 39, no. 10 (Oct): 465-74. http://dx.doi.org/10.1016/j.tibs.2014.08.010.

Sun, C., et al. 2022. "Inhibiting Src-Mediated Parp1 Tyrosine Phosphorylation Confers Synthetic Lethality to Parp1 Inhibition in Hcc." *Cancer Lett* 526 (02 01): 180-192. http://dx.doi.org/10.1016/j.canlet.2021.11.005.

Suvà, M. L., et al. 2014. "Reconstructing and Reprogramming the Tumor-Propagating Potential of Glioblastoma Stem-Like Cells." *Cell* 157, no. 3 (Apr 24): 580-94. http://dx.doi.org/10.1016/j.cell.2014.02.030.

Szakács, G., et al. 2014. "Targeting the Achilles Heel of Multidrug-Resistant Cancer by Exploiting the Fitness Cost of Resistance." *Chem Rev* 114, no. 11 (Jun 11): 5753-74. http://dx.doi.org/10.1021/cr4006236.

Szatmári, T., et al. 2006. "Detailed Characterization of the Mouse Glioma 261 Tumor Model for Experimental Glioblastoma Therapy." *Cancer Sci* 97, no. 6 (Jun): 546-53. http://dx.doi.org/10.1111/j.1349-7006.2006.00208.x.

Tabernero, A., et al. 2016. "The Role of Connexin43-Src Interaction in Astrocytomas: A Molecular Puzzle." *Neuroscience* 323 (May 26): 183-94. http://dx.doi.org/10.1016/j.neuroscience.2015.02.029.

Tabernero, A., A. Orfao, and J. M. Medina. 1996. "Astrocyte Differentiation in Primary Culture Followed by Flow Cytometry." *Neurosci Res* 24, no. 2 (Jan): 131-8. http://dx.doi.org/10.1016/0168-0102(95)00981-7.

Takasugi, M., et al. 2022. "The Role of Cellular Senescence and Sasp in Tumour Microenvironment." *FEBS J* (Feb 02). http://dx.doi.org/10.1111/febs.16381.

Tang, J. B., et al. 2011. "N-Methylpurine Dna Glycosylase and Dna Polymerase Beta Modulate Ber Inhibitor Potentiation of Glioma Cells to Temozolomide." *Neuro Oncol* 13, no. 5 (May): 471-86. http://dx.doi.org/10.1093/neuonc/nor011.

Thiel, G. 2013. "How Sox2 Maintains Neural Stem Cell Identity." *Biochem J* 450, no. 3 (Mar 15): e1-2. http://dx.doi.org/10.1042/BJ20130176.

Traag, V. A., L. Waltman, and N. J. van Eck. 2019. "From Louvain to Leiden: Guaranteeing Well-Connected Communities." *Sci Rep* 9, no. 1 (03 26): 5233. http://dx.doi.org/10.1038/s41598-019-41695-z.

Tsidulko, A. Y., et al. 2017. "Prognostic Relevance of Ng2/Cspg4, Cd44 and Ki-67 in Patients with Glioblastoma." *Tumour Biol* 39, no. 9 (Sep): 1010428317724282. http://dx.doi.org/10.1177/1010428317724282.

van Tellingen, O., et al. 2015. "Overcoming the Blood-Brain Tumor Barrier for Effective Glioblastoma Treatment." *Drug Resist*

Updat 19 (Mar): 1-12. http://dx.doi.org/10.1016/j.drup.2015.02.002.

Venkatesh, H. S., et al. 2015. "Neuronal Activity Promotes Glioma Growth through Neuroligin-3 Secretion." *Cell* 161, no. 4 (May 7): 803-16. http://dx.doi.org/10.1016/j.cell.2015.04.012.

---. 2017. "Targeting Neuronal Activity-Regulated Neuroligin-3 Dependency in High-Grade Glioma." *Nature* 549, no. 7673 (Sep 28): 533-537. http://dx.doi.org/10.1038/nature24014.

Verhaak, R. G., et al. 2010. "Integrated Genomic Analysis Identifies Clinically Relevant Subtypes of Glioblastoma Characterized by Abnormalities in Pdgfra, Idh1, Egfr, and Nf1." *Cancer Cell* 17, no. 1 (Jan 19): 98-110. http://dx.doi.org/10.1016/j.ccr.2009.12.020.

Viswanathan, V. S., et al. 2017. "Dependency of a Therapy-Resistant State of Cancer Cells on a Lipid Peroxidase Pathway." *Nature* 547, no. 7664 (07 27): 453-457. http://dx.doi.org/10.1038/nature23007.

Vivès, E., P. Brodin, and B. Lebleu. 1997. "A Truncated Hiv-1 Tat Protein Basic Domain Rapidly Translocates through the Plasma Membrane and Accumulates in the Cell Nucleus." *J Biol Chem* 272, no. 25 (Jun 20): 16010-7. http://dx.doi.org/10.1074/jbc.272.25.16010.

Voskuhl, R. R., et al. 2009. "Reactive Astrocytes Form Scar-Like Perivascular Barriers to Leukocytes During Adaptive Immune Inflammation of the Cns." *J Neurosci* 29, no. 37 (Sep 16): 11511-22. http://dx.doi.org/10.1523/JNEUROSCI.1514-09.2009.

Wainwright, D. A., et al. 2014. "Durable Therapeutic Efficacy Utilizing Combinatorial Blockade against Ido, Ctla-4, and Pd-L1 in Mice with Brain Tumors." *Clin Cancer Res* 20, no. 20 (Oct 15): 5290-301. http://dx.doi.org/10.1158/1078-0432.CCR-14-0514.

Wakahara, R., et al. 2012. "Phospho-Ser727 of Stat3 Regulates Stat3 Activity by Enhancing Dephosphorylation of Phospho-Tyr705 Largely through Tc45." *Genes Cells* 17, no. 2 (Feb): 132-45. http://dx.doi.org/10.1111/j.1365-2443.2011.01575.x.

Waldman, A. D., J. M. Fritz, and M. J. Lenardo. 2020. "A Guide to Cancer Immunotherapy: From T Cell Basic Science to Clinical Practice." *Nat Rev Immunol* 20, no. 11 (11): 651-668. http://dx.doi.org/10.1038/s41577-020-0306-5.

Wang, L., and R. Bernards. 2018. "Taking Advantage of Drug Resistance, a New Approach in the War on Cancer." *Front Med* 12, no. 4 (Aug): 490-495. http://dx.doi.org/10.1007/s11684-018-0647-7.

Wang, L., et al. 2018. "An Acquired Vulnerability of Drug-Resistant Melanoma with Therapeutic Potential." *Cell* 173, no. 6 (05 31): 1413-1425.e14. http://dx.doi.org/10.1016/j.cell.2018.04.012.

Wang, X., et al. 2018. "Reciprocal Signaling between Glioblastoma Stem Cells and Differentiated Tumor Cells Promotes Malignant Progression." *Cell Stem Cell* 22, no. 4 (Apr 5): 514-528.e5. http://dx.doi.org/10.1016/j.stem.2018.03.011.

---. 2021. "Sequential Fate-Switches in Stem-Like Cells Drive the Tumorigenic Trajectory from Human Neural Stem Cells to Malignant Glioma." *Cell Res* 31, no. 6 (06): 684-702. http://dx.doi.org/10.1038/s41422-020-00451-z.

Wang, Y., et al. 2017. "Promoting Oligodendroglial-Oriented Differentiation of Glioma Stem Cell: A Repurposing of Quetiapine for the Treatment of Malignant Glioma." *Oncotarget* 8, no. 23 (Jun 06): 37511-37524. http://dx.doi.org/10.18632/oncotarget.16400.

Watkins, S., et al. 2014. "Disruption of Astrocyte-Vascular Coupling and the Blood-Brain Barrier by Invading Glioma Cells." *Nat Commun* 5 (Jun 19): 4196. http://dx.doi.org/10.1038/ncomms5196.

Wei, J., et al. 2019. "Osteopontin Mediates Glioblastoma-Associated Macrophage Infiltration and Is a Potential Therapeutic Target." *J Clin Invest* 129, no. 1 (01 02): 137-149. http://dx.doi.org/10.1172/JCI121266.

Weinstein, I. B. 2002. "Cancer. Addiction to Oncogenes--the Achilles Heal of Cancer." *Science* 297, no. 5578 (Jul 05): 63-4. http://dx.doi.org/10.1126/science.1073096.

Weiss, N., et al. 2009. "The Blood-Brain Barrier in Brain Homeostasis and Neurological Diseases." *Biochim Biophys Acta* 1788, no. 4 (Apr): 842-57. http://dx.doi.org/10.1016/j.bbamem.2008.10.022.

Weissenberger, J., et al. 1997. "Development and Malignant Progression of Astrocytomas in Gfap-V-Src Transgenic Mice." *Oncogene* 14, no. 17 (May 01): 2005-13. http://dx.doi.org/10.1038/sj.onc.1201168.

Wen, Z., Z. Zhong, and J. E. Darnell. 1995. "Maximal Activation of Transcription by Stat1 and Stat3 Requires Both Tyrosine and Serine Phosphorylation." *Cell* 82, no. 2 (Jul 28): 241-50. http://dx.doi.org/10.1016/0092-8674(95)90311-9.

Woroniecka, K., and P. E. Fecci. 2018. "T-Cell Exhaustion in Glioblastoma." *Oncotarget* 9, no. 82 (Oct 19): 35287-35288. http://dx.doi.org/10.18632/oncotarget.26228.

Wu, G., et al. 2014. "The Genomic Landscape of Diffuse Intrinsic Pontine Glioma and Pediatric Non-Brainstem High-Grade Glioma." *Nat Genet* 46, no. 5 (May): 444-450. http://dx.doi.org/10.1038/ng.2938.

Xiong, J., et al. 2015. "Mature Brain-Derived Neurotrophic Factor and Its Receptor Trkb Are Upregulated in Human Glioma Tissues." *Oncol Lett* 10, no. 1 (Jul): 223-

227. http://dx.doi.org/10.3892/ol.2015.3181.

---. 2013. "Mature Bdnf Promotes the Growth of Glioma Cells in Vitro." *Oncol Rep* 30, no. 6 (Dec): 2719-24. http://dx.doi.org/10.3892/or.2013.2746.

Xiong, X. Y., Y. Tang, and Q. W. Yang. 2022. "Metabolic Changes Favor the Activity and Heterogeneity of Reactive Astrocytes." *Trends Endocrinol Metab* 33, no. 6 (06): 390-400. http://dx.doi.org/10.1016/j.tem.2022.03.001.

Xu, M., et al. 2014. "Mouse Glioma Immunotherapy Mediated by A2b5+ Gl261 Cell Lysate-Pulsed Dendritic Cells." *J Neurooncol* 116, no. 3 (Feb): 497-504. http://dx.doi.org/10.1007/s11060-013-1334-9.

Yang, H., et al. 2009. "De-Differentiation Response of Cultured Astrocytes to Injury Induced by Scratch or Conditioned Culture Medium of Scratch-Insulted Astrocytes." *Cell Mol Neurobiol* 29, no. 4 (Jun): 455-73. http://dx.doi.org/10.1007/s10571-008-9337-3.

---. 2012. "Sonic Hedgehog Released from Scratch-Injured Astrocytes Is a Key Signal Necessary but Not Sufficient for the Astrocyte De-Differentiation." *Stem Cell Res* 9, no. 2 (Sep): 156-66. http://dx.doi.org/10.1016/j.scr.2012.06.002.

Yang, J., et al. 2020. "Phospho-Ser727 Triggers a Multistep Inactivation of Stat3 by Rapid Dissociation of Py705-Sh2 through C-Terminal Tail Modulation." *Int Immunol* 32, no. 2 (02 07): 73-88. http://dx.doi.org/10.1093/intimm/dxz061.

Yi, L., et al. 2013. "Implantation of Gl261 Neurospheres into C57/Bl6 Mice: A More Reliable Syngeneic Graft Model for Research on Glioma-Initiating Cells." *Int J Oncol* 43, no. 2 (Aug): 477-84. http://dx.doi.org/10.3892/ijo.2013.1962.

Yoshimura, A., T. Naka, and M. Kubo. 2007. "Socs Proteins, Cytokine Signalling and Immune Regulation." *Nat Rev Immunol* 7, no. 6 (Jun): 454-65. http://dx.doi.org/10.1038/nri2093.

Young, R. M., et al. 2015. "Current Trends in the Surgical Management and Treatment of Adult Glioblastoma." *Ann Transl Med* 3, no. 9 (Jun): 121. http://dx.doi.org/10.3978/j.issn.2305-5839.2015.05.10.

Yu, H., M. Kortylewski, and D. Pardoll. 2007. "Crosstalk between Cancer and Immune Cells: Role of Stat3 in the Tumour Microenvironment." *Nat Rev Immunol* 7, no. 1 (Jan): 41-51. http://dx.doi.org/10.1038/nri1995.

Yu, H., D. Pardoll, and R. Jove. 2009. "Stats in Cancer Inflammation and Immunity: A Leading Role for Stat3." *Nat Rev Cancer* 9, no. 11 (Nov): 798-809. http://dx.doi.org/10.1038/nrc2734.

Yu, S. C., et al. 2012. "Connexin 43 Reverses Malignant Phenotypes of Glioma Stem Cells by Modulating E-Cadherin." *Stem Cells* 30, no. 2 (Feb): 108-20. http://dx.doi.org/10.1002/stem.1685.

Zamanian, J. L., et al. 2012. "Genomic Analysis of Reactive Astrogliosis." *J Neurosci* 32, no. 18 (May 2): 6391-410. http://dx.doi.org/10.1523/jneurosci.6221-11.2012.

Zanin, J. P., et al. 2019. "The P75 Neurotrophin Receptor Facilitates Trkb Signaling and Function in Rat Hippocampal Neurons." *Front Cell Neurosci* 13: 485. http://dx.doi.org/10.3389/fncel.2019.00485.

Zeisel, A., et al. 2018. "Molecular Architecture of the Mouse Nervous System." *Cell* 174, no. 4 (08 09): 999-1014.e22. http://dx.doi.org/10.1016/j.cell.2018.06.021.

Zhai, Y., et al. 2020. "Single-Cell Rna-Sequencing Shift in the Interaction Pattern between Glioma Stem Cells and Immune Cells During Tumorigenesis." *Front Immunol* 11: 581209. http://dx.doi.org/10.3389/fimmu.2020.581209.

Zhao, B., et al. 2016. "Exploiting Temporal Collateral Sensitivity in Tumor Clonal Evolution." *Cell* 165, no. 1 (Mar 24): 234-246. http://dx.doi.org/10.1016/j.cell.2016.01.045.

Zhao, Z., et al. 2015. "Establishment and Dysfunction of the Blood-Brain Barrier." *Cell* 163, no. 5 (Nov 19): 1064-1078. http://dx.doi.org/10.1016/j.cell.2015.10.067.

Zhu, D., et al. 1991. "Transfection of C6 Glioma Cells with Connexin 43 Cdna: Analysis of Expression, Intercellular Coupling, and Cell Proliferation." *Proc Natl Acad Sci U S A* 88, no. 5 (Mar 01): 1883-7. http://dx.doi.org/10.1073/pnas.88.5.1883.

Zhu, X., D. E. Bergles, and A. Nishiyama. 2008. "Ng2 Cells Generate Both Oligodendrocytes and Gray Matter Astrocytes." *Development* 135, no. 1 (Jan): 145-57. http://dx.doi.org/10.1242/dev.004895.

Zong, Hui, Roel GW Verhaak, and Peter Canoll. 2014. "The Cellular Origin for Malignant Glioma and Prospects for Clinical Advancements." *http://dx.doi.org/10.1586/erm.12.30* (9 Jan 2014). http://dx.doi.org/10.1586/erm.12.30.

Connexin43 peptide, TAT-Cx43$_{266–283}$, selectively targets glioma cells, impairs malignant growth, and enhances survival in mouse models in vivo

Myriam Jaraíz-Rodríguez,* Rocío Talaverón,* Laura García-Vicente, Sara G. Pelaz, Marta Domínguez-Prieto, Andrea Álvarez-Vázquez, Raquel Flores-Hernández, Wun Chey Sin, John Bechberger, José M. Medina, Christian C. Naus, and Arantxa Tabernero

Department of Biochemistry and Molecular Biology, Institute of Neurosciences Castilla y León (INCYL), University of Salamanca, Salamanca, Spain (M.J-R., R.T., L.G-V., S.G.P., M.D-P., A.A-V., R.F-H., J.M.M., A.T.); Department of Cellular and Physiological Sciences, The Life Sciences Institute, University of British Columbia, Vancouver, British Columbia, Canada (W.C.S., J.B., C.C.N.)

*These authors contributed equally to this work.

Corresponding Author: Arantxa Tabernero, Departamento de Bioquímica y Biología Molecular, Instituto de Neurociencias de Castilla y León Castilla y León (INCYL), Universidad de Salamanca, C/ Pintor Fernando Gallego 1, 37007 Salamanca, Spain (ataber@usal.es).

Abstract

Background. Malignant gliomas are the most frequent primary brain tumors and remain among the most incurable cancers. Although the role of the gap junction protein, connexin43 (Cx43), has been deeply investigated in malignant gliomas, no compounds have been reported with the ability to recapitulate the tumor suppressor properties of this protein in in vivo glioma models.

Methods. TAT-Cx43$_{266–283}$ a cell-penetrating peptide which mimics the effect of Cx43 on c-Src inhibition, was studied in orthotopic immunocompetent and immunosuppressed models of glioma. The effects of this peptide in brain cells were also analyzed.

Results. While glioma stem cell malignant features were strongly affected by TAT-Cx43$_{266–283}$, these properties were not significantly modified in neurons and astrocytes. Intraperitoneally administered TAT-Cx43$_{266–283}$ decreased the invasion of intracranial tumors generated by GL261 mouse glioma cells in immunocompetent mice. When human glioma stem cells were intracranially injected with TAT-Cx43$_{266–283}$ into immunodeficient mice, there was reduced expression of the stemness markers nestin and Sox2 in human glioma cells at 7 days post-implantation. Consistent with the role of Sox2 as a transcription factor required for tumorigenicity, TAT-Cx43$_{266–283}$ reduced the number and stemness of human glioma cells at 30 days post-implantation. Furthermore, TAT-Cx43$_{266–283}$ enhanced the survival of immunocompetent mice bearing gliomas derived from murine glioma stem cells.

Conclusion. TAT-Cx43$_{266–283}$ reduces the growth, invasion, and progression of malignant gliomas and enhances the survival of glioma-bearing mice without exerting toxicity in endogenous brain cells, which suggests that this peptide could be considered as a new clinical therapy for high-grade gliomas.

Key Points

1. Connexin43 peptide, TAT-Cx43$_{266–283}$, selectively targets glioma cells.

2. TAT-Cx43$_{266–283}$ impairs malignant glioma growth and enhances survival in mouse models in vivo.

Importance of the Study

Malignant gliomas are the most frequent and aggressive primary brain tumors. Here, we reveal that TAT-Cx43$_{266-283}$, an inhibitor of Src based on connexin43, selectively targets glioma cells, impairs the growth of these tumors in vivo, and enhances the survival of glioma-bearing mice. While glioma cells were strongly affected by TAT-Cx43$_{266-283}$, the toxicity in neurons and astrocytes was notably lower than that found with dasatinib, another c-Src inhibitor currently used in glioma clinical trials. Intraperitoneally administered TAT-Cx43$_{266-283}$ decreased the invasion of intracranial tumors generated by murine glioma cells in immunocompetent mice. When human glioma stem cells were intracranially injected with TAT-Cx43$_{266-283}$ into immunosuppressed mice, there was reduced expression of stemness markers and reduced tumorigenicity of these glioma cells. Furthermore, TAT-Cx43$_{266-283}$ enhanced the survival of immunocompetent mice bearing gliomas derived from murine glioma stem cells. Our results highlight the importance of this compound for the design of new therapies against gliomas.

Malignant gliomas are among the most incurable cancers, with a median survival rate of 1–2 years.[1] These tumors are composed of a heterogeneous population of cells, including many with stem cell–like properties, called glioma stem cells (GSCs). GSCs are characterized by their self-renewal capacity, high oncogenic potential, resistance to standard therapies,[2,3] and high invasive capacity.[4,5]

Connexin43 (Cx43) is a protein that forms gap junction channels and hemichannels playing important roles in cellular communication.[6] Cx43 interacts with a plethora of intracellular signaling partners,[7] such as c-Src,[8] which is a proto-oncogene that regulates a wide range of cellular events related to cancer.[9–11] Indeed, in astrocytes, ectopic expression of v-Src, the active viral form of Src, promotes the development of astrocytomas.[12]

In the context of gliomas, Cx43 has been traditionally considered a tumor suppressor protein because it is downregulated in malignant glioma cells,[13–16] including GSCs,[17–19] compared with astrocytes,[20] and because the ectopic expression of Cx43 in glioma cells reduces their rate of proliferation[21] and tumor formation in vivo.[22] Among other mechanisms, Cx43 exerts its antitumor effects through the recruitment of c-Src together with its endogenous inhibitors, C-terminal Src kinase (CSK) and phosphatase and tensin homolog (PTEN), which inhibit the activity of c-Src.[23,24] Because c-Src is overactivated in malignant gliomas,[25] the ectopic expression of Cx43 might have beneficial effects on glioma therapy. However, connexins can also play pro-tumorigenic roles in glioma.[25] Indeed, Cx46 is upregulated in GSCs and required for their maintenance.[17] In addition, restoration of Cx43 in glioma cells can favor glioma invasion.[26,27] These studies indicate that very specific Cx-related tools should be used to target glioma.

Consequently, instead of the whole protein we used the region of Cx43 responsible for Src inhibition[18] (amino acids 266 to 283), fused to the transactivator of transcription (TAT) cell-penetrating sequence (TAT-Cx43$_{266-283}$). We found that TAT-Cx43$_{266-283}$ retained the ability to recruit c-Src, CSK, and PTEN,[24] leading to c-Src inhibition in a broad spectrum of glioma cells. TAT-Cx43$_{266-283}$, by inhibiting c-Src, reduces the expression of markers of stemness, such as Sox2, neurosphere formation, proliferation, migration, and invasion in GSCs, including primary GSCs derived from patients and freshly removed surgical specimens.[18,28]

However, TAT-Cx43$_{266-283}$ toxicity in nontumor cells and in vivo effects remain unknown, hampering potential clinical applications. Therefore, in this study we explored the effects of TAT-Cx43$_{266-283}$ in neurons and astrocytes and compared them with those of other c-Src inhibitors currently being evaluated in clinical trials (https://clinicaltrials.gov/ct2/show/NCT00895960, https://clinicaltrials.gov/ct2/show/NCT00423735, and https://clinicaltrials.gov/ct2/study/NCT00892177). Once we confirmed the lack of toxic effects of TAT-Cx43$_{266-283}$ in healthy brain cells, we investigated the antitumor effects of TAT-Cx43$_{266-283}$ in vivo in 3 mouse models of glioma using mouse glioma cells, mouse GSCs, and human GSCs.

Methods

For details of media and protocols, see the Supplementary Material.

Animals

Albino Wistar rats, nonobese diabetic/severe combined immunodeficient (NOD/SCID) mice, and C57BL/6 mice were obtained from the animal facility of the University of Salamanca and the University of British Columbia. The animal procedures were approved by the ethics committee of the University of Salamanca and the Junta de Castilla y León and were carried out in accordance with European Community Council directives (2010/63/UE), Spanish law (RD 53/2013 BOE 34/11370–420, 2013) for the use and care of laboratory animals, and the University of British Columbia Animal Care Committee (protocol number: A14-0183) and performed in accordance with the guidelines established by the Canadian Council on Animal Care.

Cell Culture

Primary astrocytes and neurons were cultured as described.[29] Human G166 GSCs were obtained from Dr Steven Pollard (Medical Research Council Centre for Regenerative Medicine, University of Edinburgh) or BioRep (Milan, Italy)

and cultured in adherent conditions.[28] For the indicated experiments, cells were labeled with 2 μL/mL PKH26 (Red Fluorescent Cell kit, Sigma-Aldrich) for 5 min. GL261-GSCs were obtained from GL261 cells as previously described.[30]

For GSC-astrocyte cocultures, 25 000 GSCs/cm^2 were cultured on top of confluent astrocytes and allowed to integrate for 72 h.

Mouse GL261 glioma cells (National Cancer Institute–Frederick Division of Cancer Treatment and Diagnosis) and GSCs were transfected with pcDNA-mCherry plasmid using Lipofectamine 2000 (Invitrogen) as described.[26]

Organotypic Brain Slice Cultures

Organotypic brain slice cultures were prepared as described.[31] 350-μm-thick newborn rat brain slices were cultured onto cell culture inserts for 19–20 days in vitro. For GSC-organotypic brain slice cocultures, 2500 PKH26-labeled GSCs were placed onto each brain slice and allowed to engraft for 2 days prior to the experiment.

Intracranial Implantation of Glioma Cells

One microliter of saline containing 5000 cells was injected by a unilateral stereotaxic intracerebral injection into the right cortex with a Hamilton microsyringe. Murine mCherry-GL261 glioma cells or murine mCherry-GL261-GSCs were injected into C57BL/6 while human GSCs labeled with PKH26 were injected into NOD/SCID mice. At the indicated times, animals were transcardially perfused and brains were processed to obtain 20- to 40-μm-thick coronal sections.

Treatments

Peptides (>85% pure) were obtained from GenScript. For ex vivo and in vitro studies, the peptides and the c-Src inhibitor dasatinib (Selleck Chemicals) were used at the specified concentrations in culture medium at 37°C for the indicated times.

For in vivo studies, saline, TAT, or TAT-Cx43$_{266–283}$ were intraperitoneally injected or intracranially co-injected with GSCs at the specified concentrations and times.

Immunofluorescence

For in vitro and ex vivo studies, samples were subjected to immunocytochemistry for glial fibrillary acidic protein (GFAP), microtubule-associated protein 2 (MAP-2), human nestin, and 4′,6′-diamidino-2-phenylindole (DAPI) or TO-PRO-3 as previously described.[18] For in vivo studies, tumor sections were subjected to immunohistochemistry for human nestin, Sox2, Stem121, PTEN, Src (Y416), and activated caspase-3.

MTT Assay

Cells were incubated with culture medium containing 0.5 mg/mL MTT (3-(4,5-dimethylthiazol-2-yl)-2,5-diphenyltetrazolium bromide) (Sigma-Aldrich). After 10 min in dimethyl sulfoxide (DMSO), the absorbance was measured at 570 nm.

Matrigel Invasion Assay

750 000 cells were plated into the upper chamber and were allowed to invade Matrigel for 15 h. Cells in the lower surface were counted in 10 random fields per insert.

Quantification of the Invasiveness of Intracranial Tumors

The invasiveness of mCherry-GL261 cells was determined using Fiji software by quantifying the fractal dimension (D) of the tumor rims.[32,33] We blindly determined the D by thresholding the mCherry fluorescence images, establishing the tumor rims, and quantifying D using FracLac (Fiji) in at least 3 separate sections per animal.

Statistical Analyses

Student's *t*-test was used when 2 groups were compared. For more than 2 groups, one-way ANOVA was used, followed by a post hoc test (Tukey). The survival of glioma-bearing mice was analyzed by Kaplan–Meier curves and differences were compared by log-rank test analysis.

Results

TAT-Cx43$_{266–283}$ Selectively Targets GSCs Without Toxic Effects in Neurons and Astrocytes

To analyze TAT-Cx43$_{266–283}$ internalization, GSCs, astrocytes, and neurons in culture were exposed to increasing concentrations of TAT-Cx43$_{266–283}$ fused to biotin (TAT-Cx43$_{266–283}$-B) for 5 min. TAT-Cx43$_{266–283}$-B was internalized by astrocytes and more efficiently by GSCs, but not significantly by neurons (Fig. 1A–C and Supplementary Figure 1). To confirm these results, we used an ex vivo model of brain tumors.[34,35] PKH26-labeled GSCs were placed into brain slices (Fig. 1D), which were incubated with TAT-Cx43$_{266–283}$-B for 5 min. TAT-Cx43$_{266–283}$-B was internalized by GSCs within the brain parenchyma and by brain cells surrounding tumor cells (Fig. 1E; for complete Z-stack, see Supplementary Movie 1).

In agreement with our previous results,[24,28] TAT-Cx43$_{266–283}$ reduced GSC growth (Fig. 2A). However, we observed no differences in the morphology of neurons (Fig. 2B and Supplementary Figure 2A) or astrocytes (Fig. 2C and Supplementary Figure 2B). In fact, the expression of MAP-2 and GFAP, neuronal and astrocytic markers, respectively, was not affected by TAT-Cx43$_{266–283}$ (Fig. 2B, C). Moreover, time-lapse imaging of neurons in culture showed that neuron and neurite development was very similar among control, TAT-, or TAT-Cx43$_{266–283}$–treated cultures (Supplementary Movies 2, 3, and 4, respectively). TAT-Cx43$_{266–283}$ reduced GSC viability by about 60% (Fig. 2D), whereas neuronal viability remained unaffected and astrocyte viability was only slightly decreased (by about 15%). To confirm
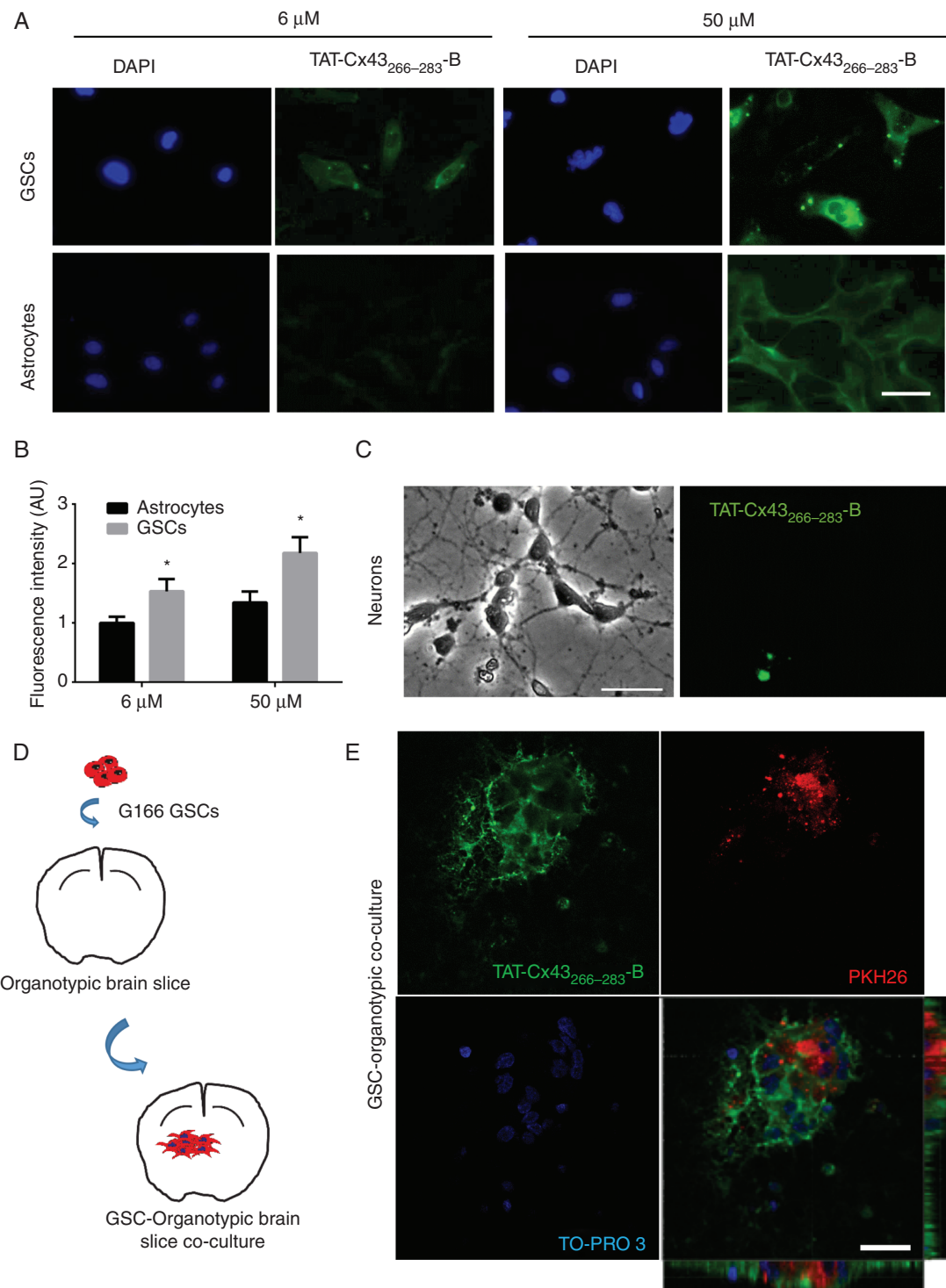
Fig. 1 TAT-Cx43$_{266-283}$ internalization in GSCs, neurons, and astrocytes. (A–C) Cells incubated with TAT-Cx43$_{266-283}$ fused to biotin at the C-terminus (TAT-Cx43$_{266-283}$-B) for 5 min and revealed with streptavidin. TAT-Cx43$_{266-283}$ (green) and DAPI (blue) staining of the same field. (A) Internalization of 6 and 50 µM TAT-Cx43$_{266-283}$-B in GSCs and astrocytes. Bar: 100 µm. (B) Quantification of TAT-Cx43$_{266-283}$-B fluorescence expressed as arbitrary units (AU) and the mean ± SEM of 3 independent experiments (*t*-test: *$P < 0.05$). (C) Images from the same field showing the lack of internalization in neurons incubated with 50 µM of TAT-Cx43$_{266-283}$-B for 5 min. Bar: 50 µm. (D) Scheme for GSC–organotypic brain slice cocultures. (E) Cocultures incubated with 50 µM TAT-Cx43$_{266-283}$-B for 5 min. TAT-Cx43$_{266-283}$-B internalization (green) in GSCs (PKH26 [red]) and surrounding cells (nuclear staining, TO-PRO-3 [blue]). Bar: 25 µm. See also Supplementary Movie 1 showing the complete Z-stack.
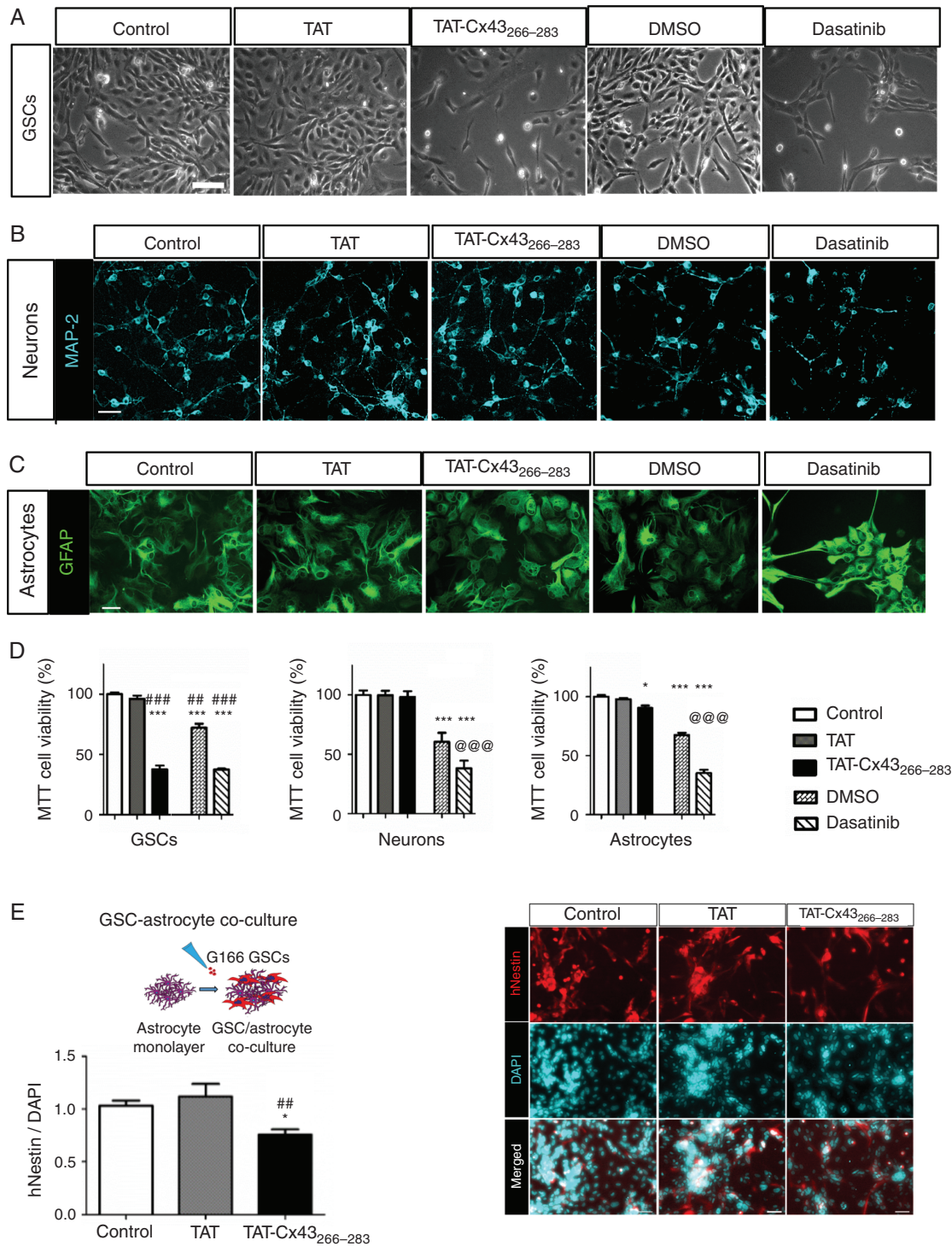
Fig. 2 Effect of TAT-Cx43$_{266-283}$ and dasatinib on cell viability in GSCs, neurons, and astrocytes. Cells treated with 50 µM TAT, 50 µM TAT-Cx43$_{264-283}$, 1 µM of the c-Src inhibitor dasatinib, or 0.1% (v/v) DMSO (vehicle for dasatinib) for 72 h. Three independent experiments were carried out with similar results. (A) Images showing the reduction in GSC viability induced by TAT-Cx43$_{264-283}$ and dasatinib. Bar: 100 µm. (B) Immunofluorescence for MAP-2 (turquoise) in neurons showing a reduction in MAP-2 by dasatinib. Bar: 50 µm. (C) Immunofluorescence for GFAP (green) in astrocytes showing an alteration induced by dasatinib. Bar: 50 µm. (D) MTT results expressed as the percentage of the control; mean ± SEM; $n \geq 3$ (ANOVA: *$P < 0.05$, ***$P < 0.001$ vs control; #$P < 0.05$, ##$P < 0.01$, ###$P < 0.001$ vs TAT; @@@$P < 0.001$ vs DMSO). (E) GSC–astrocyte cocultures treated with 50 µM TAT or TAT-Cx43$_{266-283}$ for 72 h. Images showing human nestin (hNestin, red) expressed by GSCs and DAPI nuclear staining (turquoise) of GSCs and astrocytes (right). Bar: 50 µm. Left, quantification of the nestin-positive cells vs DAPI (total cells); mean ± SEM; $n = 3$ (ANOVA: *$P < 0.05$ vs control and ##$P < 0.01$ vs TAT).

these results, we analyzed the effect of TAT-Cx43$_{266–283}$ in a GSC-astrocyte coculture. Our results showed that TAT-Cx43$_{266–283}$ specifically decreased the growth of GSCs (Fig. 2E), because the number of cells expressing human nestin over the total number of cells decreased by about 25%.

Because the effect of TAT-Cx43$_{266–283}$ is exerted through inhibition of the oncogenic activity of c-Src,[18] we compared the effect of TAT-Cx43$_{266–283}$ with that of dasatinib, a well-known inhibitor of this tyrosine kinase.[36] Both exerted a similar reduction in GSC growth (about 60%; Fig. 2A, D). However, while TAT-Cx43$_{266–283}$ did not affect neurons or astrocytes, dasatinib affected neuronal and astrocyte morphology, reducing MAP-2–positive neurites (Fig. 2B) and increasing GFAP staining (Fig. 2C), suggesting neuronal damage and increased astrocytic reactivity, respectively. MTT assays confirmed that dasatinib reduced the viability of neurons and astrocytes by about 30% and 50%, respectively (Fig. 2D).

We have shown that TAT-Cx43$_{266–283}$ strongly reduces the migration and invasion of GSCs through inhibition of c-Src and focal adhesion kinase (FAK).[28] The present study revealed that TAT-Cx43$_{266–283}$ did not modify neuron or astrocyte migration, as shown by neuronal motility (Supplementary Movies 2, 3, and 4) and by wound-healing assays performed in astrocytes (Supplementary Figure 3A, B). This is consistent with the lack of effect of TAT-Cx43$_{266–283}$ on FAK activity found in astrocytes, in contrast to the effect in glioma cells[28] (Supplementary Figure 3C). However, dasatinib significantly reduced astrocyte migration (Supplementary Figure 3A, B).

Altogether, these data suggest a specific effect of TAT-Cx43$_{266–283}$ on GSCs, with lower toxicity in healthy brain cells than another c-Src inhibitor.

TAT-Cx43$_{266–283}$ Reduces the Invasion of GL261 Glioma Cells In Vivo

To address the effects of TAT-Cx43$_{266–283}$ on glioma invasion in vivo, we selected the same model that showed a proinvasive effect of Cx43[26] consisting in the intracranial injection of mCherry-GL261 cells in C57BL/6 mice.

First, we analyzed the effect in vitro. While mCherry-GL261 cell growth was not modified (Fig. 3A), cell invasion was strongly reduced by TAT-Cx43$_{266–283}$ (Fig. 3B), which is consistent with the reduction in FAK activity (Supplementary Figure 3C). To analyze the effect in vivo, 1 week after tumor implantation TAT-Cx43$_{266–283}$ was intraperitoneally injected (Fig. 3C). After 15 days, TAT-Cx43$_{266–283}$ reduced the complexity of the tumor borders (Fig. 3D). Indeed, TAT-Cx43$_{266–283}$ significantly reduced the fractal dimension values of the tumor borders (Fig. 3E), an index of tumor invasion,[32] suggesting a reduction in tumor invasion. Although no effects were found in PTEN expression in vitro (Supplementary Figure 3C) and in vivo (Supplementary Figure 4A, B), the activity of Src (Y416 Src) was reduced by TAT-Cx43$_{266–283}$ in vivo (Supplementary Figure 4C), indicating that TAT-Cx43$_{266–283}$ reduced the activity of the Src–FAK axis with the subsequent effects in glioma cell invasion in vivo.

TAT-Cx43$_{266–283}$ Reverses the Human GSC Phenotype and Reduces GSC Tumorigenicity In Vivo

To address the effect of TAT-Cx43$_{266–283}$ on the stemness of human GSCs in vivo, PKH26-labeled human GSCs were intracranially injected together with TAT or TAT-Cx43$_{266–283}$ into the brains of NOD/SCID mice (Fig. 4A). Seven days after implantation, the levels of Sox2 and human nestin were analyzed in GSCs (Fig. 4B). We found that TAT-Cx43$_{266–283}$ strongly decreased their expression (white arrows indicate some examples; see also Supplementary Figure 5, in which the nuclear staining facilitates the distinction). Indeed, human nestin and Sox2 fluorescence levels were decreased by about 75% with TAT-Cx43$_{266–283}$.

Reduced expressions of Sox2 and nestin suggest that TAT-Cx43$_{266–283}$ decreases the stemness of the implanted GSCs in vivo. Therefore, we followed up the in vivo experiments for 30 days to analyze the tumorigenicity of GSCs. To identify human GSCs, in addition to PKH26, antibodies against the human antigen Stem121 were used[35] and the expression of human nestin was analyzed as a marker of stemness in human xenografted cells. According to the reported GSC tumorigenicity,[37] at 1 month postimplantation, we found GSCs that were able to engraft, proliferate, and migrate within the brain parenchyma in both TAT-treated (Fig. 4C, D) and control (Supplementary Figures 6, 7, 8) animals. However, TAT-Cx43$_{266–283}$ reduced the number of PKH26-labeled and Stem121-positive cells 1 month after implantation (Fig. 4C and Supplementary Figure 7), suggesting reduced GSC survival and/or proliferation under these conditions. Indeed, the analysis of activated caspase-3 suggested an increased cell death in the tumor area after TAT-Cx43$_{266–283}$ treatment, without effect in other brain areas, such as the subventricular zone (Supplementary Figure 9). Furthermore, those few remaining PKH26-labeled cells expressed low levels of human nestin (Fig. 4D and Supplementary Figure 8), suggesting the loss of stemness upon TAT-Cx43$_{266–283}$ treatment. No significant differences were found when TAT treatment was compared with the control condition (Supplementary Figure 6).

TAT-Cx43$_{266–283}$ Prolongs the Survival of Glioma-Bearing Mice

To study the effect of TAT-Cx43$_{266–283}$ on the survival of glioma-bearing mice, we combined the 2 in vivo models previously described. We isolated the highly tumorigenic subpopulation of GSCs from GL261 glioma cells (GL261-GSCs) because they generate more aggressive tumors with shorter mouse survival than their differentiated counterparts in an immunocompetent environment.[30,38] Our results showed that GL261-GSCs exhibited higher Src activity and Sox2 levels than their differentiated counterpart GL261 (Fig. 5A), consistent with the role of Src in Sox2 expression and stemness.[11] We confirmed that TAT-Cx43$_{266–283}$ reduced both Src activity and Sox2 expression in GL261-GSCs in vitro (Fig. 5B), as shown in human GSCs.[18] Then, GL261-GSCs were intracranially injected together with saline or TAT-Cx43$_{266–283}$ into the brains of immunocompetent
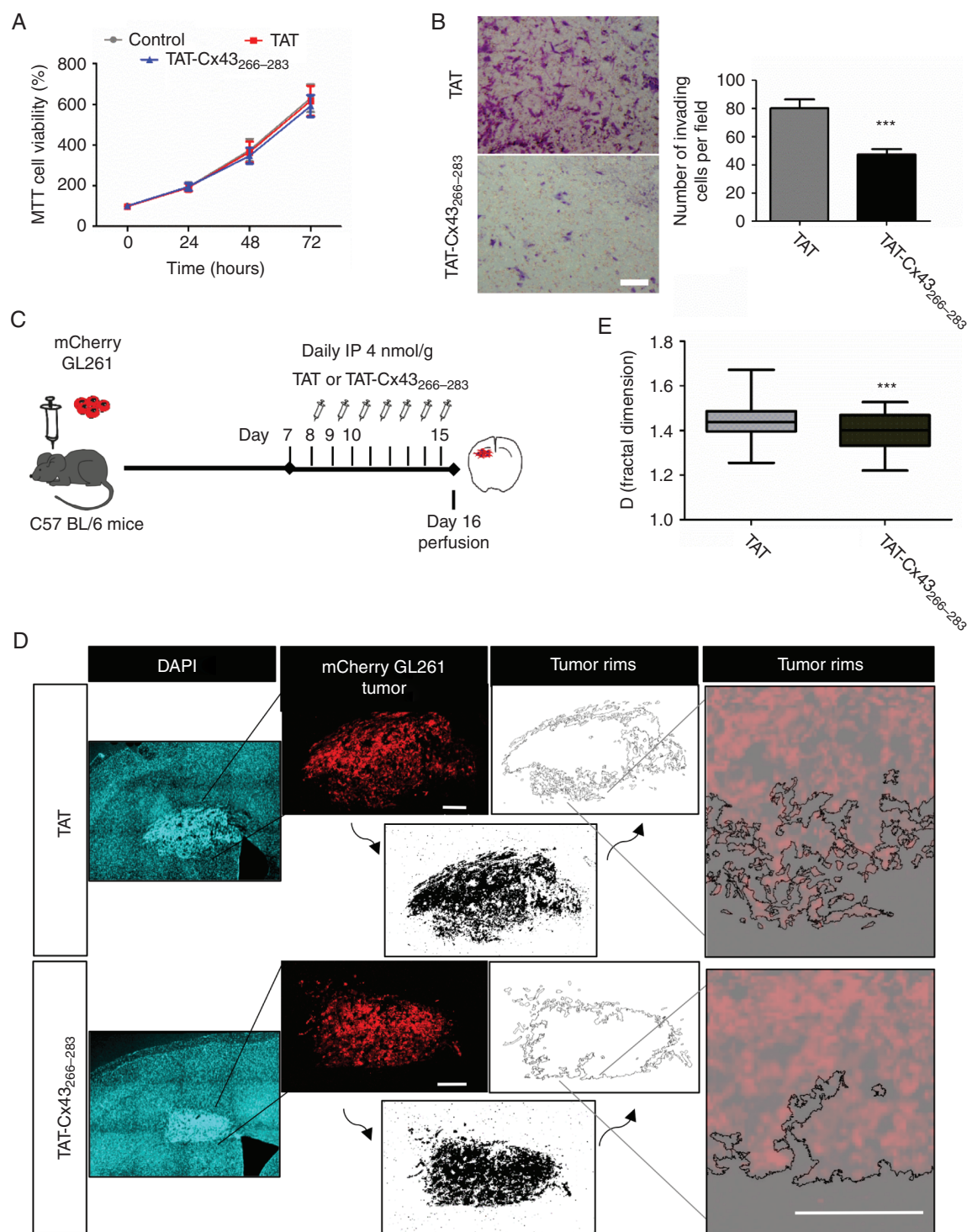
Fig. 3 TAT-Cx43$_{266-283}$ reduces the invasion of GL261 glioma cells in vivo. (A) MTT of GL261 cells incubated with 100 µM TAT or TAT-Cx43$_{266-283}$. Percentage of the control (mean ± SEM; n = 3; ANOVA). (B) Matrigel invasion assay. GL261 cells were treated with 100 µM TAT or TAT-Cx43$_{266-283}$ for 15 h. Representative images of the inserts and quantification. Bar: 100 µm; mean ± SEM; n = 3 (Student's t-test: ***P < 0.001). (C) GL261 cells were intracranially implanted in syngeneic mice (C57BL/6) and allowed to grow for 7 days. Then, a daily i.p. injection of 4 nmol/g TAT or TAT-Cx43$_{266-283}$ was administered for the next 7 days. (D) Mosaic immunofluorescence of DAPI (blue), mCherry GL261 glioma cells (red), the thresholded images (bottom, black), the tumor rims (top), and their magnifications. Bars: 200 µm. (E) The box plot shows the fractal dimension (D) of the tumor rims. D was determined in at least 3 separate sections per animal in 12 TAT and 13 TAT-Cx43$_{266-283}$ animals from 4 independent experiments. The band inside the box represents the median and the bottom and top of the box represent the first and third quartiles. The top and bottom whiskers reflect the minimum and maximum values, respectively (Student's t-test: ***P < 0.001).
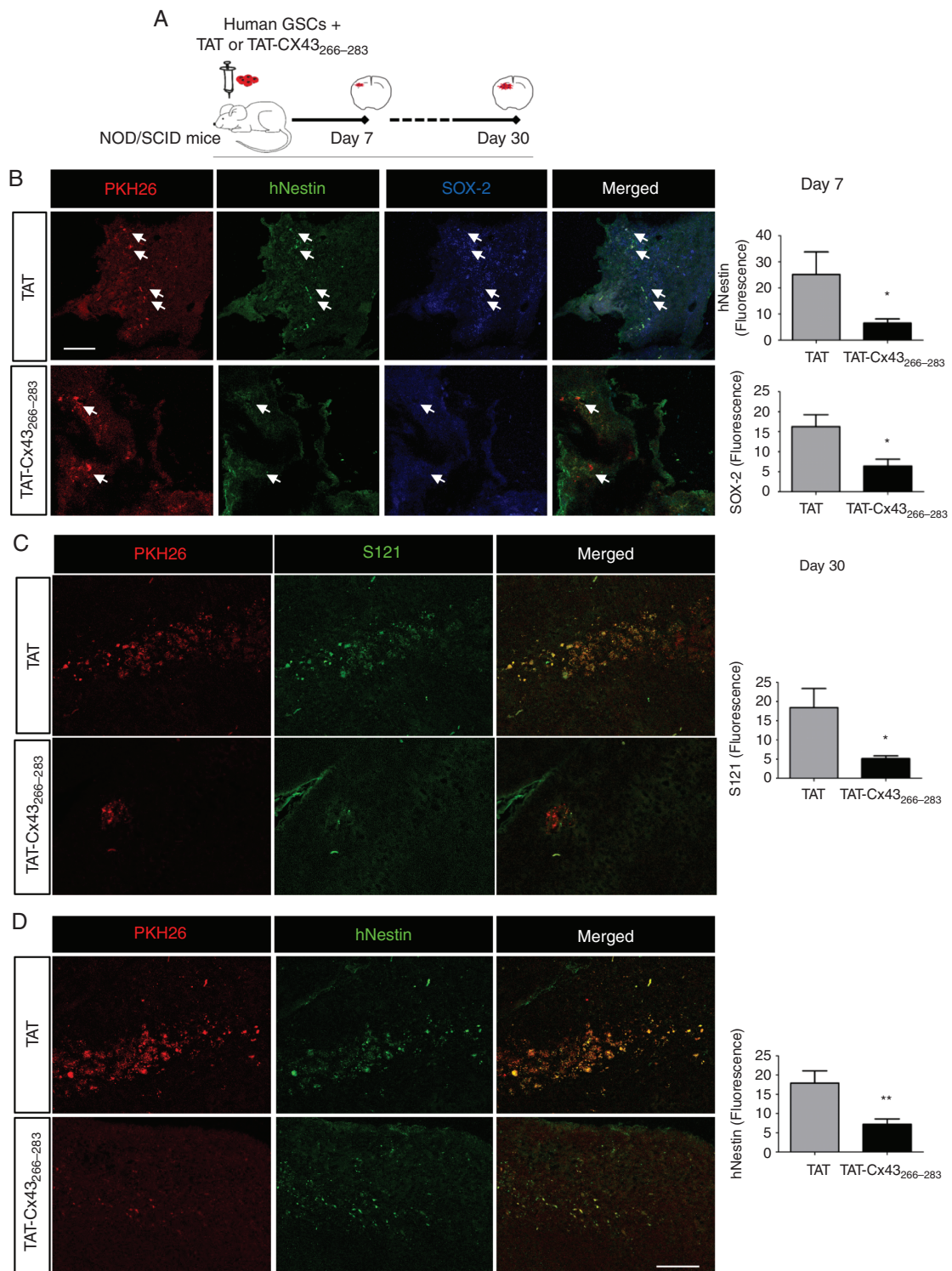
Fig. 4 TAT-Cx43$_{266-283}$ reduces Sox2 and human nestin expression and tumorigenicity in human GSCs intracranially implanted into mice. (A) Human PKH26-labeled GSCs were intracranially injected together with 100 µM TAT or TAT-Cx43$_{266-283}$ in NOD/SCID mice. After 7 (B) or 30 (C and D) days, brain sections were analyzed. (B) PKH26 (red), human nestin (hNestin; green), Sox2 (blue), and merged images of the same field. White arrows indicate some PKH26-labeled cells to illustrate the reduction in hNestin and Sox2 expression in these cells after their treatment with TAT-Cx43$_{266-283}$ for 7 days Bar: 75 µm. Quantification of hNestin and Sox2 fluorescence intensity. (C and D) Images showing a reduction in PKH26, Stem121 (S121), and hNestin after treatment with TAT-Cx43$_{266-283}$ for 30 days. Bar: 75 µm. Quantification of S121 and hNestin fluorescence (mean ± SEM). Between 2 and 5 sections per animal and 4 or 5 animals per condition from 3 independent experiments were analyzed (Student's t-test: *$P < 0.05$, **$P < 0.01$).
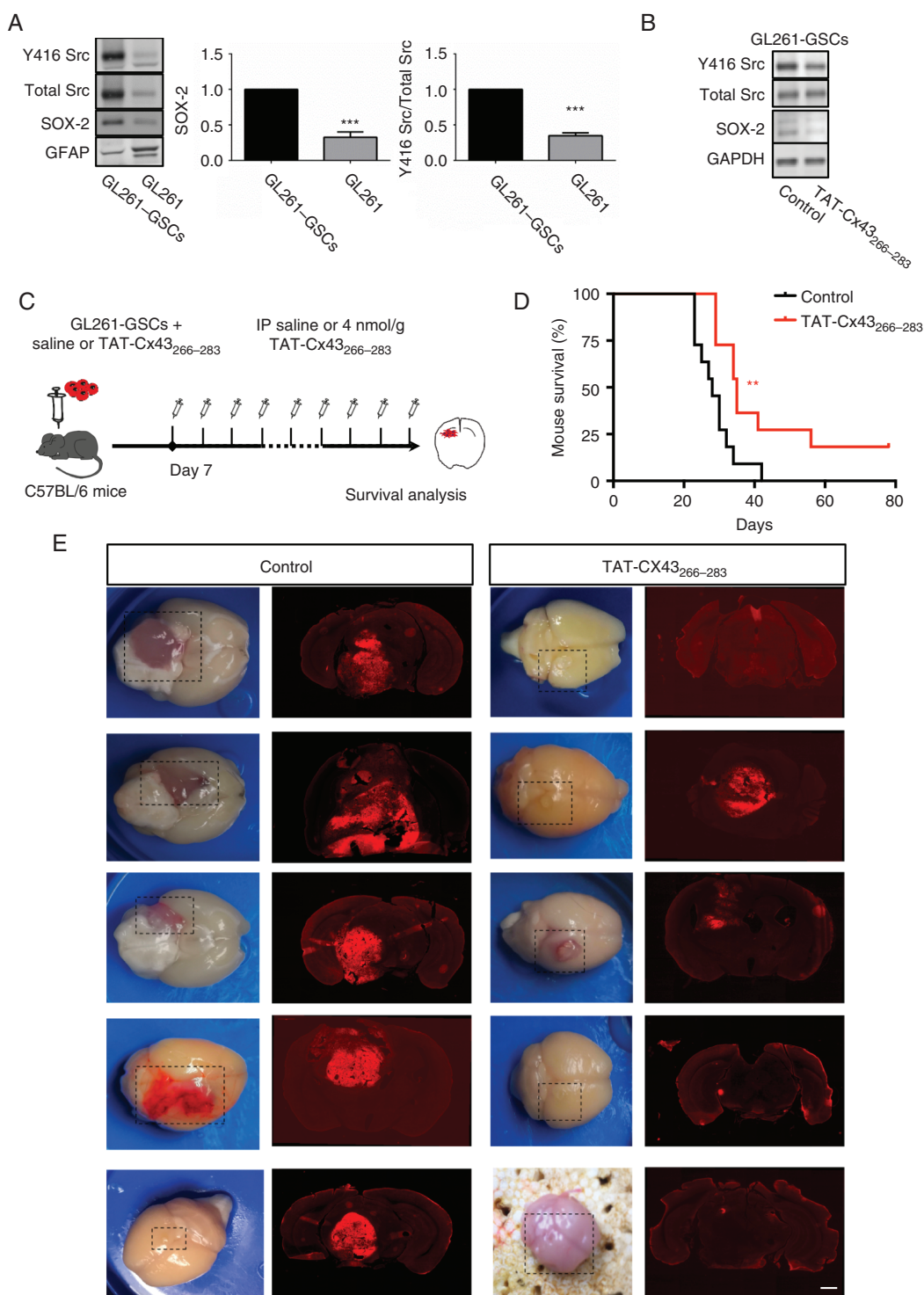
Fig. 5 TAT-Cx43_{266-283} enhances the survival of immunocompetent mice bearing GL261-GSC-derived gliomas. (A) Western blot and quantification of Y416 Src, total Src, Sox2, and GFAP in GL261-GSCs and GL261 (Dulbecco's modified Eagle's medium + fetal calf serum for 7 days); means ± SEM; $n = 8$ (Student's t-test: ***$P < 0.001$). (B) Western blot of Y416 Src, total Src, Sox2, and glyceraldehyde 3-phosphate dehydrogenase in GL261-GSCs control or treated with 50 μM TAT-Cx43_{266-283} for 24 h. (C) GL261-GSCs together with 100 μM TAT-Cx43_{266-283} or saline were intracranially injected in C57BL/6 mice. After 7 days, a twice per week i.p. injection of saline or 4 nmol/g TAT-Cx43_{266-283} was administered until neurological symptoms appeared. (D) Effect of TAT-Cx43_{266-283} on the survival of mice bearing orthotopic tumor syngrafts. Percentage of animals alive along the experiment depicted in Kaplan–Meier plot ($n = 11$ animals per condition from 3 independent experiments). Log-rank test **$P < 0.01$. (E) Representative images of the brains and tumor-bearing brain sections from control and treated animals at the end of the experiment. Bar: 1 mm.

mice, and 1 week after tumor implantation mice were intraperitoneally injected with TAT-Cx43$_{266-283}$ twice per week and followed for survival (Fig. 5C). A low amount of GL261-GSCs developed very aggressive tumors, characterized by their invasion, large size, angiogenesis, and very poor mice survival (Fig. 5D, E). Importantly, our results showed that TAT-Cx43$_{266-283}$ significantly prolonged the survival of these animals (Fig. 5D), which exhibited tumors with reduced signs of aggressiveness (Fig. 5E).

Discussion

We previously reported that the peptide based on Cx43, TAT-Cx43$_{266-283}$, inhibits c-Src activity and exerts important effects in different types of glioma cells in vitro, including freshly removed surgical specimens of glioblastoma.[28] In this study, we explored the possibility of using this peptide for therapy against malignant gliomas by studying its effect on healthy brain cells and by evaluating its antitumor effects in vivo.

The present study showed that the effect of TAT-Cx43$_{266-283}$ is cell selective. Thus, while GSC viability was strongly decreased, neuron and astrocyte viabilities were not greatly affected by TAT-Cx43$_{266-283}$. Moreover, the morphology, expression of differentiation markers, and motility of these normal brain cells were unaffected by TAT-Cx43$_{266-283}$. Conversely, TAT-Cx43$_{266-283}$ reduced stemness, proliferation, survival, invasion, and migration in GSCs.[18,24,28] The cell selectivity of TAT-Cx43$_{266-283}$ might be due to a reduced rate of internalization, especially by neurons, compared with that of GSCs. The TAT peptide is composed mainly of positively charged amino acids, and its internalization relies on electrostatic interactions with the negative charges of the plasma membrane.[39] One of the features of cancer cells, including GSCs, is a glycocalyx with a high content of negatively charged glycans, such as sialic acid, glucuronic acid, and glycosaminoglycans.[40,41] This negatively charged glycocalyx could promote stronger electrostatic interactions with TAT-Cx43$_{266-283}$ in GSCs compared with nontumor cells, contributing to the higher internalization. As expected for nontumor cells,[42] c-Src activity is lower in astrocytes than in GSCs.[18] Indeed, GSCs rely on the activity of this oncoprotein for survival, stemness, and invasion.[10] Therefore, the cell selectivity of TAT-Cx43$_{266-283}$ might depend both on its internalization and on the activity and function of c-Src. Thus, TAT-Cx43$_{266-283}$ would specifically target cells harboring a negative glycocalyx with a high c-Src activity required for their survival.

The lack of TAT-Cx43$_{266-283}$ toxicity found in neurons and astrocytes is in contrast to the results found with other Src inhibitors, such as dasatinib. Although TAT-Cx43$_{266-283}$ and dasatinib promoted similar effects on GSC viability (as shown in this study) and stemness phenotype,[18] TAT-Cx43$_{266-283}$ showed lower toxicity than dasatinib in neurons and astrocytes. The mechanism of dasatinib inhibition of c-Src involves a hydrogen bond–mediated association with the ATP binding site, resulting in competitive restriction of ATP binding by c-Src.[36] In addition to inhibiting c-Src, dasatinib also inhibits other members of the Src kinase family: BCR-ABL, c-KIT, PDGFR, and ephrin

A2.[43] However, TAT-Cx43$_{266-283}$ inhibits c-Src by acting as a docking platform for c-Src together with its endogenous inhibitors CSK and PTEN.[24,44] These data suggest that TAT-Cx43$_{266-283}$, by using a specific and endogenous mechanism to inhibit c-Src activity, exerts lower toxicity in nontumor cells than other inhibitors that act through nonendogenous mechanisms with broader targets.

Intraperitoneally administered TAT-Cx43$_{266-283}$ decreased the invasion of intracranial tumors generated by GL261 glioma cells in mice. This is the same in vivo glioma model used to show that Cx43, by increasing gap junctional communication, promotes invasion.[26] Our results suggest that TAT-Cx43$_{266-283}$ did not promote the deleterious increase in gap junctional communication between astrocytes and the GL261 Cx43-expressing glioma cells, because TAT-Cx43$_{266-283}$ did not modify astrocytic gap junctional communication.[29] However, our results suggest that TAT-Cx43$_{266-283}$ impaired glioma invasion through inhibition of c-Src and FAK, as shown in vitro.[32] These results indicate that the use of specific peptides would be a useful strategy for targeting specific connexin functions and a means to apply the vast connexin knowledge to the clinic.[27] Our study shows that the effect of TAT-Cx43$_{266-283}$ on cell invasion is not restricted to GSCs but is also significant at the bulk tumor level.

Our study reveals that intracranial injection of TAT-Cx43$_{266-283}$ with GSCs reduced the expression of nestin and Sox2, crucial markers of stemness,[45,46] in GSCs at 7 days post-implantation. Consistent with the role of Sox2 as a transcription factor required for GSC tumorigenicity,[47] we found that TAT-Cx43$_{266-283}$ strongly decreased GSC tumorigenicity, as judged by the lower number of human glioma cells found 1 month post-implantation. In fact, TAT-Cx43$_{266-283}$ importantly reduced not only the number of human glioma cells, but also their expression of nestin, suggesting that the remaining glioma cells did not exhibit stem cell properties known to drive recurrence. Furthermore, the survival of immunocompetent mice bearing gliomas derived from murine glioma stem cells was enhanced when these animals were treated with TAT-Cx43$_{266-283}$.

Altogether, these data confirm the relevance of TAT-Cx43$_{266-283}$ for the design of new therapies against gliomas. Indeed, after a thorough investigation that included in vitro and in vivo models, such as intracranial implantation of murine glioma cells and GSCs into immunocompetent mice and of human GSCs into immunosuppressed mice, we can conclude that TAT-Cx43$_{266-283}$ prolongs the survival of glioma-bearing mice because it reduces the growth, invasion, and progression of malignant gliomas with remarkably fewer toxic effects for normal brain cells than other c-Src inhibitors currently being tested in glioma clinical trials. It should be highlighted that TAT peptides have been proven to be safe and effective for stroke in preclinical models[48] and in patients after intravenous administration[49] and are currently being evaluated in a phase III clinical trial (https://clinicaltrials.gov/ct2/show/NCT02930018). These studies confirm the ability of peptides fused to TAT to cross the human blood–brain barrier and the suitability of the systemic administration of these compounds for CNS therapy. Therefore, intravenous administration of TAT-Cx43$_{266-283}$ might be efficient for malignant gliomas. Because most patients

with malignant glioma show recurrence after surgery within or in close proximity to the original site,[50] another attractive proposal would be to explore the local administration of TAT-Cx43$_{266–283}$ within the postoperative cavity through a sustained-release drug delivery system, in combination with standard therapies. According to our results, TAT-Cx43$_{266–283}$ might reduce tumor cell invasion and could target those GSCs that escape the surgery, reversing their stemness and consequently reducing their tumorigenic activity, preventing the regrowth of the tumor. Further research is required to explore this interesting possibility and its future application in the clinic.

We are aware that most preclinical positive results in the field of malignant gliomas failed when applied in the clinic. However, the effects of TAT-Cx43$_{266–283}$ in GSCs and at the bulk tumor level, the positive results in freshly removed surgical specimens of glioblastoma patients[28] as well as in immunocompetent in vivo models, and the lack of toxicity suggest that the combination of this compound with existing therapies could improve the survival of these patients.

Supplementary Material

Supplementary data are available at *Neuro-Oncology* online.

Keywords

cell-penetrating peptides | connexin | glioma | Src

Authorship statement. All authors participated in drafting and revising the article for important intellectual content and approved the final version for publication. M.J-R., R.T., L.G-V., S.G.P., M. D-P., A.A-V., R.F-H., W.C.S., and J.B. contributed to the experimental design and development, data acquisition, analysis, and interpretation. J.M.M. and C.C.N. contributed to the experimental design and data interpretation. A.T. conceived and designed the experiments, supervised the experimental development and analysis, interpreted the data, and drafted the article.

References

1. Gilbert MR, Dignam JJ, Armstrong TS, et al. A randomized trial of bevacizumab for newly diagnosed glioblastoma. *N Engl J Med.* 2014;370(8):699–708.

2. Dirks PB. Brain tumor stem cells: the cancer stem cell hypothesis writ large. *Mol Oncol.* 2010;4(5):420–430.

3. Chen J, Li Y, Yu TS, et al. A restricted cell population propagates glioblastoma growth after chemotherapy. *Nature.* 2012;488(7412):522–526.

4. Cheng L, Wu Q, Guryanova OA, et al. Elevated invasive potential of glioblastoma stem cells. *Biochem Biophys Res Commun.* 2011;406(4):643–648.

5. Garcia JL, Perez-Caro M, Gomez-Moreta JA, et al. Molecular analysis of ex-vivo CD133+ GBM cells revealed a common invasive and angiogenic profile but different proliferative signatures among high grade gliomas. *BMC Cancer.* 2010;10:454.

6. Laird DW, Lampe PD. Therapeutic strategies targeting connexins. *Nat Rev Drug Discov.* 2018;17(12):905–921.

7. Leithe E, Mesnil M, Aasen T. The connexin 43 C-terminus: a tail of many tales. *Biochim Biophys Acta Biomembr.* 2018;1860(1):48–64.

8. Kanemitsu MY, Loo LW, Simon S, Lau AF, Eckhart W. Tyrosine phosphorylation of connexin 43 by v-Src is mediated by SH2 and SH3 domain interactions. *J Biol Chem.* 1997;272(36):22824–22831.

9. Thomas SM, Brugge JS. Cellular functions regulated by Src family kinases. *Annu Rev Cell Dev Biol.* 1997;13:513–609.

10. Han X, Zhang W, Yang X, et al. The role of Src family kinases in growth and migration of glioma stem cells. *Int J Oncol.* 2014;45(1):302–310.

11. Singh S, Trevino J, Bora-Singhal N, et al. EGFR/Src/Akt signaling modulates Sox2 expression and self-renewal of stem-like side-population cells in non-small cell lung cancer. *Mol Cancer.* 2012;11:73.

12. Weissenberger J, Steinbach JP, Malin G, Spada S, Rülicke T, Aguzzi A. Development and malignant progression of astrocytomas in GFAP-v-src transgenic mice. *Oncogene.* 1997;14(17):2005–2013.

13. Huang RP, Hossain MZ, Sehgal A, Boynton AL. Reduced connexin43 expression in high-grade human brain glioma cells. *J Surg Oncol.* 1999;70(1):21–24.

14. Soroceanu L, Manning TJ Jr, Sontheimer H. Reduced expression of connexin-43 and functional gap junction coupling in human gliomas. *Glia.* 2001;33(2):107–117.

15. Pu P, Xia Z, Yu S, Huang Q. Altered expression of Cx43 in astrocytic tumors. *Clin Neurol Neurosurg.* 2004;107(1):49–54.

16. Crespin S, Fromont G, Wager M, et al. Expression of a gap junction protein, connexin43, in a large panel of human gliomas: new insights. *Cancer Med.* 2016;5(8):1742–1752.

17. Hitomi M, Deleyrolle LP, Mulkearns-Hubert EE, et al. Differential connexin function enhances self-renewal in glioblastoma. *Cell Rep.* 2015;11(7):1031–1042.

18. Gangoso E, Thirant C, Chneiweiss H, Medina JM, Tabernero A. A cell-penetrating peptide based on the interaction between c-Src and connexin43 reverses glioma stem cell phenotype. *Cell Death & Disease.* 2014;5:e1023.

19. Yu SC, Xiao HL, Jiang XF, et al. Connexin 43 reverses malignant phenotypes of glioma stem cells by modulating E-cadherin. *Stem Cells.* 2012;30(2):108–120.

20. Giaume C, Koulakoff A, Roux L, Holcman D, Rouach N. Astroglial networks: a step further in neuroglial and gliovascular interactions. *Nat Rev Neurosci.* 2010;11(2):87–99.

21. Zhu D, Caveney S, Kidder GM, Naus CC. Transfection of C6 glioma cells with connexin 43 cDNA: analysis of expression, intercellular coupling, and cell proliferation. *Proc Natl Acad Sci U S A.* 1991;88(5):1883–1887.

22. Naus CC, Elisevich K, Zhu D, Belliveau DJ, Del Maestro RF. In vivo growth of C6 glioma cells transfected with connexin43 cDNA. *Cancer Res.* 1992;52(15):4208–4213.

23. Herrero-González S, Gangoso E, Giaume C, Naus CC, Medina JM, Tabernero A. Connexin43 inhibits the oncogenic activity of c-Src in C6 glioma cells. *Oncogene.* 2010;29(42):5712–5723.

24. González-Sánchez A, Jaraíz-Rodríguez M, Domínguez-Prieto M, Herrero-González S, Medina JM, Tabernero A. Connexin43 recruits PTEN and Csk to inhibit c-Src activity in glioma cells and astrocytes. *Oncotarget.* 2016;7(31):49819–49833.

25. Du J, Bernasconi P, Clauser KR, et al. Bead-based profiling of tyrosine kinase phosphorylation identifies SRC as a potential target for glioblastoma therapy. *Nat Biotechnol.* 2009;27(1):77–83.

26. Sin WC, Aftab Q, Bechberger JF, Leung JH, Chen H, Naus CC. Astrocytes promote glioma invasion via the gap junction protein connexin43. *Oncogene.* 2016;35(12):1504–1516.

27. Aasen T, Leithe E, Graham SV, et al. Connexins in cancer: bridging the gap to the clinic. *Oncogene.* 2019;38(23):4429–4451.

28. Jaraíz-Rodríguez M, Tabernero MD, González-Tablas M, et al. A short region of connexin43 reduces human glioma stem cell migration, invasion, and survival through Src, PTEN, and FAK. *Stem Cell Reports.* 2017;9(2):451–463.

29. Gangoso E, Talaverón R, Jaraíz-Rodríguez M, et al. A c-Src inhibitor peptide based on connexin43 exerts neuroprotective effects through the inhibition of glial hemichannel activity. *Front Mol Neurosci.* 2017;10:418.

30. Yi L, Zhou C, Wang B, et al. Implantation of GL261 neurospheres into C57/BL6 mice: a more reliable syngeneic graft model for research on glioma-initiating cells. *Int J Oncol.* 2013;43(2):477–484.

31. Polo-Hernández E, De Castro F, García-García AG, Tabernero A, Medina JM. Oleic acid synthesized in the periventricular zone promotes axonogenesis in the striatum during brain development. *J Neurochem.* 2010;114(6):1756–1766.

32. Baker GJ, Yadav VN, Motsch S, et al. Mechanisms of glioma formation: iterative perivascular glioma growth and invasion leads to tumor progression, VEGF-independent vascularization, and resistance to antiangiogenic therapy. *Neoplasia.* 2014;16(7):543–561.

33. Yadav VN, Zamler D, Baker GJ, et al. CXCR4 increases in-vivo glioma perivascular invasion, and reduces radiation induced apoptosis: a genetic knockdown study. *Oncotarget.* 2016;7(50):83701–83719.

34. Chen Q, Boire A, Jin X, et al. Carcinoma-astrocyte gap junctions promote brain metastasis by cGAMP transfer. *Nature.* 2016;533(7604):493–498.

35. Marques-Torrejon MA, Gangoso E, Pollard SM. Modelling glioblastoma tumour-host cell interactions using adult brain organotypic slice co-culture. *Dis Model Mech.* 2018;11(2):dmm031435.

36. Lombardo LJ, Lee FY, Chen P, et al. Discovery of N-(2-chloro-6-methyl-phenyl)-2-(6-(4-(2-hydroxyethyl)- piperazin-1-yl)-2-methylpyrimidin-4-ylamino)thiazole-5-carboxamide (BMS-354825), a dual Src/Abl kinase inhibitor with potent antitumor activity in preclinical assays. *J Med Chem.* 2004;47(27):6658–6661.

37. Pollard SM, Yoshikawa K, Clarke ID, et al. Glioma stem cell lines expanded in adherent culture have tumor-specific phenotypes and are suitable for chemical and genetic screens. *Cell Stem Cell.* 2009;4(6):568–580.

38. Pellegatta S, Poliani PL, Corno D, et al. Neurospheres enriched in cancer stem-like cells are highly effective in eliciting a dendritic cell-mediated immune response against malignant gliomas. *Cancer Res.* 2006;66(21):10247–10252.

39. Fuchs SM, Raines RT. Internalization of cationic peptides: the road less (or more?) traveled. *Cell Mol Life Sci.* 2006;63(16):1819–1822.

40. Fuster MM, Esko JD. The sweet and sour of cancer: glycans as novel therapeutic targets. *Nat Rev Cancer.* 2005;5(7):526–542.

41. Zhou F, Cui C, Ge Y, et al. Alpha2,3-sialylation regulates the stability of stem cell marker CD133. *J Biochem.* 2010;148(3):273–280.

42. Okada M. Regulation of the SRC family kinases by Csk. *Int J Biol Sci.* 2012;8(10):1385–1397.

43. Chang Q, Jorgensen C, Pawson T, Hedley DW. Effects of dasatinib on EphA2 receptor tyrosine kinase activity and downstream signalling in pancreatic cancer. *Br J Cancer.* 2008;99(7):1074–1082.

44. Jaraíz-Rodríguez M, González-Sánchez A, García-Vicente L, Medina JM, Tabernero A. Biotinylated cell-penetrating peptides to study intracellular protein-protein interactions. *J Vis Exp.* 2017(130):e56457.

45. Neradil J, Veselska R. Nestin as a marker of cancer stem cells. *Cancer Sci.* 2015;106(7):803–811.

46. Garros-Regulez L, Garcia I, Carrasco-Garcia E, et al. Targeting SOX2 as a therapeutic strategy in glioblastoma. *Front Oncol.* 2016;6:222.

47. Gangemi RM, Griffero F, Marubbi D, et al. SOX2 silencing in glioblastoma tumor-initiating cells causes stop of proliferation and loss of tumorigenicity. *Stem Cells.* 2009;27(1):40–48.

48. Freitas-Andrade M, Wang N, Bechberger JF, et al. Targeting MAPK phosphorylation of connexin43 provides neuroprotection in stroke. *J Exp Med.* 2019;216(4):916–935.

49. Hill MD, Martin RH, Mikulis D, et al; ENACT trial investigators. Safety and efficacy of NA-1 in patients with iatrogenic stroke after endovascular aneurysm repair (ENACT): a phase 2, randomised, double-blind, placebo-controlled trial. *Lancet Neurol.* 2012;11(11):942–950.

50. Lemée JM, Clavreul A, Menei P. Intratumoral heterogeneity in glioblastoma: don't forget the peritumoral brain zone. *Neuro Oncol.* 2015;17(10):1322–1332.